VIBRATION AND FLEXURAL STRENGTH CHARACTERISTICS OF COMPOSITE CASTELLATED BEAMS

by

Rahsean Jackson

Thesis submitted to the Faculty of the

Virginia Polytechnic Institute and State University

in partial fulfillment of the requirements for the degree of

MASTERS OF SCIENCE

in

Civil Engineering

APPROVED:

_____

Dr. Thomas M. Murray, Chairman

_____ _____

Dr. Mehdi Setareh Dr. Finley A. Charney

February, 2002

Blacksburg, Virginia

VIBRATION AND FLEXURAL STRENGTH CHARACTERISTICS OF CASTELLATED BEAMS

by

Rahsean Jackson

Dr. Thomas M. Murray, Chairman

Department of Civil and Environmental Engineering

(ABSTRACT)

With the development of lightweight concrete and design optimizations, floor vibration problems are becoming a serious serviceability problem. The castellated beam is a prime example and was the focus of this study. The vibration and flexural strength performance were verified in this paper.

The vibration characteristics of castellated beams were examined using experimental and analytical test methods. The effective moment of inertia is essential to accurately predict the frequency and deflection of a floor system due to human occupancy. Since castellated beams have non-prismatic cross-sections, their effective moment of inertia is an uncertainty and was verified in this study. This paper confirmed the accuracy of the AISC Design Guide procedures used in for prismatic beam, when applied to castellated beams.

The flexural strength of various composite castellated beam were studied. Three full-scale specimens were tested to failure to evaluate their yield and maximum applied load. Each specimens' moment strength was verified based on span, beam properties, concrete slab, and amount of shear connection.

ACKNOWLEDGEMENTS

I would like to express my appreciation to Dr. Thomas M. Murray for serving as my committee chairman and his valuable guidance with this thesis. Gratitude is also extended to Dr. Mehdi Setareh and Dr. Finley A. Charney for serving as committee members. I would like to acknowledge CIT who make this research possible.

I‘d also like to thank Aaron L. Ratliff whom I met here at VT, for being a true friend. I would also like to thank Crystel M. Cole for her love, patience and support throughout my stay in Blacksburg.

Finally, I would like to thank my mother, without her, there would be no me. This is dedicated to her for the enormous sacrifices, and love she has given me my entire life.

TABLE OF CONTENTS

LIST OF FIGURES

LIST OF TABLES

Table

LIST OF EQUATIONS

Equation

CHAPTER I

INTRODUCTION AND LITERATURE REVIEW

1.1 Introduction

Since the invention of castellated beams in the mid-1930's, they have been frequently used in Europe but commonly over looked in the United States. The first known use of castellated beams in the US was by H. E. Horton of the Chicago Bridge and Iron Works in the 1940's (Dorgherty 1993). G. M. Boyd developed the concept of the castellated beams in 1935 while working for a steel fabricator in Argentina. The idea came to Boyd when posed with a design problem with beam depth restrictions. At the time, the fabricator only had beams of minimal depths available. His first idea was to stack two beams of minimal depth on top of one another to increase depth. Boyd then decided to cut a hot rolled section along the web in a saw tooth pattern, separate the two halves, and weld the web posts back together at the high points as shown in Figure 1.1.

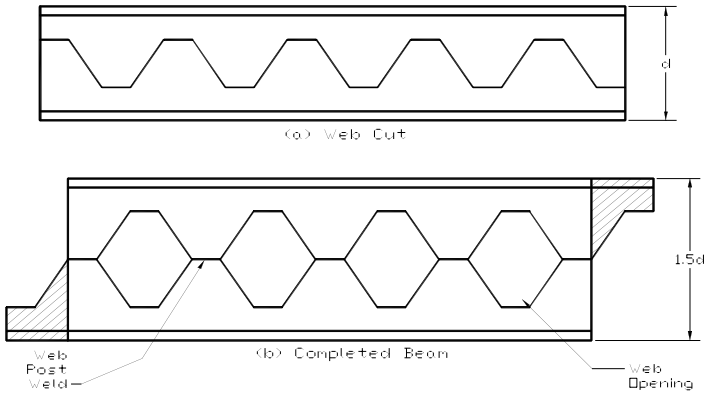

Figure 1.1 Fabrication Process

This process increases the depth of the beam by approximately 50%, therefore increasing the strength and stiffness by about 20 to 30% without increasing the weight of the beam. Also the holes in the web allow ductwork to run through beams instead of underneath ultimately reducing the depth of the floor system.

Although there are many advantages to using castellated beam, the one disadvantage is fabrication cost. The extra cost of cutting and welding the web is usually the deciding factor for their feasibility. Castellated beams are more popular in areas where the cost of steel is high and labor costs are low. The use of castellated beams in Europe has existed ever since the adoption of the fabrication process developed by Litzka Stahlbau of Bavaria, Germany (Boyer 1964). His equipment and production process is very efficient, making mass production cheaper. Since its adoption in the United States several steel fabrication companies have made castellated beams available.

The design concept for castellated beams is based on typical beam limit states, but the presence of web openings and welds can cause other modes of failure. The potential modes of failure associated with castellated beams are:

- Flexural Failure Mechanism
- Lateral-Torsional Buckling
- Vierendeel Bending Mechanism
- Weld Rupture at Web Post
- Shear Buckling of Web Post
- Compression Web Post Buckling

Vibration has become a serious serviceability problem due to design optimizations such as castellated beams. Other factors contributing to this problem are the use of lightweight and high strength materials, design code improvements and how

the floor system is used. Although vibration issues pose no strength problems, they can cause severe human discomfort and in some cases render a structure unusable.

Many times vibration controls over strength and deflection. Although it is not a required design check in specifications, it can be very costly to retrofit if neglected in initial design. Passive and active damping systems may be used to mitigate vibration problems once construction is complete. Because damping systems can be very expensive, is best to avoid them through application of methodologies designed to minimize vibrations.

The AISC has recently published floor vibration design criteria developed by Murray, Allen and Ungar (1997). The criteria include accurate methods for predicting floor vibration and will be used in this research to evaluate the performance of castellated beams.

1.2 Scope of Research

The first objective of this research is limited to the investigation of the vibration performance of composite castellated beams. Because vibration is a function of the stiffness, and the cross-sectional properties of castellated beams are non-prismatic, the effective moment of inertia will be closely examined. The second objective of this research is to examine the first yielding and ultimate flexural strength of composite castellated simply supported beams.

1.3 Terminology

Throughout this paper various terms will be used to discuss vibration, castellated

beam concepts and testing results. This section introduces the reader to the definition of these terms.

Dynamic Force – Load which changes with respect to time.

Forced Vibration – The repeated alternating motion (up and down in the case of floors) of a system when excited by a dynamic force.

Free Vibration – The continued alternating motion (up and down in the case of floors) of a system after the dynamic excitation force has been discontinued.

Cycle – is a complete oscillation starting at any given magnitude and direction that ends at the same magnitude and direction.

Period (*T*) – The time is takes for one complete cycle. (see Figure 1.2)

Amplitude – is the maximum absolute value of a periodic curve measured along its vertical axis. In the case of vibration this value is usually the dependent variable in a displacement or acceleration verses time plot as shown in Figure 1.2.

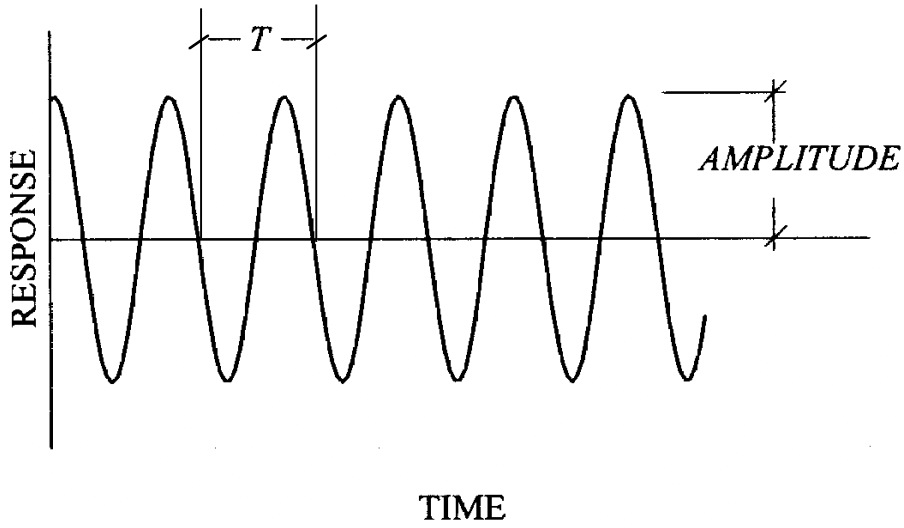

Figure 1.2 Base Cosine Wave

Frequency – Number of cycles in any given period of time, usually measured in Hertz (Hz).

Natural Frequency – The frequency at which a system will vibrate freely once excited.

Fundamental Natural Frequency – All systems have multiple natural frequencies. The fundamental frequency is the lowest natural frequency at which a system will freely vibrate.

Damping – is the loss of mechanical energy of a vibrating system. This usually reduces the dynamic response (amplitude or displacement) in a particular system by dissipating energy. Response decay is directly related to damping.

Acceleration Trace – is a plot of measured acceleration verses time as the independent variable. (see Figure 1.3)

Fast Fourier Transformation (FFT) – a mathematical procedure used to transform a set of time dependant values into a set of frequency dependent values.

FFT Spectrum – is a frequency verses acceleration plot as shown in Figure 1.4. This is the graphical result of a FFT of an acceleration trace.

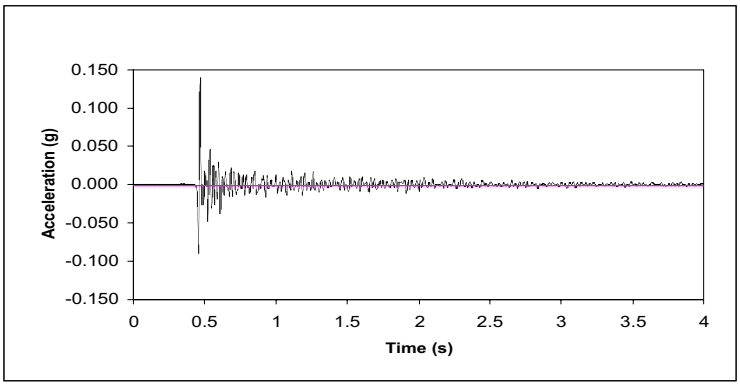

Figure 1.3 Acceleration Trace

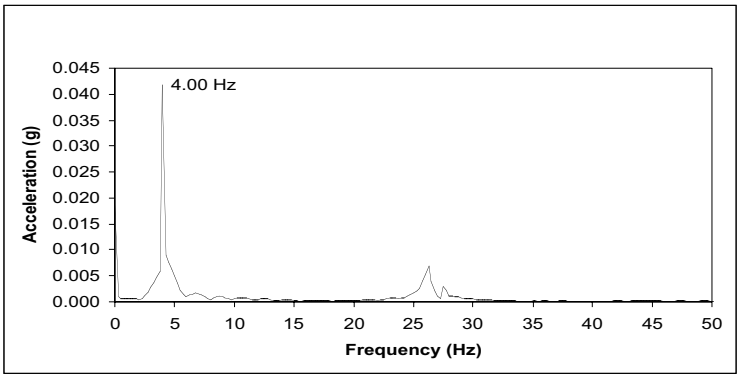

Figure 1.4 FFT Frequency Spectrum

Tee-section – is the "T" shaped bottom or top portion of the cross-section through the web opening of a castellated beam.

1.4 Literature Review

1.4.1 Castellated Beams

Since the late 1930's there has been a moderate amount of theoretical and experimental research associated with castellated beams. Flexural strength research of castellated beams was first initiated by Toprac and Cooke (1959). Their research found that castellated beams under pure bending yielded in the upper and lower tee sections of web openings first.

United Steel (1960) realized that, although the web opening of castellated beams did not affect flexural strength, they posed an effective stiffness issue. Typically the net moment of inertia associated with the cross-section through the web opening of castellated beams is used when calculating deflection. Their research found this underestimates deflection due to shear deformation. These results are based on tests

where castellated beams were loaded to failure at quarter points. All beams tested were relatively small with depths less than 15 in.

The first known composite castellated beam work was by Larnach and Park (1964). Their tests used six different castellated beams with shear transferred from the concrete slab to the beam via spiral shear connectors. A distributed load was used to fail the specimen by web post buckling and transverse cracking of the concrete. From this testing it was found that the neutral axis at the web post was lower than that associated with the web opening.

Baldwin and Douty (1966) conducted tests on beams identical to three beams used in the design of the American Dental Association Building (ADA) in Chicago, Illinois. Two of the three beams tested had enlarged web openings to accommodate special ductwork. Each beam was loaded to failure at or in excess of 160 percent of the design load for the ADA building. In all three tests, the measured deflection was greater than the predicted deflection based on gross moment of inertia by about 10 percent. It is also noted that yielding occurred before the building service load was reached.

Giriyappa and Baldwin (1966) performed two tests on composite castellated beams with different top and bottoms sections under a distributed load systems. Although web post buckling was the predicted failure mode, yielding in the tension flange occurred first, indicating flexural failure.

Composite action of castellated beams without shear studs was considered by encasing the top flange of the beam in a 2-in. concrete slab. Watson, O'Neal, Barnoff, and Mead (1974) found sufficient adhesion between the steel flange and concrete from

slip data measured during tests. Load verses deflection experiments also revealed 95 to 99 percent theoretical full composite action.

Kerdal and Nethercot (1984) conducted a study based on previous tests comparing the experimental moment capacity, M_{exp} and plastic bending moment, $M_{p.}$ This study found the $M_{exp}/M_{p(hole)}$ ratio to be slightly higher than 1.0, where $M_{p(hole)}$ is the plastic moment capacity of castellated beam considering only the cross-section through web opening. This value drops to about 0.8 for the ratio $M_{exp}/M_{p(post),}$ where $M_{p(post)}$ is the plastic moment capacity of the castellated beam considering the cross-section through web post.

Modeling castellated beams as a Vierendeel truss with points of infection at the mid-span of tee sections and web posts was used by Knowles (1991) to examine deflection effects due to pure shear. This work concluded that inflection points in the tee sections are not located at the midpoints. The result was further investigated by Megharief (1997), which is the most recent known composite castellated beam work. In this study, three beams in high shear and two beams in high flexure were tested to failure. The three shear oriented tests revealed that the bottom tee takes 11 to 25 percent of shear, and that the concrete slab and top tee together take 75 to 89 percent. The two flexural test specimens ultimately failed due to lateral-torsional buckling but only after the bottom flanged yielded and the shear studs failed over half of the length of the beam. Tension strain was measured above web openings. This indicated the neutral axis was located higher than predicted.

1.4.2 Vibration

Treadgold, (1828) was the first to suggest a vibration and stiffness relationship in 1828. He suggested wooden floor beams be made deeper to reduce residential floor vibration induced by walking.

Vibration acceptance criteria is ultimately related to how sensitive humans are to various frequencies. Reiher and Meister (1931) were the first to examine this phenomenon by subjecting a controlled group of people to different combinations of vibration frequencies and amplitudes. The frequencies ranged from 5 to 70 Hz and amplitudes varied from 0.001 to 0.04 in. Each individual was asked to classify their response as "slightly perceptible", "distinctly perceptible", "strongly perceptible", "disturbing" and "very disturbing". These results were used to develop the Reiher-Meister Scale shown in Figure 1.5.

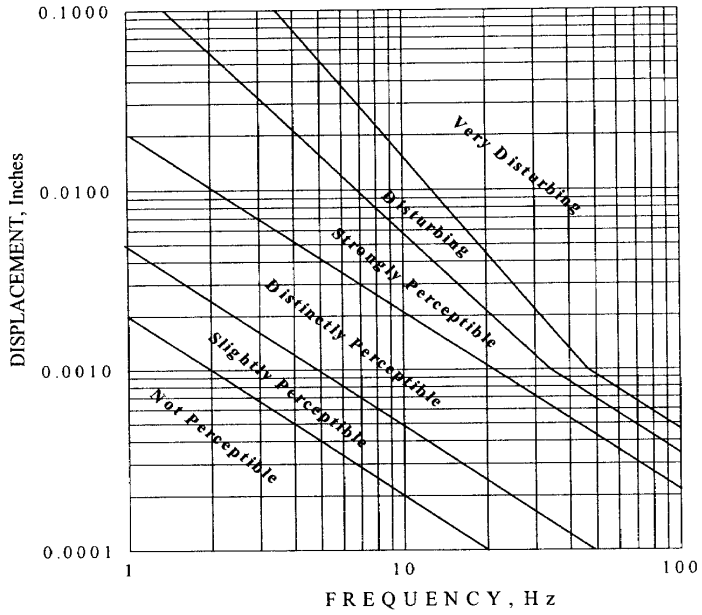

Figure 1.5 Reiher-Meister Scale

Lenzen (1966) suggested the Reiher-Meister Scale amplitudes be adjusted by a

factor of ten to account for the transient nature of vibrations. The modified version of the Reiher-Meister Scale is shown in Figure 1.6.

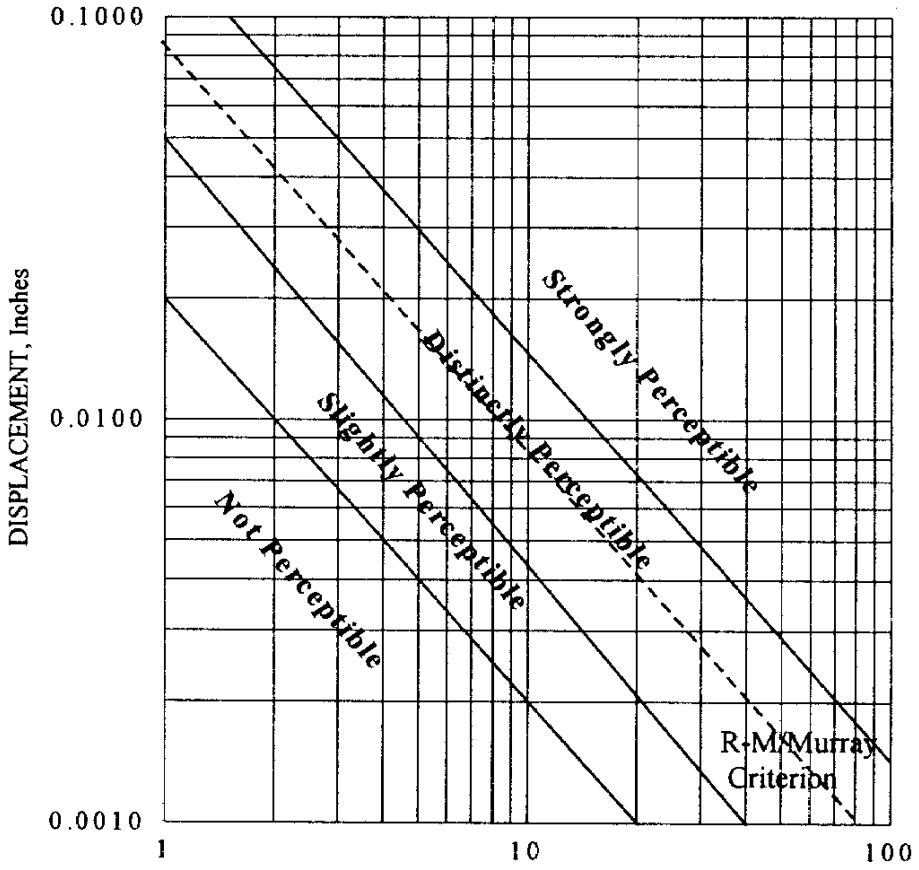

Figure 1.6 Modified Reiher-Meister/Murray Scale

An additional criterion was added to the Reiher-Meister Scale by Murray (1975), indicated by the dashed line through the middle of the "distinctly perceptible" portion of the scale also shown in Figure 1.6. Murray found that "steel beam-concrete slab systems, with relatively open areas free of partitions and damping between 4 and 10 percent critical, which plot above the upper one-half of the distinctly perceptible range, will result in complaints from the occupants". All frequencies and amplitudes below the dashed line

are considered acceptable by what is known as the Modified Reiher-Meister/Murray criterion.

The Modified Reiher-Meister/Murray criterion is based on log decrement damping between 4 and 10 percent. This was found to be slightly conservative based on further research by Murray (1981). Critical damping required is directly related to amplitude and natural frequency due to heel drop excitation. These properties were used to do a statistical analysis based on ninety-one systems to determine an acceptable damping criterion given by:

$$D \geq 35 A_0 f_n + 2.5 \tag{1.1}$$

where f_n = first natural frequency of floor system, in Hz; A_0 = initial amplitude from heel-drop impact, in. and D = percent of critical log decrement damping. This criterion is applicable only for floor systems with spans and natural frequencies less than 40 ft and 10 Hz, respectively. The natural frequency, f_n, is determined using

$$f_n = \frac{0.18}{\sqrt{g/\Delta_j}} \tag{1.2}$$

where g = the acceleration of gravity, and Δ = mid-span deflection of the member relative to its supports due to the weight supported.

Based on Murray (1991) “humans react adversely to frequencies in the 5-8 Hz range.” This is due to the natural frequencies of the internal organs of the body falling within this range.

Humans have also been found to be sensitive to floor accelerations. Various floor systems are used and excited in different ways. Figure 1.7, developed by Murray and Allen (1993), shows four different classifications of floors and the corresponding acceptable acceleration criterion.

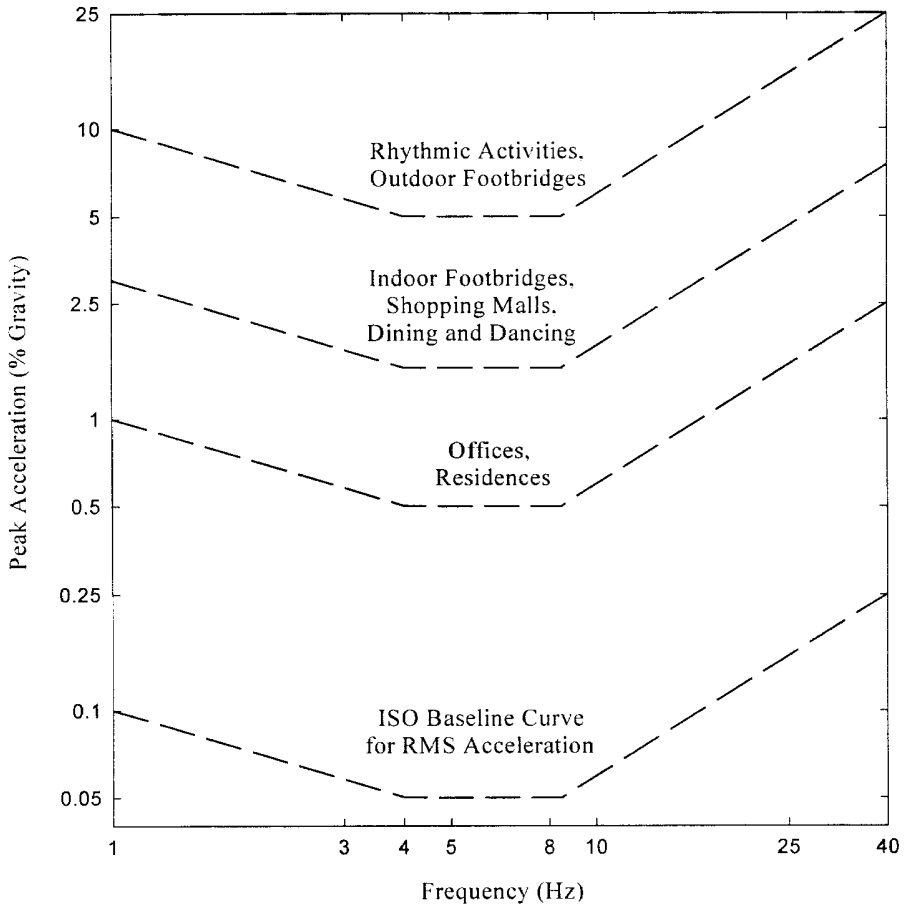

Figure 1.7 Recommended Peak Acceleration Criterion (Allen and Murray 1993)

The AISC Steel Design Guide Series 11, by Murray, Allen and Ungar (1997), provides methods to predict the floor framing natural frequency. Included in the Design Guide is criterion based on the dynamic response of steel beam and joist supported floor systems to walking forces. The criterion states that the peak acceleration of a floor

system, a_p due to a walking excitation, expressed as a fraction of the acceleration of gravity, g, is determined from

$$\frac{a_p}{g} = \frac{P_o \exp(-0.35 f_n)}{\beta W} \tag{1.3}$$

where a_p/g, the computed acceleration should not exceed the acceleration limit a_o/g for the appropriate occupancy, P_o = a constant force representing the excitation, f_n = the fundamental natural frequency of a beam or joist panel as applicable, β = modal damping ratio, and W = effective weight supported by the beam, joist, or girder panel, as applicable.

The recommended values for P_o and β are based on the type of occupancy of floor system. Figure 1.7 can be used to determine the acceleration limit a_o/g. The combined effective panel weight, W_c, is found from

$$W_c = \frac{\Delta_j}{\Delta_j + \Delta_g} W_j + \frac{\Delta_g}{\Delta_j + \Delta_g} W_g \tag{1.4}$$

where, Δ_j and Δ_g = maximum deflections of the beam or joist and girder, respectively, due to weight supported by member as if simply supported. W_j and W_g = effective panel weights for the beams or joists and the girder, respectively. The effective panel weights is determined using

$$W_{j/g} = wBL \tag{1.5}$$

where w = the supported weight per unit area, L = member span, and B = the effective width. The effective width for a beam or joist is

$$B_j = C_j (D_s / D_j)^{1/4} L_j \tag{1.6}$$

where C_j = 2.0 for typical beams or joists and 1.0 for beams or joists parallel to an interior edge as for a mezzanine, D_s = transformed slab moment of inertia per unit width, and D_j = joist or beam transformed moment of inertia per unit width, and L_j = joist or beam span. For the girder panel, the effective width is:

$$B_g = C_g (D_j / D_g)^{1/4} L_g \tag{1.7}$$

where C_g = 1.6 for girders supporting joist connected to girder flange, or 1.8 for beams connected to the girder web, D_g = girder transformed moment of inertia per unit width, and L_g = girder span.

In the field or laboratory, natural frequencies are determined through measured response of the floor subjected to a dynamic force. Floors are commonly excited with a "heel-drop" impact. "Standard" heel drops are made by a 170 lb. person rocking up on the balls of his feet with heels approximately 2.5 in. off the floor and then relaxing allowing the heels to impact the floor (Murray 1981). Figure 1.8 illustrates standard and approximate heel drop impact curve developed by Ohmart (1968). Floor systems can also be excited by walking in different directions and bouncing on the floor at frequencies which cause resonance.

Finite element analysis may also be used to predict natural frequencies of floor systems. Different methods of modeling have been adopted depending on the type floor system. Megharief (1997) used shell elements to model castellated beams with the web oriented in the x-y plane and flanges in the z-x plane as shown in Figure 1.9. Composite

slab elements were modeled using one-dimensional beam elements with nonlinear capabilities. Beavers (1998) used a simpler means to model composite beams, using all one-dimensional elements shown in Figure 1.10.

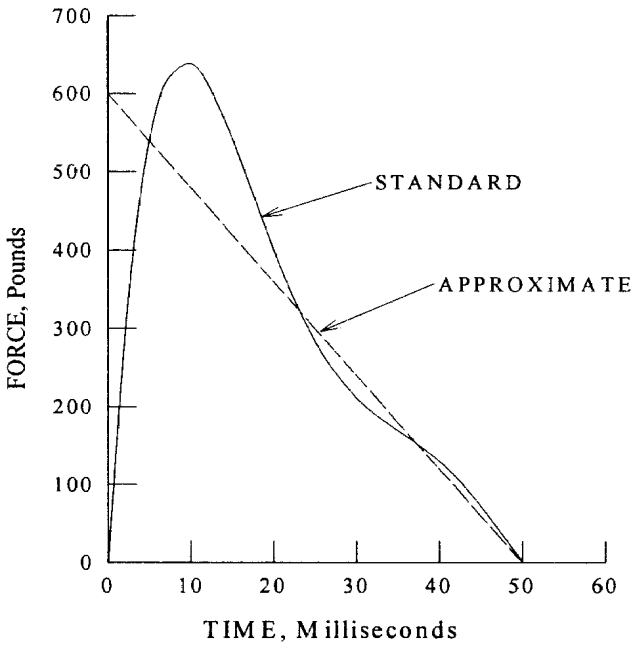

Figure 1.8 Heel Drop Force Verses Time Functions

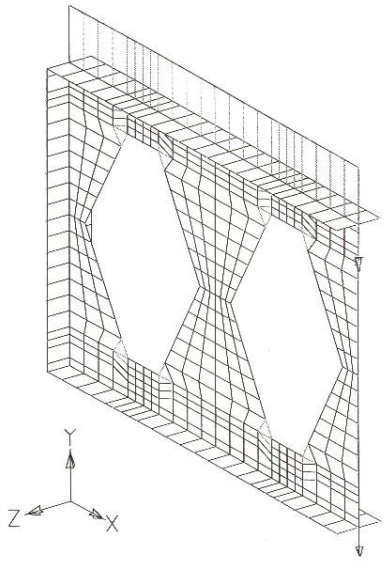

Figure 1.9 FE Model of Composite Castellated Beam (Megharief 1997)

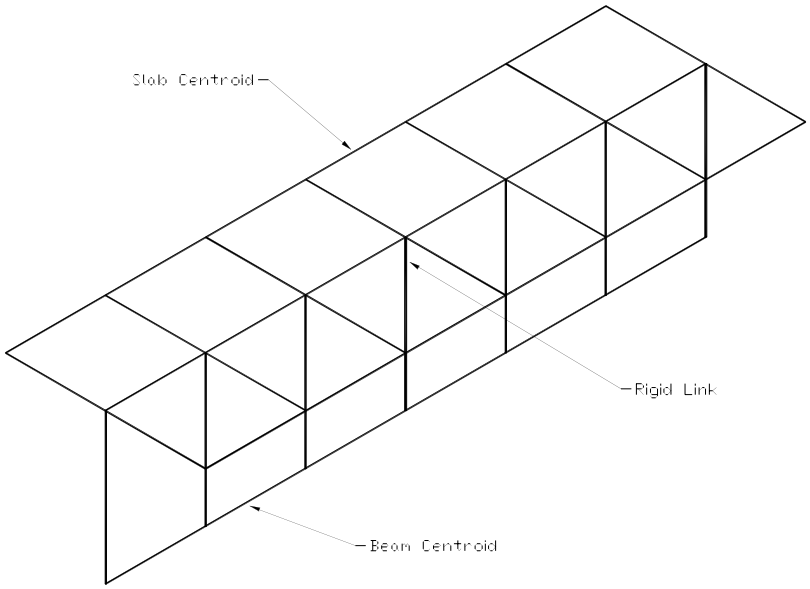

Figure 1.10 Slab and Beam FEM (Beaver 1998)

1.5 Need For Research

Since vibration is a function of stiffness an accurate vibration prediction may be problematic because the effective moment of inertia of castellated beams is an uncertainty. This study evaluated the accuracy of the methods used to predict natural frequencies for prismatic beams when applied to castellated beams.

The flexural strength of composite castellated beams is usually critical at the center of long span beams. The most recent composite flexural tests were conducted by using a concentrated load at mid span, not typical of most building floor systems. A distributed load is the best way to model a typical loading for a floor framed system. The geometry of the castellation cut becomes an issue when considering flexural strength. Each steel manufacturer cuts their castellation in a different manner. This ultimately affects the depth of the top and bottom tee-sections through web openings, which can

significantly affect the flexural strength of a beam. The tests conducted in this study evaluated long span composite castellated beams with uniform distributed loading.

1.6 Overview

Chapter II covers the evaluation of the vibration characteristics of composite castellated floor systems. The chapter includes a description of specimens used for all tests in the study. It also describes the vibration and stiffness test procedures. Load verses deflection measurements were used to establish the effective stiffness of non-composite and composite castesllated beams. These stiffness values are compared to tabulated values in the manufacture's design manual. These stiffness results are then used to evaluate frequency predictions and measurements.

Chapter III discusses the flexural strength of castellated beams. This evaluation is based on three different castellated beams that were tested to failure. The test procedures and instrumentation are described in this chapter. First yield and ultimate strength results are evaluated.

Chapter IV includes all final results and conclusions for each part of the study. Final recommendations for future research are found in this chapter. All supporting data and drawings are tabulated in Appendices following this chapter.

CHAPTER II

EVALUATION OF VIBRATION CHARACTARISTICS OF COMPOSITE CASTELLATED BEAMS

2.1 Introduction

To evaluate the vibration behavior of typical composite castellated beam floor systems, three sets of full-scale vibration tests were conducted. These tests were performed at the Virginia Tech Department of Civil and Environmental Engineering Structures and Materials Research Laboratory. Each test set-up consisted of two simply supported castellated beams. The beams were fabricated by SMI Steel Products in Farmville, Virginia. The composite floor slab had a total thickness of 6 _ in., over a 22 gauge 3 in. metal deck. The specimen configuration and nominal concrete properties are shown in Figure 2.1. The tests are designated CB12 x 13, CB15 x 15/19, and CB27 x 35/50. Table 2.1 is a summary of the test specimen parameters.

Table 2.1 Summary of Specimen Parameters

Beam Test	Span (ft)	Nominal Concrete strength (psi)	Concrete weight (pcf)	Concrete effective width (in)	Total slab depth (in)	Deck Rib depth (in)	Total Slab width (ft)	No. of Shear Studs per span
CB12X13	30	3000	145	42	6.25	3	7	16
CB15X15/19	40	3000	145	42	6.25	3	7	14
CB27X35/50	58	3000	145	42	6.25	3	7	22

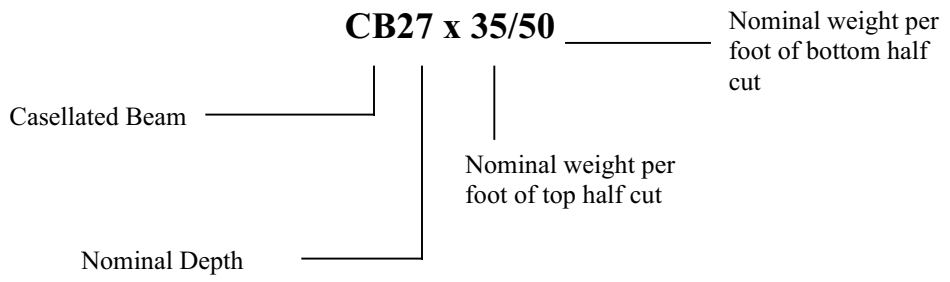

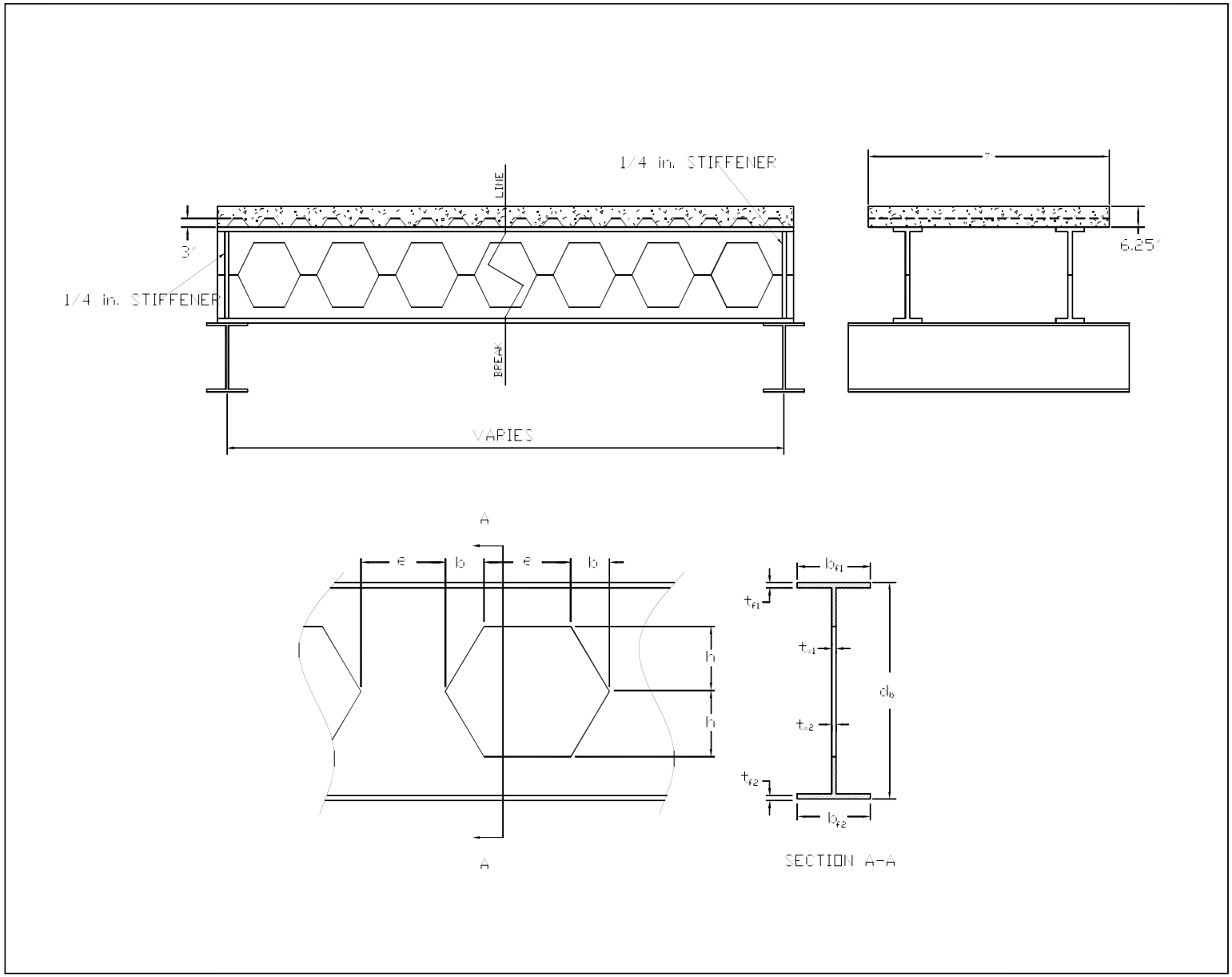

Figure 2.1 Typical Test Specimen Parameters

Table 2.2
CB12 x 13 Dimensions

SECTION PROPERTY	MEASURED DIMENSION SIZE (in)
e	3.523
b	2.062
h	3.313
t_{f1}	0.270
t_{f2}	0.270
b_{f1}	3.900
b_{f2}	3.900
t_{w1}	0.230
t_{w2}	0.230
d_b	11.625

Table 2.3
CB15 x 15/19Dimensions

SECTION PROPERTY	MEASURED DIMENSION SIZE (in)
e	5.126
b	2.930
h	5.126
t_{f1}	0.290
t_{f2}	0.371
b_{f1}	4.040
b_{f2}	4.073
t_{w1}	0.200
t_{w2}	0.250
d_b	15.173

Table 2.4
CB27 x 35/50 Dimensions

SECTION PROPERTY	MEASURED DIMENSION SIZE (in)
e	7.875
b	6.063
h	9.668
t_{f1}	0.401
t_{f2}	0.563
b_{f1}	6.100
b_{f2}	7.300
t_{w1}	0.297
t_{w2}	0.355
d_b	27.375

2.2 Test Specimen

2.2.1 CB12 x 13 Specimen

The first test specimen was a CB12 x 13 castellated beam cut from a W8 x 13 hot-rolled section. The nominal depth of this specimen was 11.75 in. Measured web opening and beam dimensions for this specimen are given in Table 2.2 in conjunction with Figure 2.1. Both the top and bottom flanges have identical dimensions. The CB12 x 13 specimen had an overall span length of 30 ft. The concrete slab had a nominal width of 7 ft., total thickness of 6 _ in., and was placed on a 3-in. metal deck. The entire specimen was supported on two W18 x 35 hot rolled beams, 30 ft apart. The support beams were bolted to the laboratory reaction floor. Each beam had two _ in. x 2 in. full depth stiffeners at each support as shown in Figure 2.1.

Shear transfer between the compression flange of the beam and the concrete was provided by 16 – 3/4 in. diameter, 5.25 in long headed shear studs. This number of studs provides 77% composite action. The shear stud strength was calculated according to AISC (1999) specification provisions as found in Appendix C. A certified technician welded one stud per rib on the strong side of deck rib. A uniform distribution of studs could not be achieved, instead, three studs were placed in three consecutive ribs from each support, and then five were placed in every other rib there after.

2.2.2 CB 15 x 15/19 Specimen

This specimen was comprised of two asymmetric CB15 x 15/19 sections. The top section was cut from a W10 x 15 hot-rolled member and the bottom portion of the section was cut from a W10 x 19 member. This makes the beam more efficient since the bottom half the beam is a region of high stress. The nominal depth of the beam was 15.25 in. Top

and bottom section dimensions are listed in Table 2.3. Each beam spanned 40 ft, was spaced 5 ft apart below a 6.25 in. thick and 7 ft. wide concrete slab. The entire specimen rested on the same support and reaction floor as the CB12 x 13 specimen.

A total of fourteen _ in. diameter, 5 3/8 in. long shear studs were welded through the decking by a lab technician. All studs were uniformly distributed and placed on the strong side of deck rib to provide 54 % composite action.

2.2.3 CB27 x 35/50 Specimen

The third test specimen was very similar to the CB15 x 15/19 specimen but spanned 58-ft. The two asymmetric CB27 x 35/50 beams were spaced 5 ft. apart with a nominal depth of 27 1/8 in. The top and bottom beams were cut from W18 x 35 and W18 x 50 hot-rolled sections, respectively. The section properties for this specimen are listed in Table 2.3. The concrete slab was of the same dimensions as the pervious two specimens. Two _ in. x 3 in. full depth stiffeners were welded at all the support ends of each beam by the manufacturer. Both beams were supported by W14 x 25 hot-rolled sections, which were bolted to the reaction floor.

Twenty-two _ in. diameter, 5 3/8 in. long studs were used to transfer shear. To insure 34 % composite action one stud was placed on the strong side of each deck rib. Again, an approximate uniform distribution of shear studs in deck ribs was used.

2.3 Measurement and Prediction of Effective Stiffness

The multiple openings through the web of castellaed beams make it difficult to predict the effective moment of inertia. Typically in design, the moment of inertia through the web opening is used. To verify this assumption, non-composite and

composite static load verses deflection tests were conducted for each specimen, 14 and 28 days after the concrete slab was poured.

2.3.1 Calculation of Effective Stiffness

There are two moment of inertia values associated with castellated beams. The first is referred to as the gross moment of inertia, I_g,, which is calculated using the cross-section through the web post. The other is the net moment of inertia, I_n,, which is calculated considering the cross-section through the web opening. The predicted non-composite gross, I_g, and net, I_n, moment of inertia values listed in Table 2.5 are values found in the manufacturer's castellated beam catalog. The predicted gross, $I_{tr(gross)}$, and net, $I_{tr(net)}$, are composite moment of inertia values based on 100% composite action, and calculated using the respective member moment of inertia.

Table 2.5 Calculated Moment of Inertia

Member Stiffness	Specimen		
	CB12 x 13	CB15 x 15/19	CB27 x 35/50
Non-composite I_g in^4	91.8	221.0	1670.2
Non-composite I_n in^4	85.3	188.4	1474.7
Composite $I_{tr(gross)}$ in^4	411.6	1076.7	5174.5
Composite $I_{tr(net)}$ in^4	383.4	770.3	4265.1

2.3.2 Testing Procedure

Deflection indicators were used to measure support and mid-span deflections caused by applied loads. Six dial indicators were attached to magnetic bases and placed 6-in. from each support and at the mid-span of each castellated beam. Each specimen was preloaded by applying a 1.2 kip load at mid-span. After the load was removed, all dial

indicators were zeroed and five 20-lb weights were placed at mid-span of both beams to simulate one 100 lb concentrated static load. All six dial gauge deflection readings were then recorded. This procedure was repeated by adding weight in 100 lb increments until each beam supported 600 lb.

The net deflection of each beam was calculated by taking the average of the support deflections and subtracting it from the mid-span deflection for each load increment. The average net deflection of both beams was then used to form a linear line of best-fit function to establish a specific deflection for a given load. An arbitrary load is then input to the line-of-best-fit equation to ascertain a specific deflection. This known deflection and load were used to determine the effective moment of inertia by solving for I in deflection equation:

$$\Delta = \frac{Pl^3}{48EI} \tag{2.1}$$

where Δ = known deflection from line-of-best-fit function; P = known load used in line-of-best-fit function; l = length of beam; E = Young's modulus of steel; and I = calculated effective moment of inertia.

2.3.3 Comparison of Measured and Predicted Stiffness

CB12 x 13 Results. The non-composite CB12 x 13 test results are very linear as shown in Figure 2.2(a), indicating elastic behavior. The measured stiffness for this test was slightly lower than net moment of inertia prediction as clearly illustrated by the north and south beam slopes in the figure.

Fourteen days after the concrete slab was poured composite deflection tests for the CB 12 x 13 specimen were performed. Figure 2.2 (b) also indicates linear behavior

but the measured stiffness fall between the net and gross theoretical slopes. This shows that the effective composite stiffness is greater then composite moment of inertia using the net member moment of inertia, 85.3 in^4, and less than that using the gross moment of inertia, 91.8 in^4.

The 28-day deflection test results are very similar to the 14-day test. Both beams indicate elastic behavior as shown in Figure 2.2 (c). The effective stiffness value also falls in between gross and net theoretical stiffnesses.

.

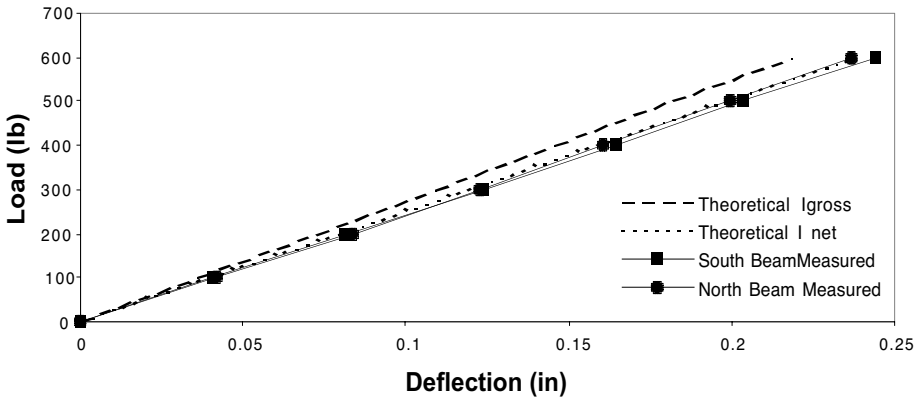

(a) Non-Composite Test

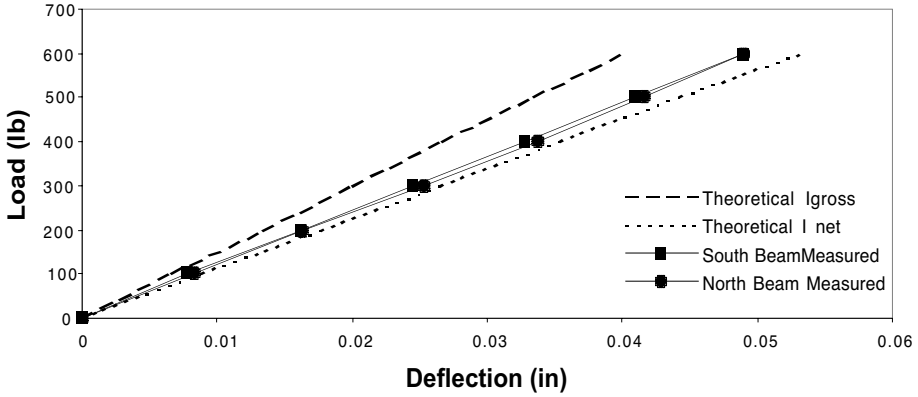

(b) Composite 14-Day Test

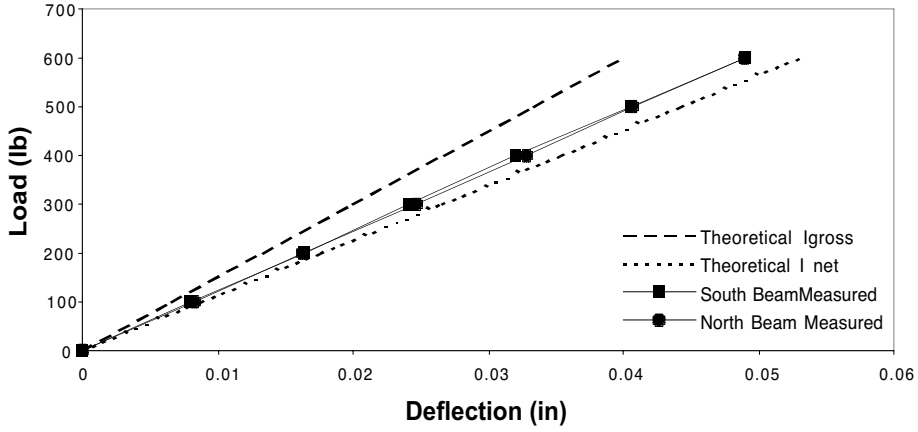

(c) Composite 28-Day Test

Figure 2.2 CB12 x 13 Load vs. Deflection Plots

CB 15 x 15/19 Results. Non-composite tests for CB 15 x 15/19 were conducted during construction to verify theoretical values given in Table 2.5. The slopes in Figure 2.3(a) indicate that the north beam is somewhat less stiff than the south beam. The north beam slope is very close to theoretical gross moment of inertia and the south beam is not as stiff as the net moment of inertia slope. This is believed to be due to about 3 to 4 in. of lateral sweep in the south beam discovered during construction. The average stiffness of both beams again falls between the net and gross values.

The 14-day composite test was also very linear, but yielded a slightly lower stiffness value than the theoretical composite net stiffness slope shown in Figure 2.3(b).

Two weeks later the 28-day test was conducted and resulted in higher stiffness values than the 14-day test. Both the north, south and theoretical net deflection lines have the same approximate slope which are shown in Figure 2.3(c). The calculated value is slightly lower than the average measured value of both beams.

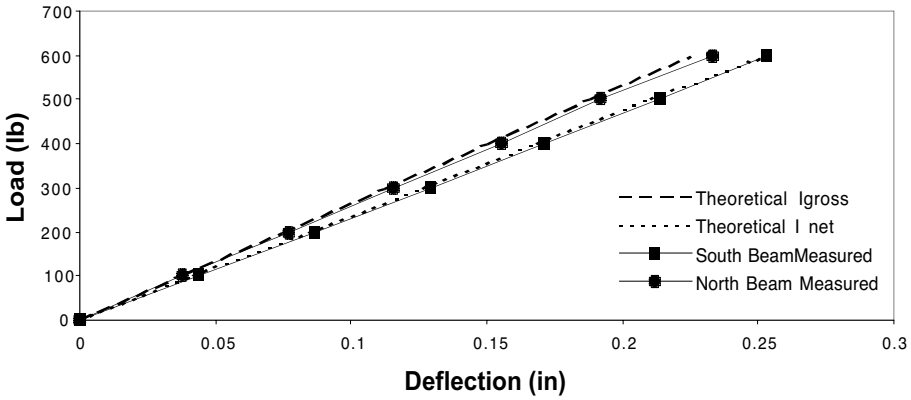

(a) Non-Composite Test

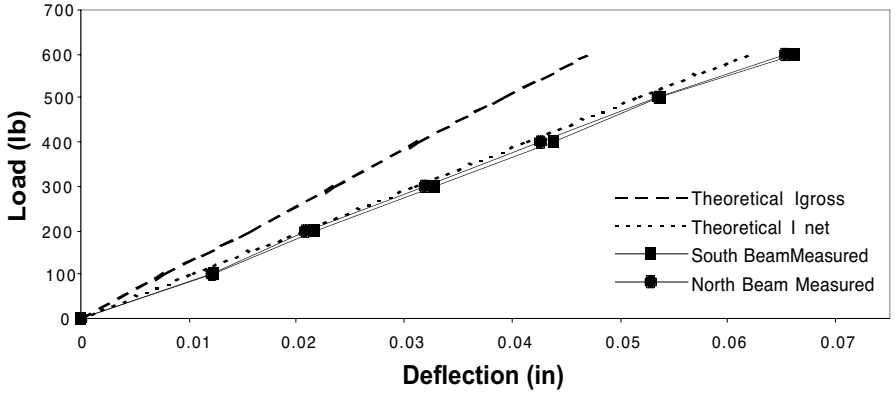

(b) Composite 14-Day Test

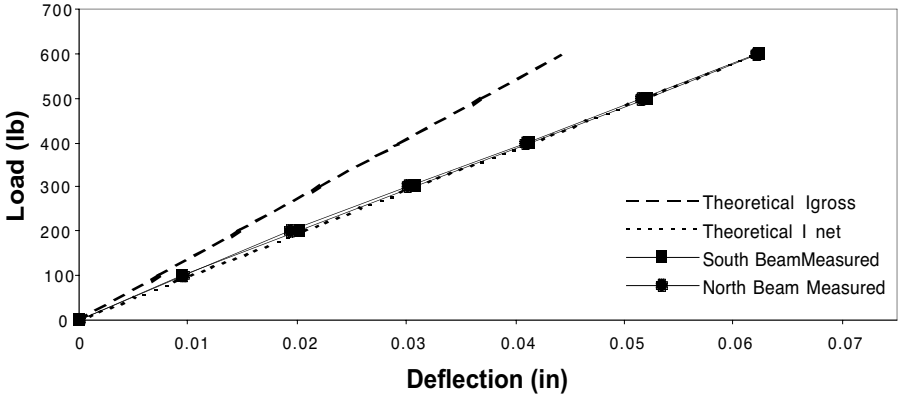

(c) Composite 28-Day Test

Figure 2.3 CB15 x 15/19 Load vs. Deflection Plots

CB 27 x 35/50 Results. Figure 2.4 (a) shows the results of the CB27 x 35/50 non-composite test. The south beam has a higher slope than the gross theoretical line and the north beam falls in between gross and net slopes.

The 14-day composite results for the CB27 x 35/50 were very similar to the CB15 x 15/19 test. Again, the measured stiffness was not as stiff as the theoretical net slope as shown in Figure 2.4 (b).

The final 28-day test also yielded results similar to the CB15 x15/19 test. Figure 2.4 (c) shows the north and south beam slopes fall between net and gross theoretical lines. This indicates the measured stiffness is greater than net stiffness value, but less than gross value.

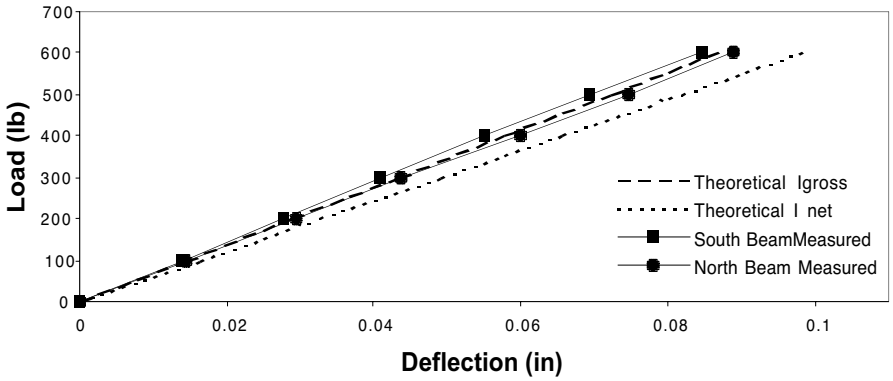

(a) Non-Composite Test

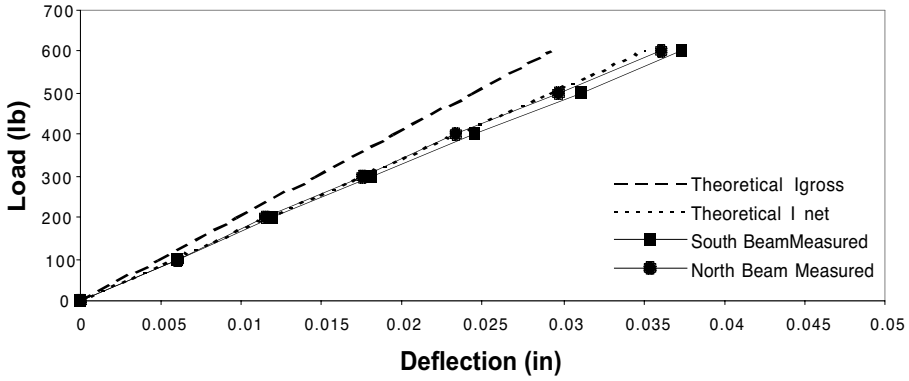

(b) Composite 14-Day Test

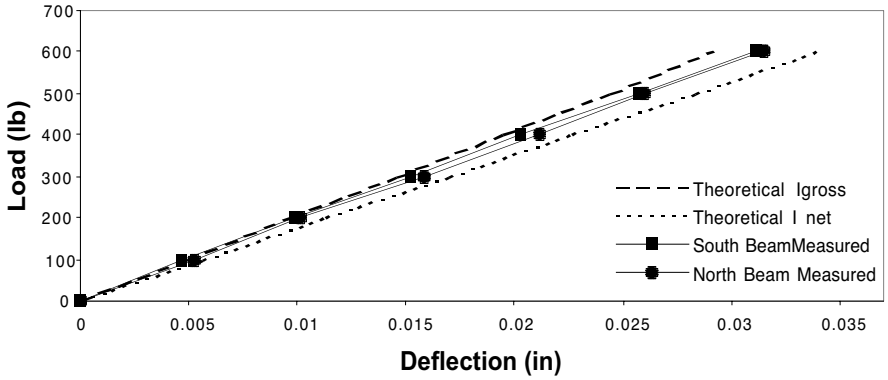

(c) Composite 28-Day Test

Figure 2.4 CB27 x 35/50 Load vs. Deflection Plots

2.3.4 Summary of Test Results

Static deflection test results were analyzed using the load verses deflection plots shown in Figures 2.2 through 2.4. Theoretical data is included in each plot to help evaluate effective stiffness of each beam. The measured and theoretical moment of inertia results are compiled in Table 2.6. Columns four and five are the non-composite theoretical gross and net moment of inertia (I_g and I_n) values, respectively. These values are based on tabulated beam properties from the manufacturer's design manual. The predicted gross and net composite moment of inertia ($I_{tr(gros)}$ and $I_{tr(net)}$) values are found in columns seven and eight, respectively. The composite theoretical moments of inertia are based on the respective non-composite moments of inertia in columns five and six, full composite action, and a 42 in. concrete slab effective width. The theoretical composite values are based on recommendations from AISC Design Guide Series 11 (Murray, Allen, and Ungar, 1997). The guide recommends 100% composite action between concrete slab and beam, even if shear connectors are not used. For vibration purposes the shear forces at the slab/beam interface are extremely small and can easily be resisted by the deck-to-member spot welds if no shear connectors are used. The measured compressive strength of the concrete used in the moment of inertia calculations are listed in column three of Table 2.6.

2.3.5 Conclusions

The effective moment of inertia of a non-composite castellated beam is a function of the beam depth. The deeper the beam, the closer the effective stiffness is to the gross moment of inertia. The effective stiffness is approximately equal to that calculated using

the net moment of inertia for shallower beams. This is clearly shown by the moment of inertia values listed in non-composite columns of Table 2.6.

The effective moment of inertia of composite castellated beams is approximately equal to the calculated moment of inertia based on net section properties. Table 2.6 shows measured moment of inertia, $I_{tr(eff)}$, values roughly equal to predicted net composite, $I_{tr(net)}$, values.

Table 2.6 **Static Test Results**

Configuration	Composite Test Day	Concrete Strength (ksi)	Non-Composite			Composite		
			Non-Composite Predicted I_g (in^4)	Non-Composite Predicted I_n (in^4)	Non-Composite Measured I (in^4)	Composite Predicted $I_{tr(gross)}$ (in^4)	Composite Predicted $I_{tr(net)}$ (in^4)	Composite Measured $I_{tr(eff)}$ (in^4)
(1)	(2)	(3)	(4)	(5)	(6)	(7)	(8)	(9)
CB12x13-N/S	14-day	2.50	91.8	85.3	83.5	501.5	378.3	407.6
CB12x13-N/S	28-day	3.00	91.8	85.3	83.5	510.3	383.4	411.6
CB15x15/19-N/S	14-day	3.57	221.0	188.4	195.3	1071.8	767.9	731.6
CB15x15/19-N/S	28-day	3.74	221.0	188.4	195.3	1076.7	770.3	772.5
CB27x35/50-N/S	14-day	2.50	1670.2	1474.7	1682.9	4960.4	4135.4	3991.9
CB27x35/50-N/S	28-day	3.30	1670.2	1474.7	1682.9	5174.5	4265.1	4677.1

where, N/S – indicates test results are based on the average of north and south beams

2.4 Beam Frequency Tests

The three floor specimens were also tested to investigate their vibration characteristics. Two sets of dynamic load tests were conducted at 14 days and 28 days composite strength for each floor specimen.

2.4.1 Testing Procedure

Four vibration measurements were taken for each specimen using a Fast Fourier Transformation (FFT) Analyzer and a low-frequency accelerometer. All floor specimens were tested in the same manner. Acceleration measurements were taken at mid-span (center) and all four supports of each test set-up as shown in Figure 2.5. Heel drops, bouncing in resonance, and walking are used to excite typical floor framed systems. All three of these excitations, as well as an ambient response, were used for mid-span measurements. Support accelerations were measured for heel drop and ambient conditions above the beam stiffener and support as shown in Figure 2.5. Separate sets of measurements were made with no additional loading and with added weight to simulate a 15 psf live loading. This was done by evenly distributing 20 lb boxes filled with metal chads across each concrete slab.

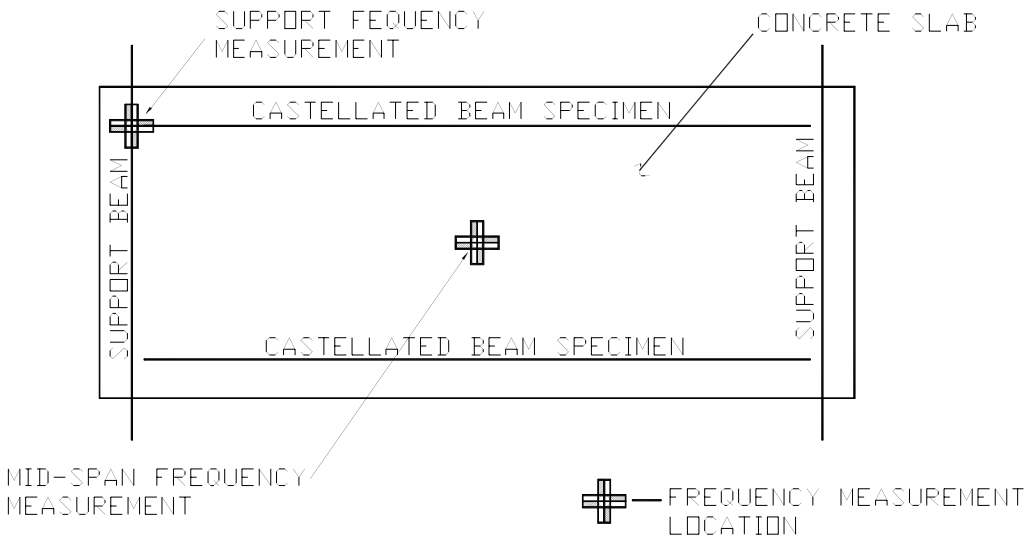

Figure 2.5 Acceleration Measurement Locations

FFT procedures were than used to determine the frequencies associated with each measurement. Support frequencies were filtered out of the mid-span measurements to obtain the beam frequency, f_b, using Dunkerly's equation:

$$\frac{1}{f_s^2} = \frac{1}{f_b^2} + \frac{1}{f_g^2} \tag{2.2}$$

where f_g = the measured support frequency, f_s = the measured mid span frequency, and f_b = the unknown beam frequency.

These measurement results were compared to predicted frequencies using the AISC Design Guide (Murray, Allen and Ungar 1997) procedure.

SAP 2000 Non-linear (2000) was also used to conduct a finite element analysis to predict natural frequency of all floor specimens. Each finite element model was based on a modified version of the model developed by Beavers (1998). The actual model used in this study is shown in Figure 2.6. All models used a combination of shell and beam elements to reconstruct each composite floor system. The castellated beam was modeled using two beam elements with tee cross-sections identical to those in cross-section through web opening as shown in Figure 2.6. The concrete slab was modeled using shell elements with the average thickness of total depth actual floor slab as shown in Figure 2.6. The cross-sectional properties used in the finite element model are listed in Table 2.7.

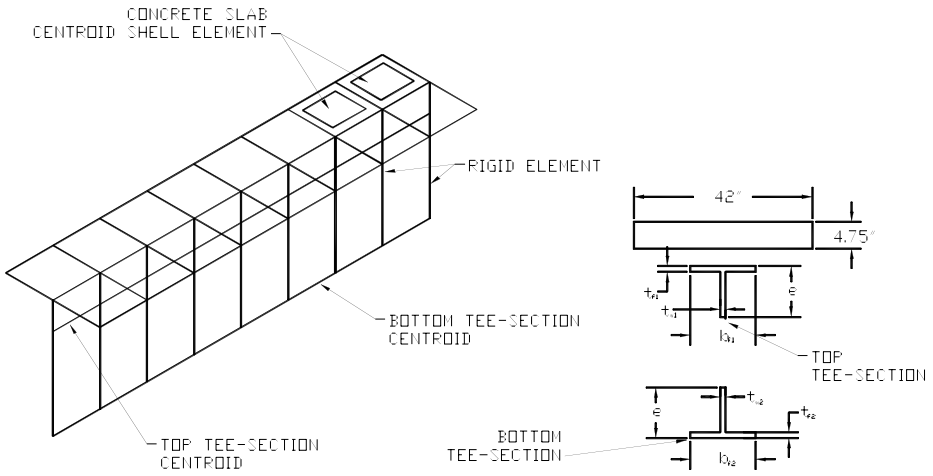

Figure 2.6 Typical FEM Parameters

Table 2.7 **FEM Beam and Shell Element Properties**

SECTION PROPERTY	CB12 x 13	CB15 x 15/19	CB27 x 35/50
t_{f1} in.	0.27	0.29	0.40
t_{f2} in.	0.27	0.37	0.56
b_{f1} in.	3.90	4.04	6.10
b_{f2} in.	3.90	4.07	7.30
t_{w1} in.	0.23	0.20	0.29
t_{w2} in.	0.23	0.25	0.36
e in.	2.50	2.53	4.02

2.4.2 Dynamic Test Results

Dynamic vibration test results were evaluated using a FFT frequency spectrum plot from data provided by the analyzer. A typical frequency spectrum is shown in Figure 1.4. The lowest frequency with significant energy content was used in all subsequent calculations and analysis. The predicted, measured mid-span, and measured support frequencies are summarized in Tables 2.8(a), through (f). The corrected measured beam frequency and both predicted frequencies are also included in these tables. An example

calculation for predicted results are found in Appendix A. FFT frequency spectra plots are found in Appendix B. Only heel drop measurements are included in Appendix B since the walking and bouncing measurement yield the same natural frequency as the heel drop. No ambient measurements were considered due to poor excitations from surrounding environment.

CB 12 x 13 Results. The measured and predicted frequency results for the CB 12 x 13 specimen are found in Table 2.6(a). The adjusted natural frequencies for the loaded and unloaded cases were 5.51 and 6.03 Hz, respectively. The frequency results for the loaded floor system were slightly lower than the unloaded results. This is a typical response due to the additional weight added to system. Increasing the load on the floor increases the deflection, Δ_j value in the frequency relationship

$$f_n = \frac{0.18}{\sqrt{g/\Delta_j}} \tag{2.3}$$

which decreases the natural frequency, f_n. The support frequencies were significantly higher than mid-span frequency due to the large stiffness in this area as shown in Table 2.6(a). The measured fundamental natural frequencies for the 14 and 28-day results were identical for both loading situations.

Predicted floor frequencies using, I_{net}, measured are in good agreement with the measured frequencies, with percent differences from measured results ranging from 0.53% to 1.34 %. The FEM percent difference results are only compared to the unloaded measured responses. The FEM model used was divided into six elements per beam section and twelve shell elements for the concrete slab. The measured unloaded frequency falls between the FEM value and that given by Equation 2.3.

CB 15 x 15/19 Results. Again, the floor system exhibited typical behavior illustrated by a decrease in frequency when the floor was loaded. It should also be noted that the support frequencies decreased with increased load. A small amount of accuracy was lost in AISC Design Guide prediction with a percent difference as high as 3.18 %. This could be due the FFT analyzer being accurate to only 0.25 Hz. It was also noticed in this test that the higher the support frequency was, the closer the mid-span frequency was to the adjusted beam frequency back calculated from Equation 2.2. The 28-day frequencies were slightly higher than 14-day measurements indicating an increase in stiffness as the concrete cured. In comparing the predicted and measured results it can be seen in Table 2.6(b) that the FEM model closely predicted the frequency of the CB15 x 15/19 specimen. This model was divided into eight beam elements to account for is longer span length. The concrete slab model was divided into sixteen elements to maintain joint continuity between slab and beam. The number of elements was increased to decrease the length and area of each element, hence increasing the accuracy of the results.

CB 27 x 35/50 Results. The results for this results were very similar to the CB 15 x 15/19 test with the exception of the 28-day loaded measurements as shown in Table 2.6(c). Although this anomaly yielded the lowest percent difference, the frequency measured is a little lower than the 14-day value. This is due to the uncharacteristic high support frequency in the 28-day loaded situation, which decreased the adjusted beam frequency. All the support frequencies in this test changed with respect to the loading situation, which is consistent with previous tests. The number of elements for this FEM model was also increased to improve prediction accuracy. Sixteen beam elements were

Table 2.8 Measured and Predicted Frequency Results

Configuration	Tested Day	**Predicted Frequency (Hz)**	Support Measured Frequency (Hz)	System Measured Frequency (Hz)	**Adjusted Beam Measured Frequency (Hz)**	% Difference b/w Floorvib and Meas.	SAP Frequency (Hz)	% Difference b/w SAP Predicted and Meas.
CB12x13	14-day	**6.06**	19.25	5.75	**6.03**	0.58%		
CB12x13-Loaded	14-day	**5.44**	17.25	5.25	**5.51**	1.34%		
CB12x13	28-day	**6.10**	19.25	5.75	**6.03**	1.23%	**6.16**	2.24%
CB12x13-Loaded	28-day	**5.48**	17.25	5.25	**5.51**	0.57%		

(a) CB12 x 13 Specimen

Configuration	Tested Day	**Predicted Frequency (Hz)**	System Measured Frequency (Hz)	Support Measured Frequency (Hz)	**Adjusted Beam Measured Frequency (Hz)**	% Difference b/w Floorvib and Meas.	SAP Frequency (Hz)	% Difference b/w SAP Predicted and Meas.
CB15x15/19	14-day	**4.65**	4.50	45.00	**4.52**	2.74%		
CB15x15/19-Loaded	14-day	**4.18**	4.00	26.25	**4.05**	3.18%		
CB15x15/19	28-day	**4.66**	4.50	30.00	**4.55**	1.98%	**4.48**	1.57%
CB15x15/19-Loaded	28-day	**4.19**	4.00	14.25	**4.17**	0.54%		

(b) CB15 x 15/19 Specimen

Configuration	Tested Day	**Predicted Frequency (Hz)**	System Measured Frequency (Hz)	Support Measured Frequency (Hz)	**Adjusted Beam Measured Frequency (Hz)**	% Difference b/w Floorvib and Meas.	SAP Frequency (Hz)	% Difference b/w SAP Predicted and Meas.
CB27x35/50	14-day	**5.09**	4.75	26.25	**4.83**	5.11%		
CB27x35/50-Loaded	14-day	**4.62**	4.50	24.75	**4.58**	0.95%		
CB27x35/50	28-day	**5.17**	4.75	25.00	**4.84**	6.42%	**4.73**	2.23%
CB27x35/50-Loaded	28-day	**4.69**	4.50	26.25	**4.57**	0.05%		

(c) CB27 x 35/50 Specimen

Table 2.8 Measured and Predicted Frequency Results Based on Predicted Section Properties

Configuration	Tested Day	**Predicted Frequency (Hz)**	Support Measured Frequency (Hz)	System Measured Frequency (Hz)	**Adjusted Beam Measured Frequency (Hz)**	% Difference b/w Floorvib and Meas.	SAP Frequency (Hz)	% Difference b/w SAP Predicted and Meas.
CB12x13	14-day	**5.92**	19.25	5.75	**6.03**	1.77%		
CB12x13-Loaded	14-day	**5.31**	17.25	5.25	**5.51**	3.79%		
CB12x13	28-day	**5.96**	19.25	5.75	**6.03**	1.09%	**6.16**	2.24%
CB12x13-Loaded	28-day	**5.34**	17.25	5.25	**5.51**	3.21%		

(d) CB12 x 13 Specimen

Configuration	Tested Day	**Predicted Frequency (Hz)**	System Measured Frequency (Hz)	Support Measured Frequency (Hz)	**Adjusted Beam Measured Frequency (Hz)**	% Difference b/w Floorvib and Meas.	SAP Frequency (Hz)	% Difference b/w SAP Predicted and Meas.
CB15x15/19	14-day	**4.71**	4.50	45.00	**4.52**	3.98%		
CB15x15/19-Loaded	14-day	**4.23**	4.00	26.25	**4.05**	4.32%		
CB15x15/19	28-day	**4.72**	4.50	30.00	**4.55**	3.57%	**4.48**	1.57%
CB15x15/19-Loaded	28-day	**4.24**	4.00	14.25	**4.17**	1.71%		

(e) CB15 x 15/19 Specimen

Configuration	Tested Day	**Predicted Frequency (Hz)**	System Measured Frequency (Hz)	Support Measured Frequency (Hz)	**Adjusted Beam Measured Frequency (Hz)**	% Difference b/w Floorvib and Meas.	SAP Frequency (Hz)	% Difference b/w SAP Predicted and Meas.
CB27x35/50	14-day	**4.99**	4.75	26.25	**4.83**	3.21%		
CB27x35/50-Loaded	14-day	**4.52**	4.50	24.75	**4.58**	1.25%		
CB27x35/50	28-day	**5.07**	4.75	25.00	**4.84**	4.57%	**4.73**	2.23%
CB27x35/50-Loaded	28-day	**4.59**	4.50	26.25	**4.57**	0.49%		

(f) CB27 x 35/50 Specimen

used to model the beam and thirty-two shell elements were used for the concrete slab. The loaded measurements yield the most accurate results in comparison to the AISC Design Guide results for this test.

2.4.3 Conclusions

In general the predicted frequencies were in good agreement with experimental measurements. The AISC Design Guide predictions assumed the measured effective stiffness of the beam was equal to the net section properties. Although the FEM was based on net section properties given by the fabricator, the average percent difference results were only 2.01%, which clearly verifies this assumption. The average deviation of all AISC Design Guide results was 2.75% also confirming the assumption. Each prediction was very accurate, thereby showing that the vibration characteristics of composite castellated beams are a function of its net moment of inertia.

CHAPTER III

EVALUATION OF FLEXURAL STRENGTH OF COMPOSITE CASTELLATED BEAMS

3.1 Test Overview

All three test specimens described in the previous chapter were loaded to failure to evaluate the flexural strength of composite castellated beams. These tests were also conducted at the Virginia Tech Structures and Materials Research Laboratory. Sixteen point loads, eight per beam, were applied to each specimen to simulate a distributed load on each beam. Two three-level spreader beam pyramids were loaded at a single point on the top spreader beam to create the sixteen point loads.

The test beams were designed to fail in flexure at mid-span. Load, mid-span deflection, and slip of the concrete slab with respect to the beam top flange were measured during testing. All measured data was monitored and recorded using a PC-based computerized data acquisition system. The beam specimens were white washed to identify areas of steel yielding. The data obtained from each test was used to determine first yield and ultimate strengths of each specimen.

3.2 Test Set-up & Instrumentation

3.2.1 Loading Apparatus

Two hydraulic ram loads were distributed into sixteen point loads (eight on each beam) by two, three tier, loading pyramids as shown in Figure 3.1. Each pyramid consisted of four W6 x 20 sections on the bottom tier, and two W6 x 25 sections for the middle tier. All beams in the middle and bottom tiers rested on two 1 in. thick plates.

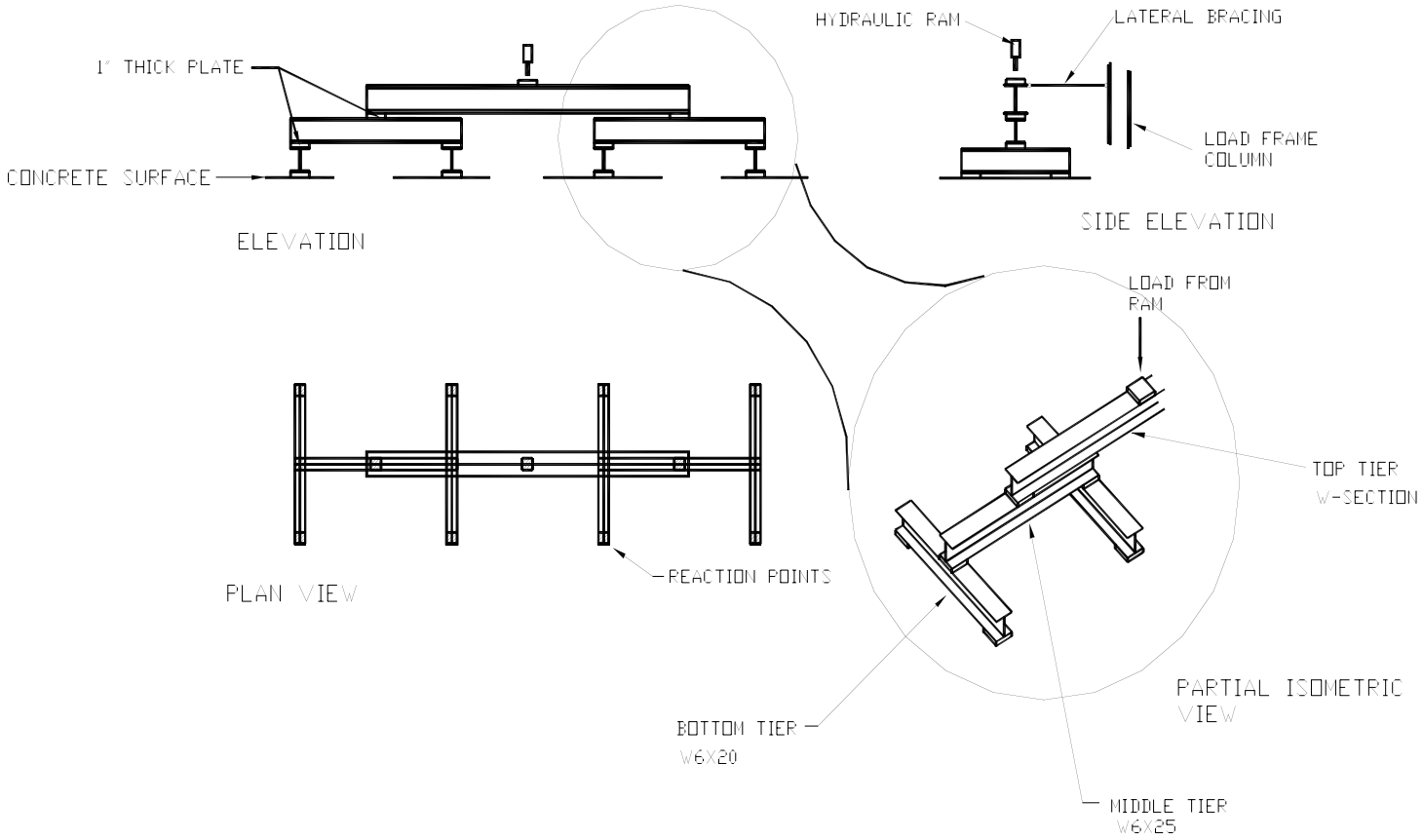

Figure 3.1 Details of Loading Pyramid

Different top tier beams were used for each test to compensate for the variation in spacing and ram loads. Load cells between the hydraulic rams and the loading pyramids were used to measure applied loads to the top spreader beams. Ram loads were applied to the mid-span of the top spreader beam, which in turn applied to the mid-span of the middle spreader beams. The load applied to mid-span of middle tier beam is then distributed to bottom tier beams through it's reactions. The end reactions of the bottom level beams provide point loads to the concrete slab. The top level beam of both pyramids was laterally braced at quarter points to provide additional stability.

Figure 3.2 Test Set-up Photo

3.2.2 CB 12 x 13 Test Set-up

The CB12 x 13 specimen was the first of three tests to failure conducted for this study. The loading apparatus was laid out as shown in Figure 3.3. A W8 x 30 hot-rolled section was used for top spreader beam. Two hydraulic rams were used to apply load at the top of the spreader beams as shown in Figure 3.3.

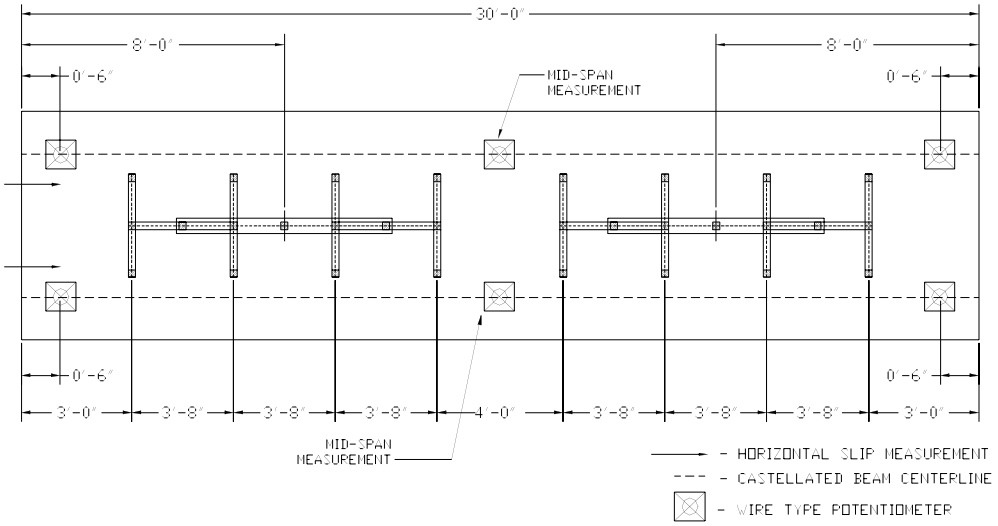

Figure 3.3 CB12 x 13 Load Apparatus Spacing

Wire type potentiometers were used to measure vertical deflection at supports and mid-span of each beam. Two of the six potentiometers were placed at mid-span of each beam and the other four were put 6 in. inboard from each support as shown in Figure 3.3. Linear displacement transducers were used to measure horizontal slip between the concrete slab and the top flange of the beams at one support end. Several holes were cut through the deck rib closest to the support to provide a connection between the concrete slab and the transducer clamped to the top flange of the beam. This measurement provided the relative movement between the concrete slab and the beam.

3.3.3 CB 15 x 15/19 Set-up

This test was very similar to the CB 12 x 13 test and was also loaded with two pyramid spreader beam arrangements. A W12 x 53 section was used as the top spreader beam to resist the increased ram load predicted for this test. The bottom spreader beam spacing for this test was adjusted to account for the change in span length as illustrated in Figure 3.4.

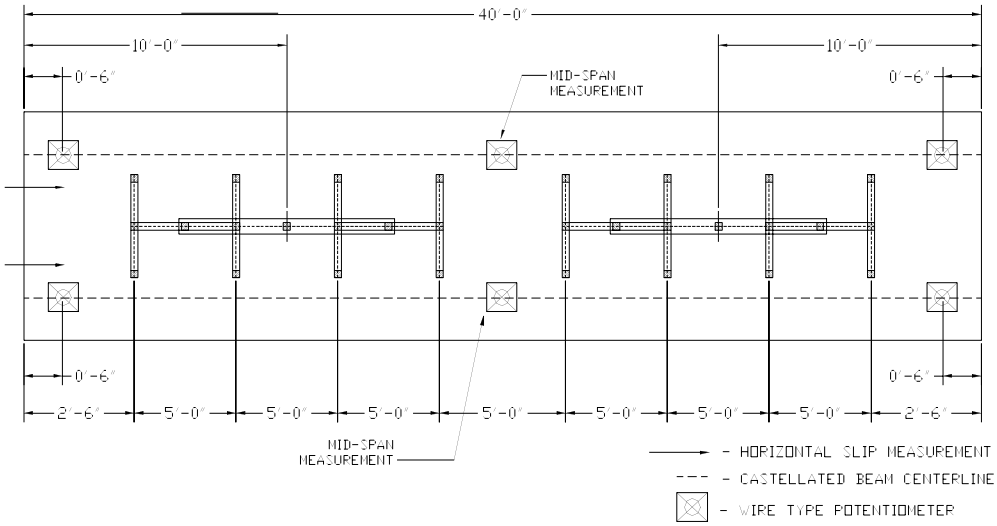

Figure 3.4 CB15 x 15/19 Load Apparatus Spacing

The same wire type potentiometers were used to measure support and mid-span deflections as shown in Figure 3.4. Slip between the concrete slab and the top flange of the test beam was measured in the same manner as for the previous CB 12 x 13 test.

3.3.4 CB 27 x 35/50 Test Set-up

The CB27 x 35/50 specimen had the longest span tested in this study requiring the bottom spreader beams to be spaced farther apart as shown in Figure 3.5. The same top tier spreader beam used in CB15 x 15/19 test was used in this test. Concrete slip, mid-

span, and support deflections were measured in the same way as for the previous tests. Deflection measurement locations for this test are shown in Figure 3.5.

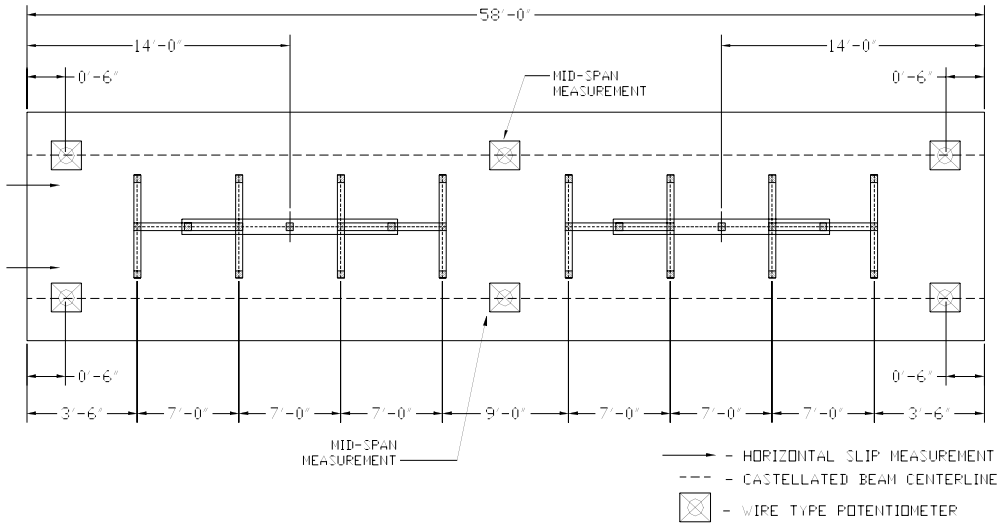

Figure 3.5 CB27 x 35/50 Load Apparatus Spacing

3.3 Testing Procedures

Each specimen was first pre-loaded by applying 10 % of the predicted failure load in three step increments and then unloaded. This was done to insure that all load apparatus, hydraulic rams, and instrumentation were working properly and all components were seated. Once the initial pre-load was complete, each specimen was loaded in proportional increments depending on the predicted failure load until first yielding occurred. The area of first yield is illustrated in Figure 3.6, by the first changes in slope of the load verses deflection curve. Once the curve began to reach it's yield plateau, the specimen was again unloaded. Load was then reapplied until the prior load was reached, also shown in Figure 3.6. The specimens were also unloaded several more

times to plum the hydraulic rams to prevent damage because of the large vertical deflection of the specimen. After significant yielding accured, loading was controlled by mid-span deflection increments.

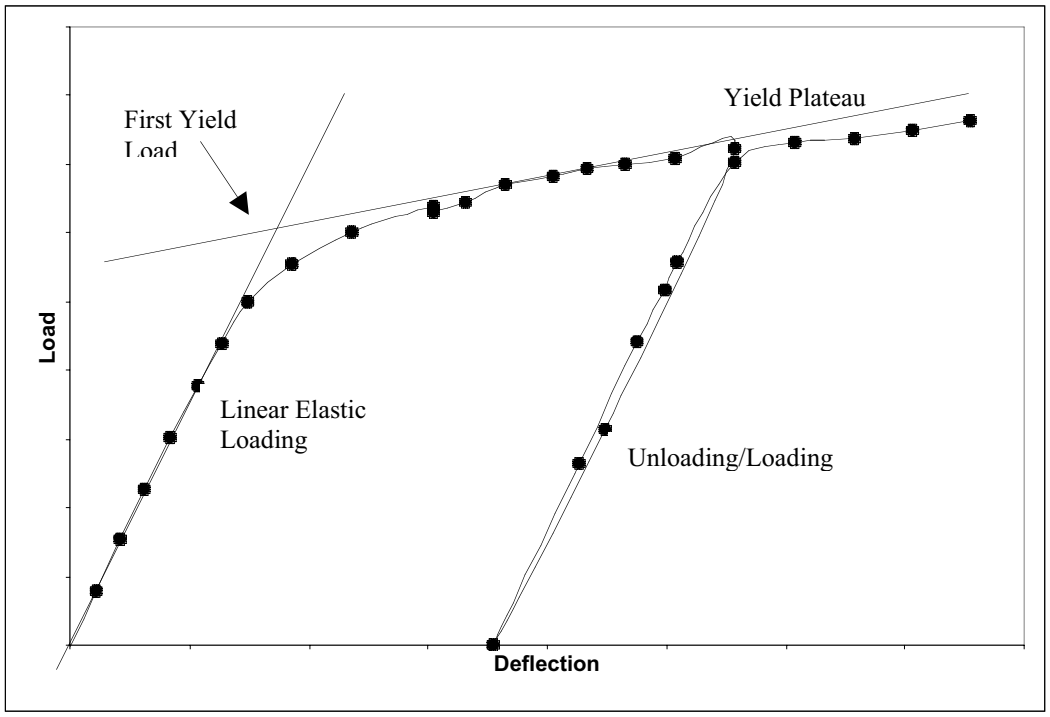

Figure 3.6 Test Procedure Curve

3.4 Supplemental Tests and Materials

Concrete cylinders were used to determine compressive strength of the concrete. Each cylinder had a 4 in. diameter and was broken the day of the specimen test. Ultimate loads and strength for each cylinder test are shown in Table 3.1.

Table 3.1 **Measured Concrete**

SPECIMEN	Load (kips)	f'_c (ksi)
CB12 x 13	37.7	3.00
CB15 x 15/19	47.0	3.74
CB27 x 35 50	41.5	3.30

Upon the completion of the failure test standard ASTM steel coupons were cut from the top and bottom flanges near the supports of each specimen to determine yield and ultimate strength of the steel. Results are summarized in Table 3.2.

Table 3.2 Steel Yield and Ultimate Yield

SPECIMEN	Elongation %	Yield (ksi)	Ultimate (ksi)
CB12 x 13	28.5	53.0	74.0
CB15 x 15/19	28.0	53.0	67.0
CB27 x 35/50	26.0	55.0	73.0

3.5 Full Specimen Test Results

The yield load for each specimen was determined as shown in Figure 3.6. With this value and the maximum applied load, the yield and maximum applied moment was determined. The moment due to the dead weight of loading pyramid, concrete, beam and metal decking weight were subtracted from the predicted moment strengths of each specimen. The resulting values are compared to the applied yield and ultimate loads from each test. Test summaries are found in Appendices C through E. Each test summary provides the theoretical and applied hydraulic ram loads, and the equivalent maximum moments.

3.5.1 CB 12 x 13 Test Results

This was the first specimen tested in this study. Figure 3.6 shows that the north and south beam net deflections were approximately equal throughout this test. Both beams behaved linearly until the applied load was approximately 18 kips, which is equivalent to 72 ft-kips. The net deflections in the linear range corresponded closely to the predicted values shown in Figure 3.7. The yield load was reached at an applied moment of about 80 kips-ft. This is defined by the intersection of the linear elastic portion and yield plateau tangents of Figure 3.7. The maximum applied moment for each beam was 113.8 kip-ft. at a deflection of 9.22 in.

Figure 3.7 shows the applied moment verses slip deflection plot for CB12 x 13 test. The slip between the concrete slab and beams did not behave linearly. The difference in maximum slip defections of each beam shows that both slipped independently of one another. The maximum south and north slip deflections were 0.193 and 0.217 in respectively.

Visual observations during the test included yield lines in the white wash at the corners of web opening at the supports as shown in Figure 3.9 just before the yield load was reached. This was an obvious sign of vierendeel bending. Identical lines were found at mid-span openings and formed at the same time as yield the load was reached. Yield underneath the bottom flanges were also found at yield load. These yield lines expanded away from the centerline of beam to the supports as more load was applied. A small amount of lateral sway of the entire specimen was notice toward the end of test.

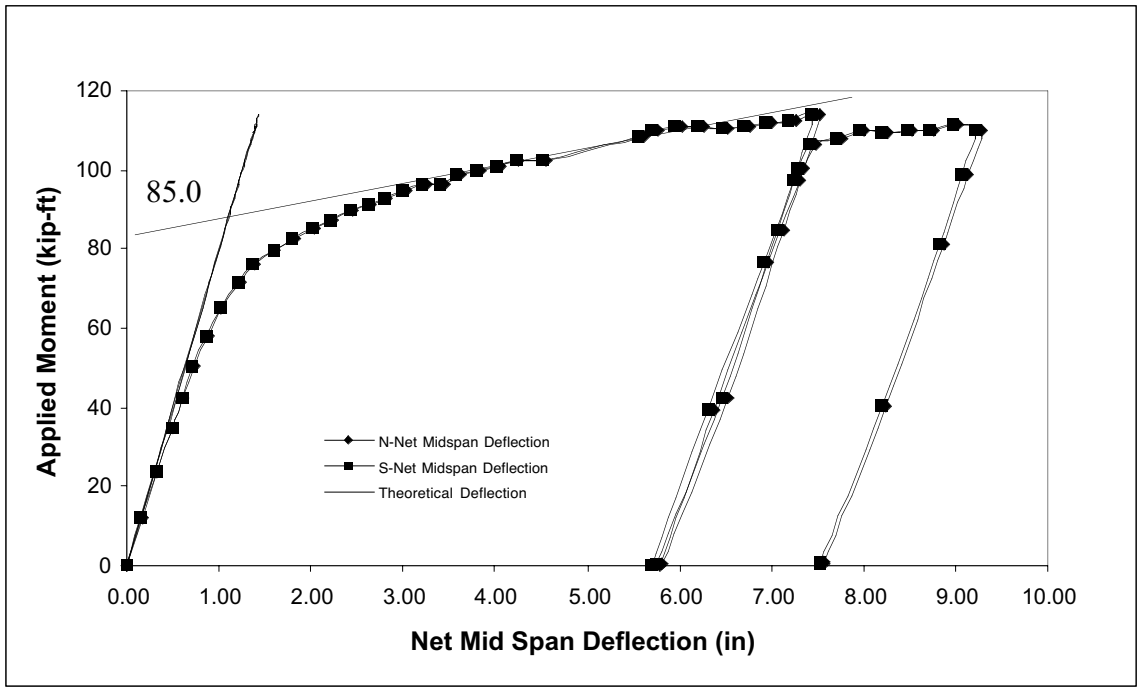

Figure 3.7 CB12 x 13 Load vs. Mid Span Deflection Plot

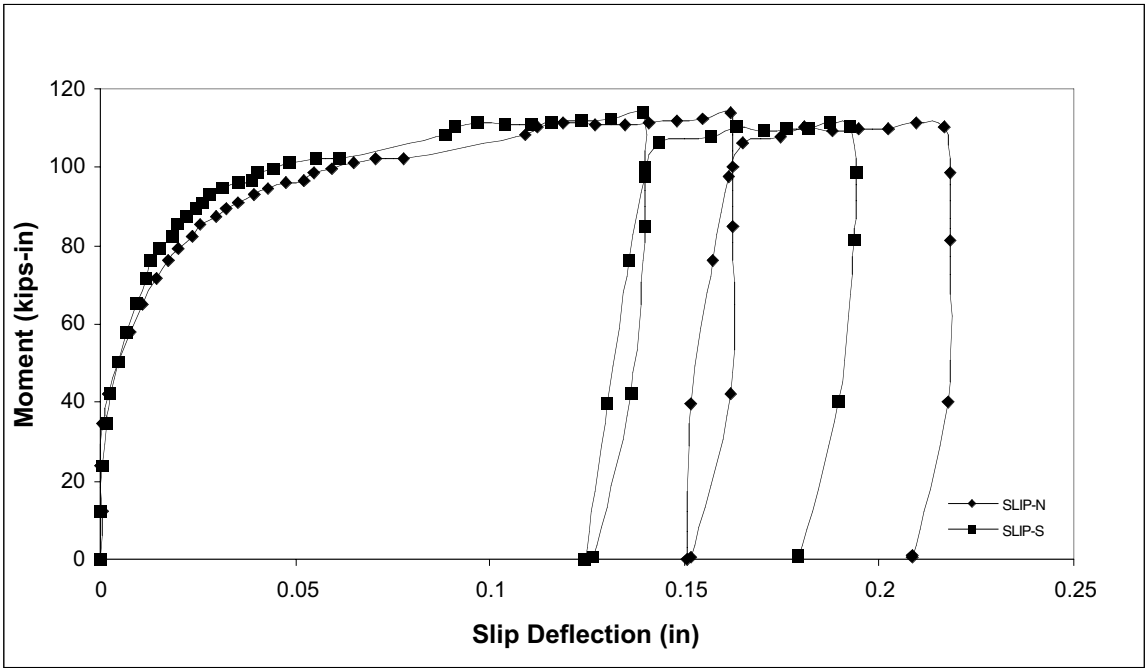

Figure 3.8 CB12 x 13 Load vs. Slip Deflection Plot

The CB12 x 13 specimen flexural test was stopped because of an excessive mid-span deflection of 9.22 in. At this defection the load remained roughly constant as mid span deflection was increased as shown in Figure 3.7.

Figure 3.9 Vierendeel Bending White Wash Lines in CB12 x 13 Test

3.5.2 CB15 x 15/19 Test Results

The CB15 x 15/19 specimen behaved similar to the CB12 x 13 test. The net deflections for both beams were nearly equal, with the exception of two data points toward the end of test, as shown in Figure 3.8. Both beam deflections were linear until a load of 20 kips was applied, which is equivalent to a moment of 100 kip-ft. The deflections in the linear range compared closely with calculated theoretical values. The applied yield moment for this test was 117.0 kip-ft for each beam. The maximum applied moment for each beam was 160.0 kip-ft. as a deflection of 12.1 in.

The slip deflection measurements for this specimen were also similar to the CB12 x 13 test and are shown in Figure 3.9. The maximum slip deflections for the north and south beams were 0.189 and 0.211 in. respectively.

The first yield lines were noticed at the mid-span web post when 20 kips was applied to each load pyramid. These lines expanded from the mid span toward supports as shown in Figure 3.12. Vierendeel bending was also noticed at web openings closest to the support, as well as, diagonal streaks through the white wash underneath bottom flange as shown in Figure 3.13.

This specimen reached a mid-span deflection of 12.1 in and was stopped because of an excessive mid-span deflection. When the test was stopped the load remained roughly constant as deflection increased.

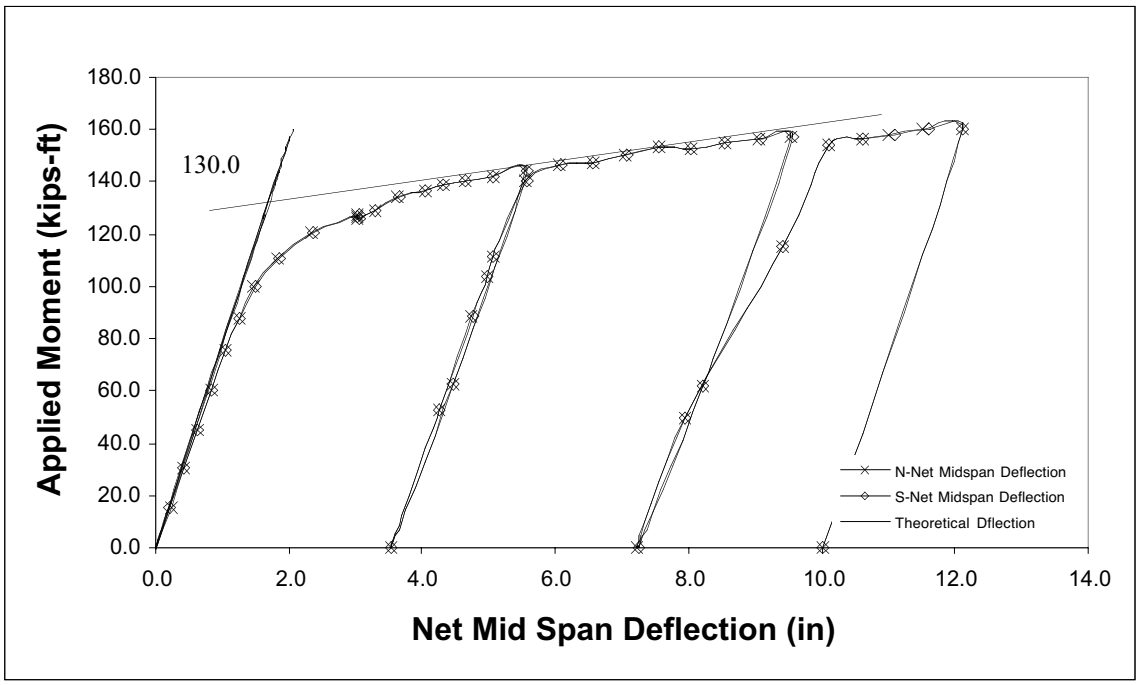

Figure 3.10 CB15 x 15/19 Load vs. Mid Span Deflection Plot

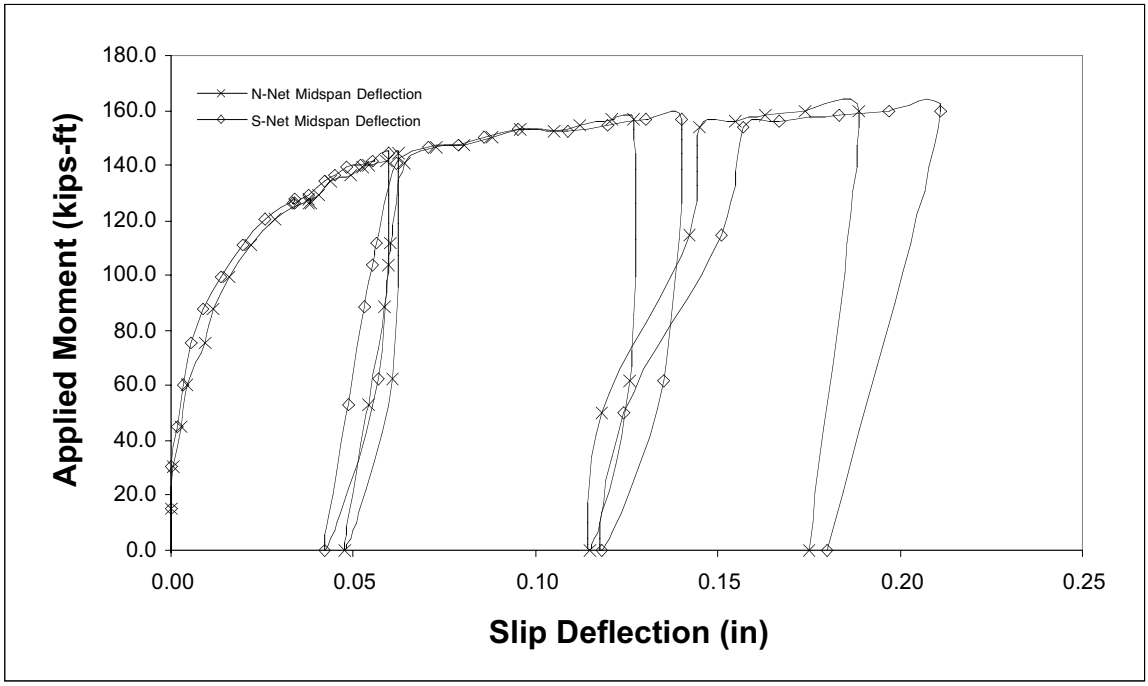

Figure 3.11 CB15 x 15/19 Load vs. Slip Deflection Plot

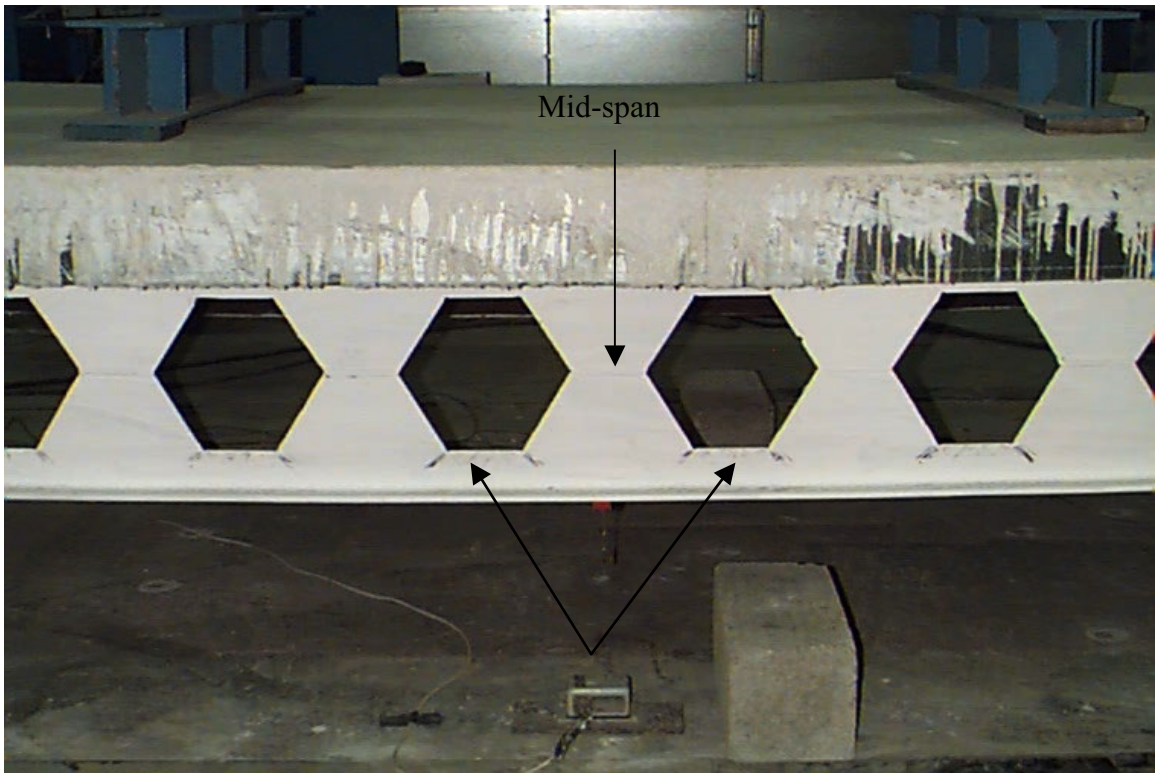

Figure 3.12 Flexural Bending White Wash Lines During CB15 x 15/19 Test

Figure 3.13 Diagonal Streaks on Bottom Flange During CB15 x 15/19 Test

3.5.3 CB27 x 35/50 Results

The north and south beam deflections for the CB27 x 35/50 specimen were nearly identical as shown in Figure 3.14. Linear behavior was observed until 62.9 kips was applied. This is equivalent to an applied moment of 450 kip-ft. The yield load applied by each ram was 85.7 kips, which is equivalent to an applied moment of 600.0 kip-ft. Both beams reached a maximum applied moment of 640.0 kip-ft.

The measured slip defection for this test was significantly higher than the previous tests. In Figure 3.15, the differences in maximum deflections indicates both beams slipped independently of each other. Maximum slip deflections for the north and south beams were 0.497 and 0.378 in., respectively.

The first yield lines were noticed at the web opening closest to the supports which is an area of high shear. These yield lines expanded from the support opening to mid-span shown in Figure 3.16. Vierendeel bending was most prominent in this specimen because of shear deformations due to both beams low span to depth ratio. Yielding at the corners of mid-span holes and bottom flange was observed shortly after the yield load was reached as shown in Figure 3.17. Three transverse cracks were found near the mid-span of concrete slab toward the end of test.

The CB27 x 35/50 test was stopped at a load of 91.43 kips. This corresponds to a maximum deflection of 10.1 in. which the caused test to be terminated.

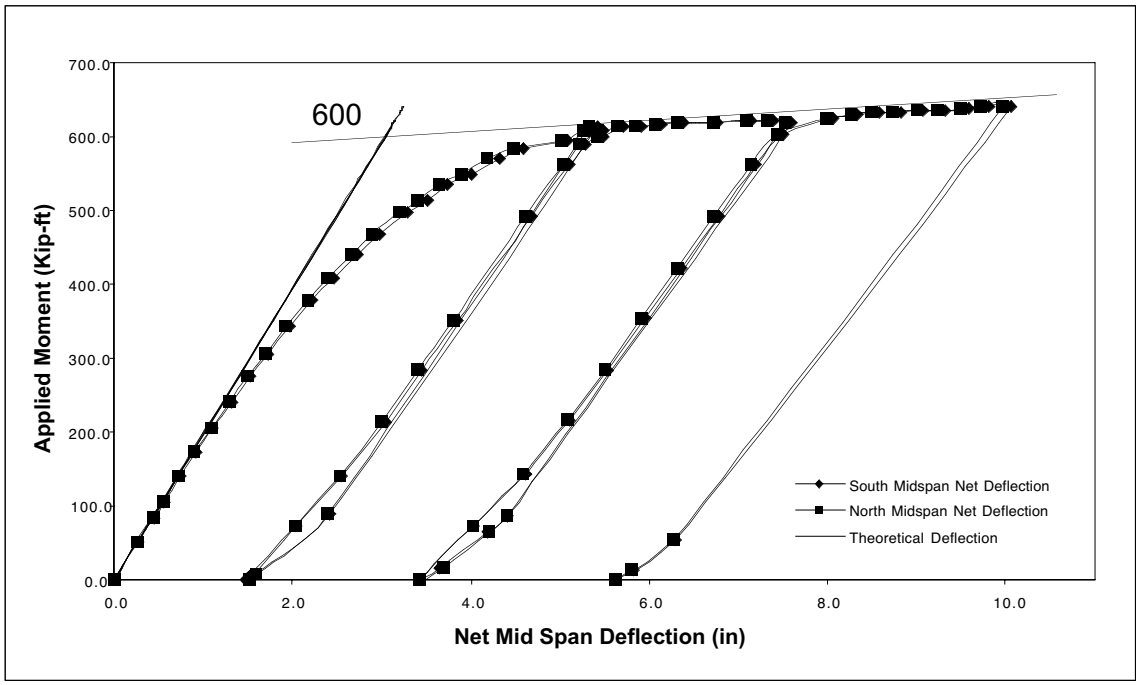

Figure 3.14 CB27 x 35/50 Load vs. Mid Span Deflection Plot

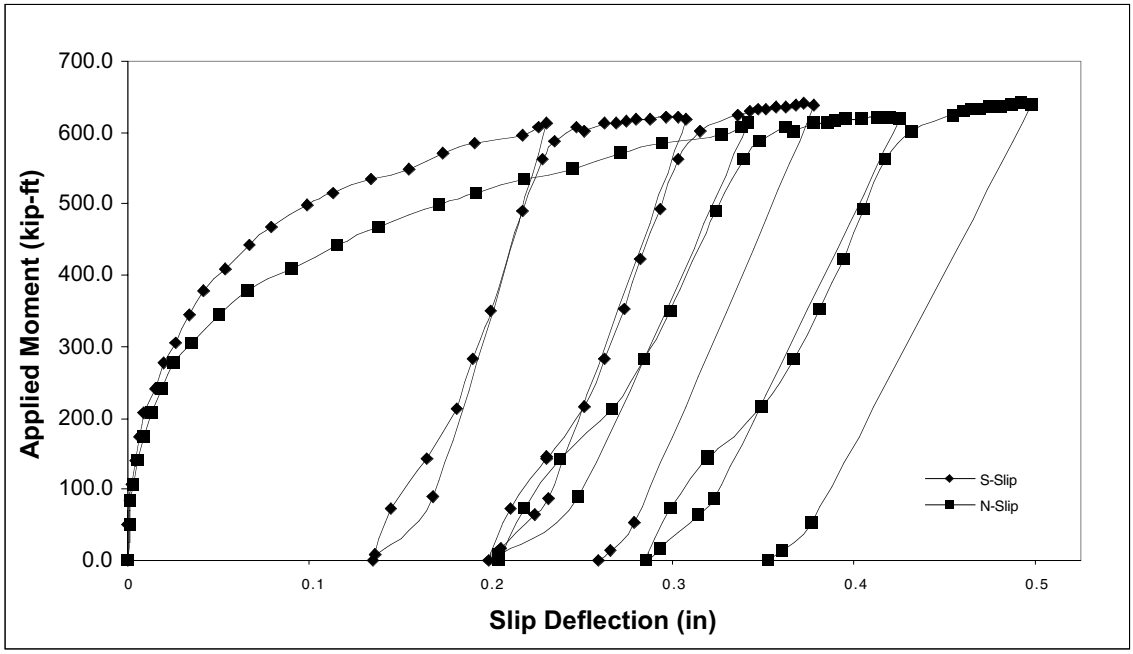

Figure 3.15 CB27 x 35/50 Load vs. Slip Deflection Plot

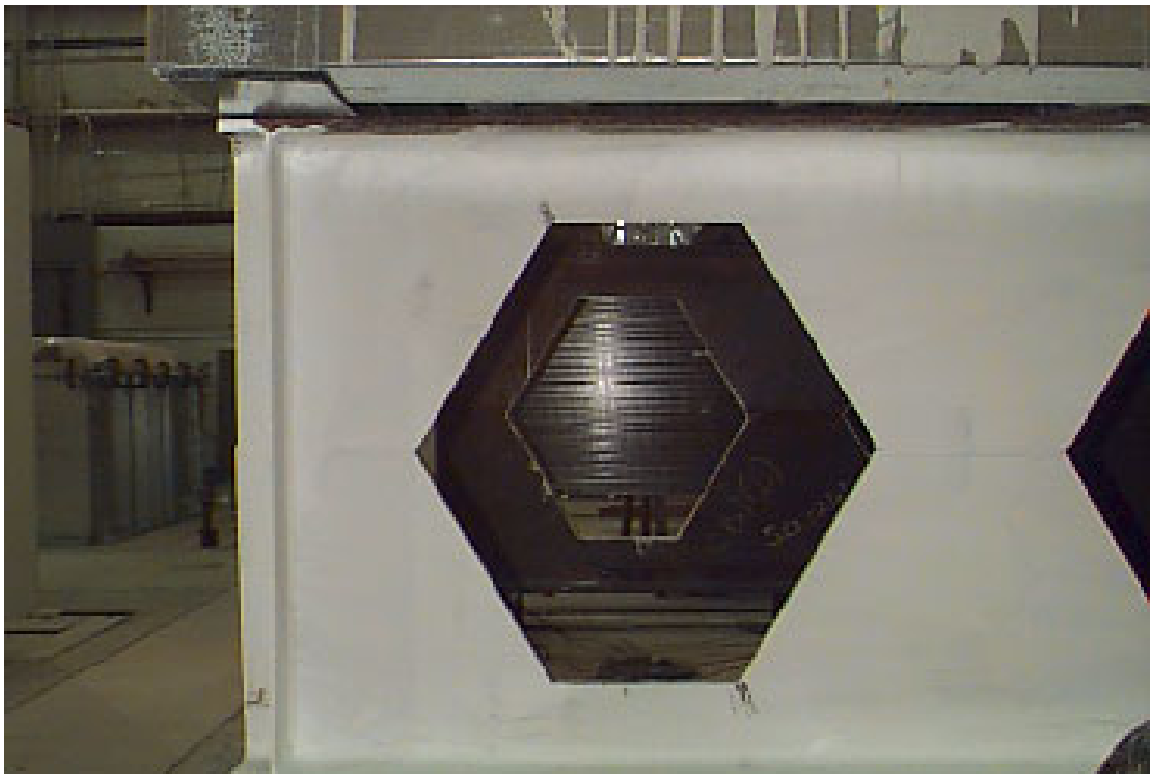

Figure 3.16 Vierendeel Bending at Support During CB27 x 35/50 Test

Figure 3.17 Flexural Bending at Mid-Span During CB27 x 35/50 Test

3.6 Evaluation of Test Results

The predicted yield moment was based on the moment produced by the weight of the beam sections, concrete, and metal decking acting on the non-composite section, and the weight of the loading pyramid and applied load acting on the composite section. The composite and non-composite section modulus were used to predict the applied yield moment from

$$\sigma_y = \frac{M_C + M_D}{S_n} + \frac{M_L}{S_c} + \frac{M_{y,applied}}{S_c} \qquad (3.1)$$

where σ_y = measured yield stress of the beam steel, M_c = calculated moment due to concrete, and metal deck weights, M_D = calculated moment due to beam weight, M_L = calculated moment from weight of loading pyramid, S_n = measures net section modulus of non-composite castellated beam, S_c = measured net composite section modulus of the castellated test beam, and $M_{y,\ applied}$ = unknown applied yield moment calculated from the equation.

Predicted ultimate strengths were calculated by determining the bending moment developed by the resultant of the compression and tension forces as shown in Figure 3.12. The entire CB12 x 13, and CB15 x 15/19 beams were in tension as shown in Figure 3.12(a). The CB27 x 35/50 moment calculations resulted in a portion of the top flange to be in compression as shown in Figure 3.18(b).

The corresponding hydraulic ram loads were developed by using simple statics.

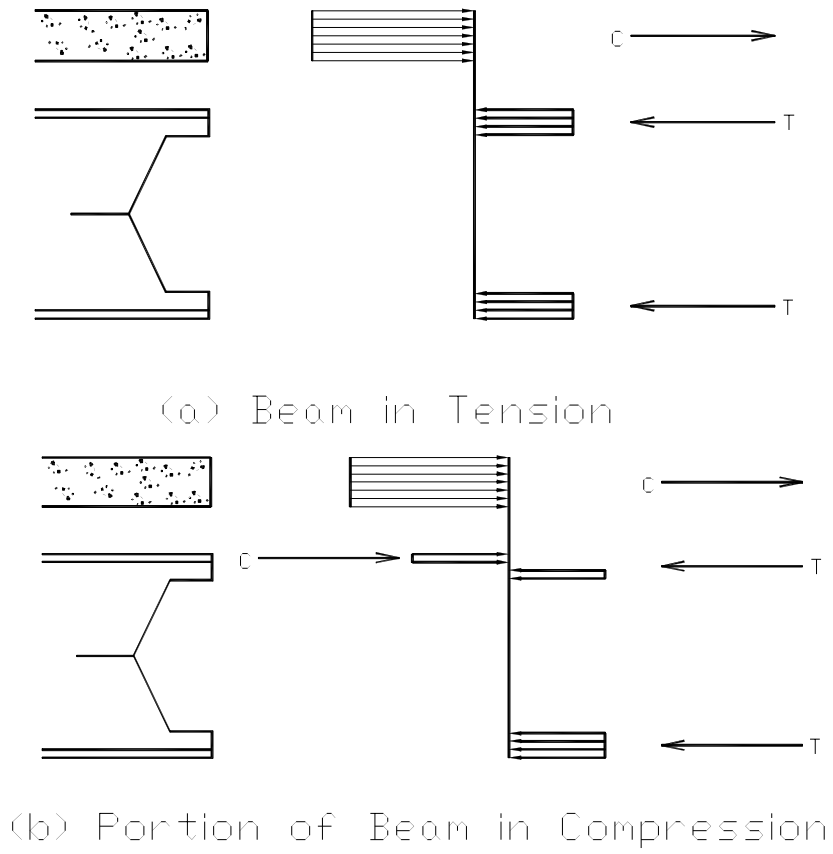

Figure 3.18 Calculated Couple Strength Diagram

3.6.1 Yield Load Evaluations

The overall behavior of each test specimens was similar. This is clearly shown in the three load-deflection plots in Figures 3.6 through 3.11. Each curve has two distinct regions of first elastic and then plastic behavior. Located somewhere in between these two regions is the yield load. The yield load is defined as the intersection of each region's tangent line as shown in Figures 3.7, 3.10, and 3.15, and are listed in Table 3.3. In Table 3.3 M_{exp} = Maximum applied moment, and M_y = Calculated moment at yield load using equation (3.1) and actual material properties.

The experiential yield load values were all higher than those predicted for the CB12 x 13 and CB15 x 15/19 tests. The ratio of M_{exp}/M_y found in last column of Table

3.3 shows a value lower than 1.0 for the CB27 x 35/50 test, indicating the specimen yielded at a lower load than predicted. The average ratio of all specimens was is 0.98.

Table 3.3 **Experimental and Predicted Yield Load Results**

SPECIMEN	EXPERIMENTAL YIELD LOAD		PREDICTED YIELD LOAD		M_{exp}/M_y
	SINGLE RAM LOAD (kips)	EQIVALENT MAXIMUM MOMENT (kip-ft)	SINGLE RAM LOAD (kips)	EQIVALENT MAXIMUM MOMENT (kip-ft)	
CB12 x 13	18.0	72.0	16.7	66.7	1.08
CB15 x 15/19	26.0	130.0	22.4	126.4	1.03
CB27 x 35/50	85.7	600.0	105.5	738.5	0.81

The bottom flange and mid-span web opening were locations where yielding was most prominent for the CB12 x 13 and CB15 x 15/19 specimens. Veirendeel bending at web openings closest to the supports was the most obvious observed yielding for the CB27 x 35/50 specimen. The observed first yielding as indicated by flaking whitewash for the CB12 x 13 and CB15 x 15/19 specimens corresponded closely with experiential yield loads. All yield strength calculations for each test are shown in Appendices C through E.

3.6.2 Ultimate Load Evaluations

The predicted ultimate strength of each specimen was calculated as described in Section 3.6. The predicted and experimental results for all tests are listed in Table 3.4. In Table 3.4, M_{exp} = Maximum applied moment, and M_p = Calculated plastic moment using measured material properties. The plastic moment, M_p, calculations were based on partial composite action. All predicted values were calculated using two different shear reduction factor (SRF) assumptions. Columns four and six are the predicted ultimate applied moments using a shear reduction factor of 0.75, and 1.0, respectively.

Table 3.4 **Experimental and Predicted Ultimate Load Results**

SPECIMEN	EXPERIMENTAL ULTIMATE LOAD		PREDICTED ULTIMATE LOAD			
	SINGLE RAM LOAD (kips)	EQIVALENT MAXIMUM MOMENT (kip-ft)	SRF=0.75		SRF=1.0	
			ULTIMATE MOMENT (kip-ft)	M_{exp}/M_p	ULTIMATE MOMENT (kip-ft)	M_{exp}/M_p
CB12 x 13	28.4	113.8	89.0	1.28	125.8	0.90
CB15 x 15/19	32.0	160.0	77.2	2.07	118.4	1.35
CB27 x 35/50	91.4	640.0	637.2	1.00	664.8	0.96

All tests were stopped because of excessive deflection in each test. The general maximum deflection limit for serviceability is L/360. The serviceability limits for all tests are found in Table 3.5. For the SRF = 0.75 prediction each specimens' ultimate experimental load was greater than or equal to its predicted value. The ratios in the last column of Table 3.4 are for the SRF = 1.0 prediction. Only the CB15 x 15/19 test resulted in a value greater than 1.0 for this prediction. Although several M_{exp}/M_p ratios were less than 1.0 the average of all values for both SRF predictions are 1.26. In general the SRF = 1.0 result are somewhat inconsistent with the exception of the CB15 x 15/19 test, which yielded a ratio greater than 1.0 for both SRF factors. All ultimate strength calculation for each test are shown in Appendices C through E.

Table 3.5 **Test Deflection Limits**

SPECIMEN	SPAN/360 (in)	MAXIMUM DEFLECTION (in)
CB12 x 13	1.00	9.22
CB15 x 15/19	1.33	12.10
CB27 x 35/50	1.93	10.10

CHAPTER IV

SUMMARY, CONCLUSION AND RECOMMENDATIONS

4.1 Summary

The purpose of this study was to evaluate the vibration and flexural strength characteristics of castellated beams. Three full-scale tests were performed. Since vibration is a function of stiffness, static load tests were conducted to verify the non-composite and composite moments of inertia for each specimen. Vibration measurements were taken at the mid-span and all four supports of each specimen. The measurements were taken using an accelerometer and a handheld FFT analyzer. The support frequencies were filtered out of the mid-span measurements to obtain an adjusted beam frequency using Dunkerly's equation. These adjusted results were compared to predicted frequencies using the procedures in the AISC Design Guide (Murray, Allen, and Ungar 1997) and with the finite element method.

The three specimens were then loaded to failure to evaluate their flexural strength. Applied load, and support and mid-span deflections were measured during tests. The resulting data was analyzed to determine the first yield and ultimate strength of each composite beam using load verses net deflection plots. Predicted values were then compared to those found from the testing.

4.2 Conclusions

From the test and analysis results of this study, the following conclusions can be reasonably drawn:

1. The AISC Design Guide procedures for composite prismatic beams can be used for determining predicted natural frequency of composite castellated beams.

2. The composite moment of inertia of castellated beams should be calculated using the net moment of the castellated beam section as found in manufacturer's catalogs.

3. The net castellated beam section properties should be used to calculate the flexural strength of castellated beams.

4. The SRF = 0.75 can yield smaller horizontal shear values for composite sections.

4.3 Areas of Further Research

Though the analysis of test data the following area requires further in investigation.

1. The non-composite stiffness characteristics tested in this study found the measured stiffness is closer to the gross moment of inertia for deeper beams and is closer to the net for sallower beams. This should be confirmed through additional static testing of non-composite castellated beams.
2. The results for both Shear reduction factors predictions were rather inconsistent for the CB12 x 13 and CB27 x 35/50 tests. Both test resulted in lower experimental values than predicted for one of the two SRF predictions. This should be studied further through additional composite failure tests.

REFERENCE LIST

AISC (1999) "Load and Resistance Factor Design Specification for Structural Steel Buildings" AISC, Inc., Dec. 27, pp 40-48

Baldwin, W. and Douty R.T. (1966) "Measured and Computed Stresses in Three Castellated Beams" *AISC Engineering Journal*, Jan. pp 15-18

Beavers, T.A. (1998). "Fundamental Natural Frequency of Steel Joist Supported Floors" M.S. Thesis, Virginia Polytechnic Institute and State University, Blacksburg, Virginia.

Boyer J. P. (1964). "Castellated Beams – New Developments" *AISC Engineering Journal,* 2nd qtr, pp 104-108.

Dougherty, B.K. (1993). "Castellated Beams: A State of the Art Report" *Journal of the South African Institution of Civil Engineering,* 2nd qtr. pp 12-20.

Giriyappa, J., and Baldwin, J.W. (1966). "Behavior of Composite Castellated Hybrid Beams" University of Missouri Engineering Experimental Research Station, Columbia, MO.

Kerdal, D., and Nethercot, D.A. (1984). "Failure Modes for Castellated Beams" J. Construct. Steel Research, 4th qtr. pp 295-315.

Knowles, P.R. (1991). "Castellated Beams*" Proc. Instn. Civ. Engrs, Part 1,* No. 90, pp 521-536.

Larnach, J. W., and Park R. (1964). "The Behavior under Load of Six Castellated Composite T-beams" *Civil Engineering and Public Works*, No. 69, pp 339-343

Lenzen, K.H. (1966). "Vibration of Steel Joist Concrete Slab Floors." Engineering Journal, AISC, 2(3), pp 133-136.

Megharief, J.D. (1997). "Behavior of Composite Castellated Beams" M.S. Thesis, McGill University, Montreal Canada.

Murray, T.M. (1975) "Design to Prevent Floor Vibrations." *Engineering Journal*, AISC, 28(3), pp 102-109

Murray, T.M. (1981) "Acceptability Criteria for Occupant-Induced Floor Vibrations." Engineering Journal, AISC, 18(2), pp 62-69.

Murray, T.M. (1991) "Building Floor Vibrations." *Engineering Journal*, AISC, 28(3), pp 82-87.

Murray, T.M. Allen, D.E. (1993). "Design Criterion for Vibrations Due to Walking." Engineering Journal, AISC, 4th qtr. pp 117-129.

Murray, T.M. Allen, D.E. and Ungar, E. E. (1997). *AISC Steel Design Guide Series 11: Floor Vibrations Due to Human Activity*. American Institute of Steel Construction, Chicago.

Ohmart, R. D. (1968). "An Approximate Method for the Response of Stiffened Plates to a Periodic Excitation." Studies in Engineering Mechanics, Report No. 30, The University of Kansas Center of Research in Engineering Sciences, Lawrence, Kansas.

Reiher, H. and Meister, F.J. (1931). "The Effect of Vibration on People" (in German). *Forchung auf dem Gebetite des Ingenieurwesens*, 2(2), p. 381. (Translation: Report no. F-TS-616-Re H.Q. Air Material Command, Wrigh Field, Ohio, 1949).

Toprac, A. A. and Cooke (1959). "An Experimental investigation of Open-Web beams" *Welding Research Council Bulletin Series*, No. 47, New York

Treadgold, T. (1828). *Elementary Principles of Carpentry*, 2nd Ed., Publisher unknown

United Steel Companies. (1960). *Properties and Strengths of Castella Beams. Deflection Characteristics*. United Steel Companies Research and Development, Rotherham, Aug. report.

Watson, J., O'Neil, R., Barnoff, R., and Mead, E. (1974) "Composite Action Without Shear Connectors" *AISC Engineering Journal*, 2nd qtr. pp 29-33

APPENDIX A

COMPOSITE MOMENT OF INERTIA AND FREQUENCY CALCULATION EXAMPLES

A.1 Example of Transformed Moment of Inertia Calculations

The following procedure is an example of the calculations used to predict the moment of inertia values in section 2.3.4. All predictions are based on 100% composite action as recommended by the AISC Design Guide Series 11 (Murray and Allen1999).

Given:

Beam Properties:

Span = 30 ft

Depth = 11.50 in

$A_{(net)}$ = 3.03 in^3

y = 5.74 in. (from bottom flange)

$I_{(net)}$ = 85.32 in^4

Slab Dimensions:

Measured f_c' = 3000 psi

Effective width = 42 in.

Slab depth = 6.25 in.

Deck Dimensions:

h_r = 3.0 in

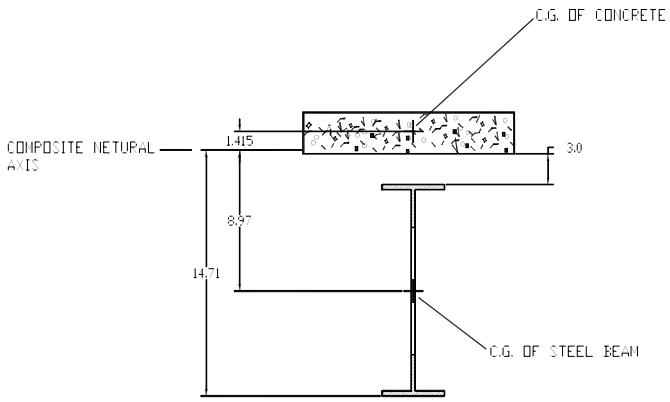

Concrete modulus

$$E_c = W^{1.5}\sqrt{f'_c}$$

$$E_c = 145^{1.5}\sqrt{3} = 3024 \text{ ksi}$$

$$n = \frac{E_s}{1.35 \times E_c} = \frac{29000}{1.35 \times 3024.21} = 7.10$$

where $1.35E_c$ is the dynamic concrete modulus of elasticity

Transformed effective width

$$b_{eff} = \frac{42}{7.10} = 5.92 \text{ in}$$

$$y = \frac{Ay}{A_{tot}} = \frac{3.03(5.74) + 5.92(3.25)16.12}{3.03 + 5.92(3.25)} = 14.71 \text{ in} \qquad \text{(from bottom flange)}$$

Net moment of inertia

$$I_{net} = \sum \frac{bh^3}{12} + Ad^2$$

$$I_{net} = \frac{5.92(3.25)^3}{12} + 3.25(5.92)(1.415)^2 + 83.32 + 3.03(8.97)^2 = 382.8 \text{ in}^4$$

A.2 Example of Frequency Calculations

The following procedure is an example of the calculations used to predict the natural frequency values in section 2.4.2. This prediction is based on the loaded situation for the CB12 x 13 castellated beam.

Given:

Loading Data:

Concrete slab = 145 pcf
Metal Decking = 1.87 psf
Live load = 11.0 psf
Dead load = 4.0 psf
Beam weight = 13.0 plf

Beam Properties:

Span = 30 ft
$I_{tr(net)}$ = 411.6 in^4 (measured)

Slab Dimensions:

Effective width = 42 in.
Depth = 6.25 in.
Effective depth = 4.75
f_c' = 3000 psi (measured)

Deck Dimensions:

h_r = 3.0 in

Total loading weight

Concrete slab $= 145 \, {lb}/{ft^3} \times \frac{4.75}{12} \times \frac{42}{12} = 200.8$ lb/ft

Metal Decking $= 1.87 \, {lb}/{ft^2} \times \frac{42}{12} = 6.55$ lb/ft

Live load $= 11.0 \, {lb}/{ft^2} \times \frac{42}{12} = 38.5$ lb/ft

Dead load $= 4.0 \, {lb}/{ft^2} \times \frac{42}{12} = 14.0$ lb/ft

Beam weight = 13.0 lb/ft

Total weight = 272.88 lb/ft

Beam deflection

$$\Delta = \frac{5wL^4}{384EI_{tr}} = \frac{5 \times 272.88 \times 30^4 \times 1728}{384 \times 29000 \times 411.6 \times 1000} = 0.417 \text{ in.}$$

Beam natural frequency

$$f_n = 0.18 \times \sqrt{\frac{g}{\Delta}} = 0.18 \times \sqrt{\frac{386}{0.417}} = 5.48 \text{ Hz}$$

APPENDIX B

FREQUENCY TEST AND PREDICTION DATA

B.1 CB12 x 13 Summary and Description of Specimen

The CB12 x 13 specimen was a symmetric section with identical top and bottom tee-section properties. It was cut from a W8 x 13 hot rolled section and spanned 30 ft between each support. Figure B.1 shows the concrete and beam dimensions as found in Table B.1 and the manufactures' catalog. The calculated and experimental frequency results for the specimen are listed in Tables B.1 and B.2, respectively.

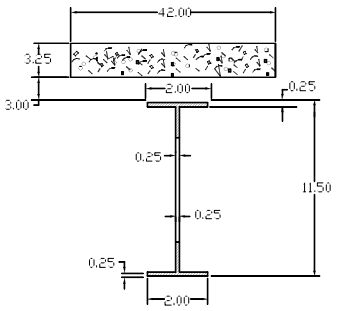

Figure B.1 Cross-section Dimensions

Table B.1 Nominal Beam Properties

CB12 X 13	
Root Top	W8 x 13
Root Bottom	W8 x 13
Weight (plf)	13.00
A_S (net)	3.03
A_S (gross)	4.64
I_x (net)	85.32
I_x (gross)	91.84
S_x net bottom	14.86
S_x net top	16.00

Table B.2 Vibration Analysis Parameters

LOADING	w (plf)	Δ (νι)	I_{tr} (in^4)
Loaded	272.8	0.417	383.8
Unloaded	220.3	0.337	

Table B.3 Vibration Results

Measurement	Frequency (Hz)	
	Unloaded	Loaded
Mid-span	5.75	5.25
Avg. Support	19.25	17.25
Corrected Mid-span	6.03	5.51
Predicted	6.10	5.48
% Difference	1.09%	3.21%

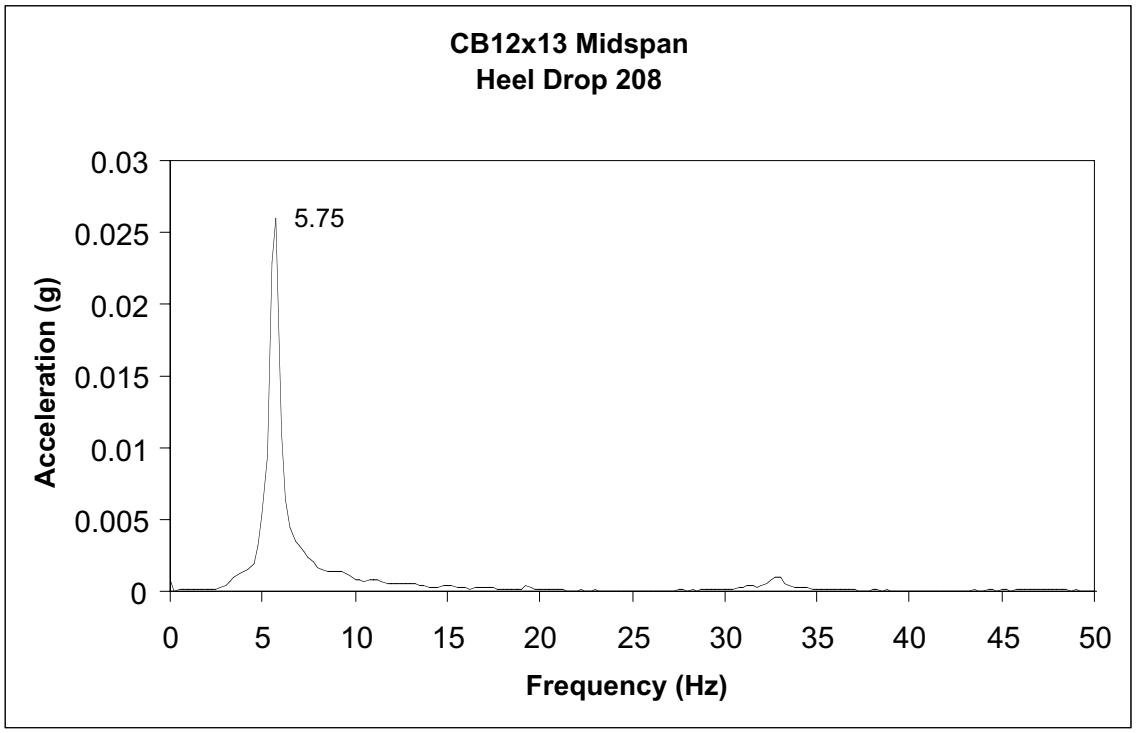

(a) Unloaded

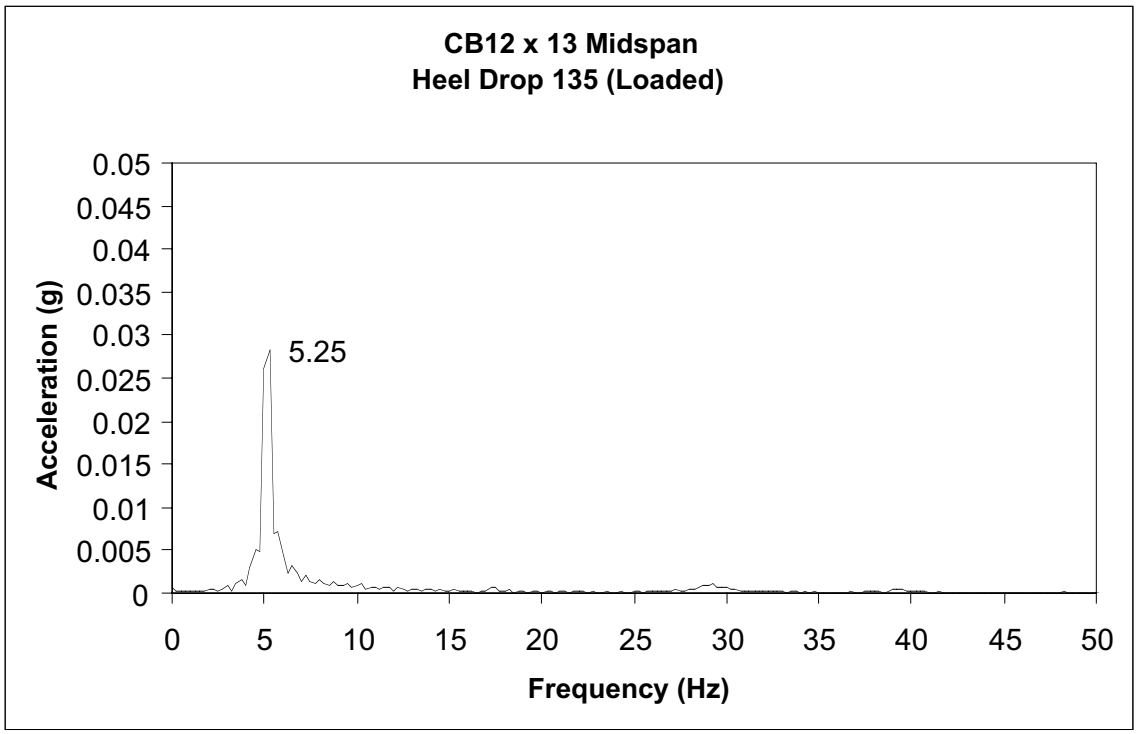

(b) Loaded

Figure B.2 CB12 x 13 Mid-span Frequency Spectra

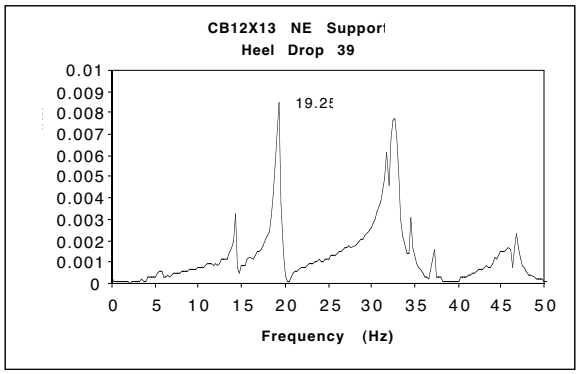

(a) NE Support

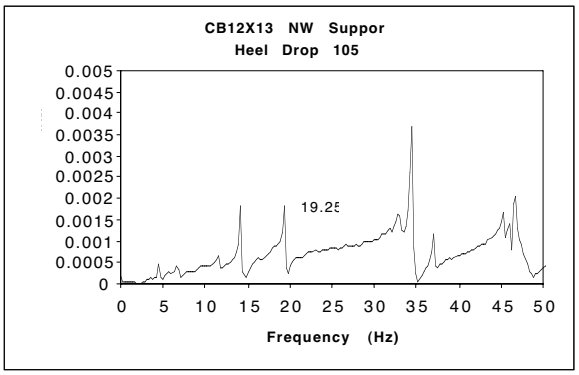

(b) NW Support

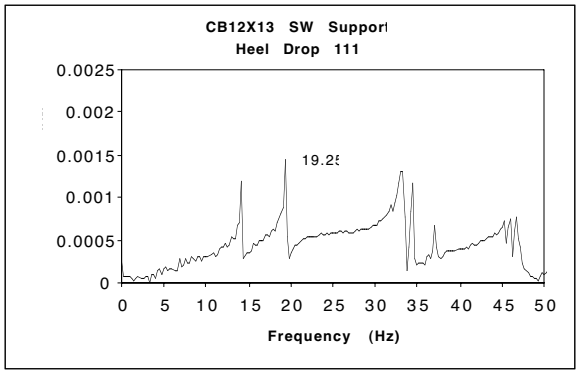

(c) SW Support

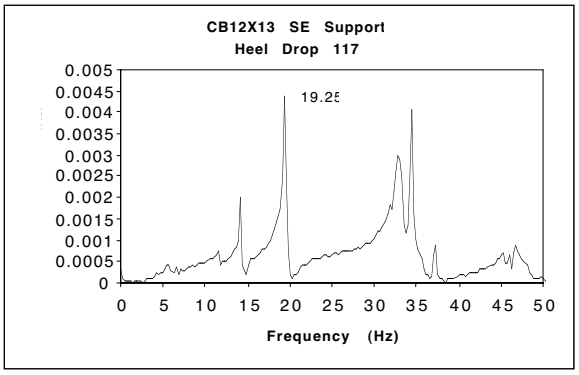

(d) SE Support

Figure B.3 CB 12 x 13 Support Frequency Spectra

B.2 CB15 x 15/19 Summary and Description of Specimen

The CB15 x 15/19 specimen was an asymmetric section with different top and bottom root sections. It was cut from a W10 x 15 and W10 x 19 hot rolled section and spanned 40 ft between each support. Figure B.5 shows the concrete and beam dimensions as found in the manufactures' catalog. The calculated and experimental frequency results for the specimen are listed in Tables B.5 and B.6, respectively.

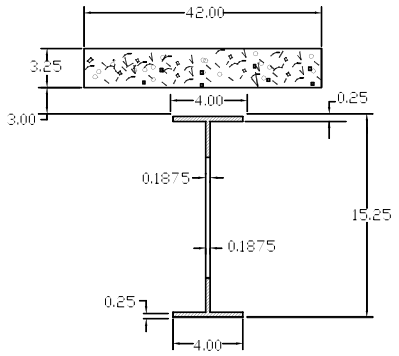

Figure B.5 Cross-section Dimensions

Table B.4 Nominal Beam Properties

CB15 X 15/19	
Root Top	W10 x 15
Root Bottom	W10 x 19
Weight (plf)	17.00
A_S (net)	3.78
A_S (gross)	6.24
I_x (net)	188.47
I_x (gross)	211.01
S_x net bottom	21.90
S_x net top	28.45

Table B.5 Vibration Analysis Parameters

LOADING	w (plf)	Δ (νι)	I_{tr} (in^4)
Loaded	276.8	0.712	772.5
Unloaded	224.3	0.577	

Table B.6 Vibration Results

Measurement	Frequency (Hz)	
	Unloaded	Loaded
Mid-span	4.50	4.00
Avg. Support	30.00	14.25
Corrected Midspan	4.55	4.17
Predicted	4.66	4.19
% Difference	3.57%	1.71%

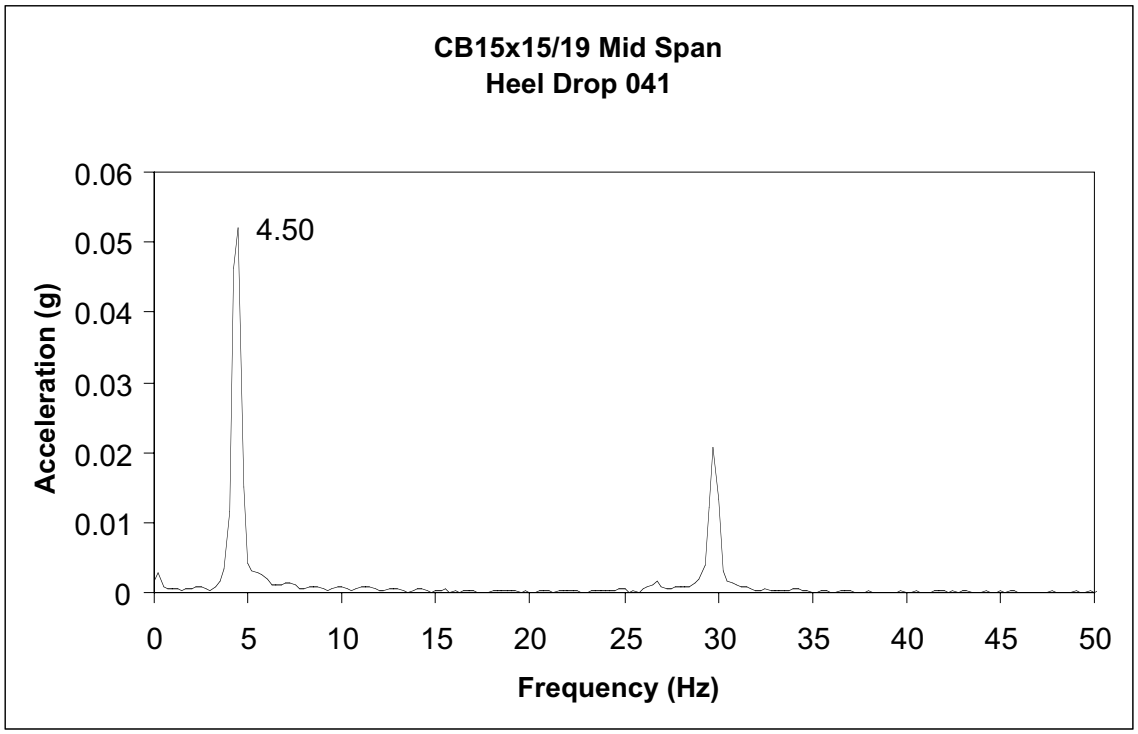

(a) Unloaded

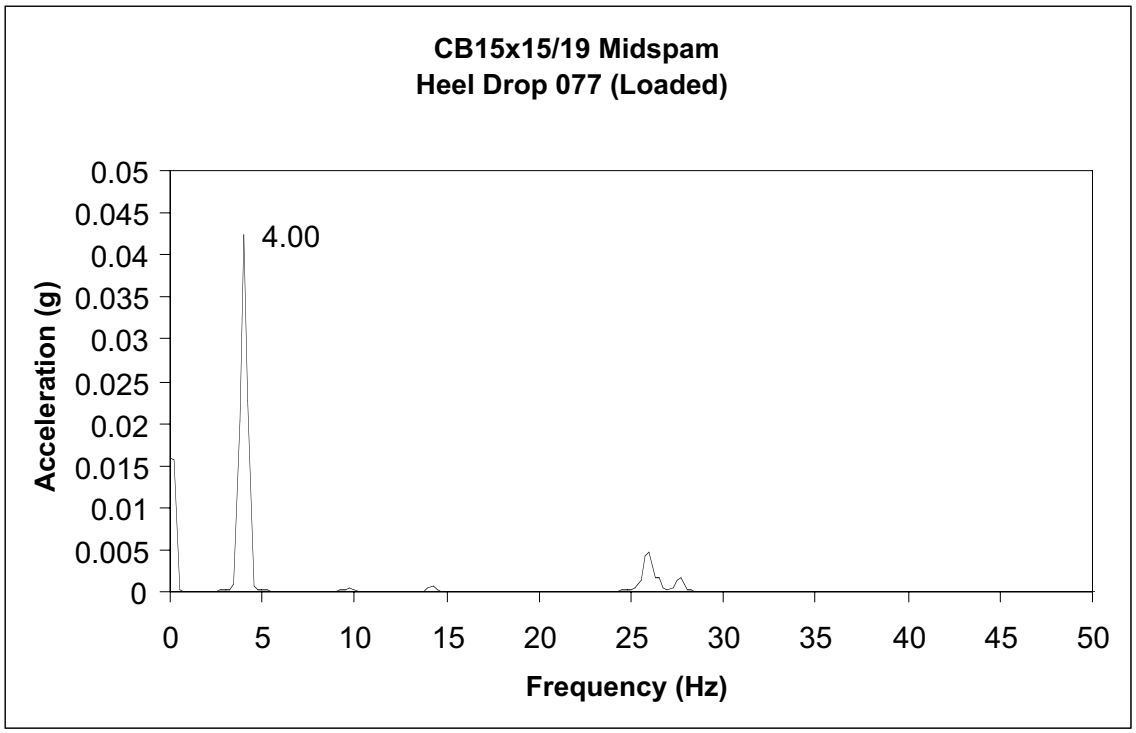

(b) Loaded

Figure B.6 CB 15 x 15/19 Mid-span Frequency Spectra

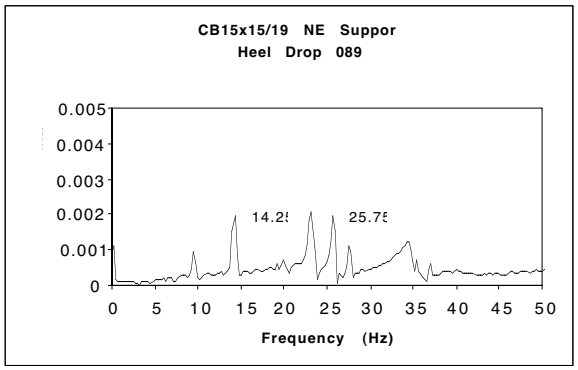

(a) NE Support

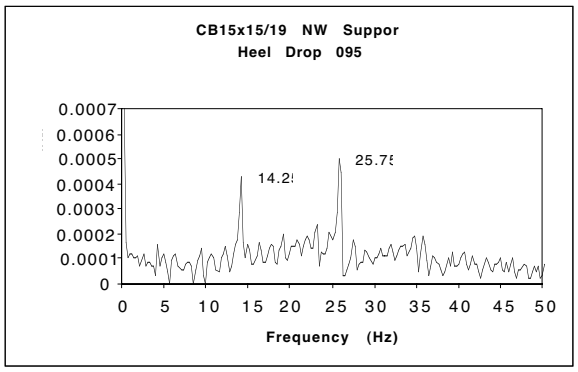

(b) NW Support

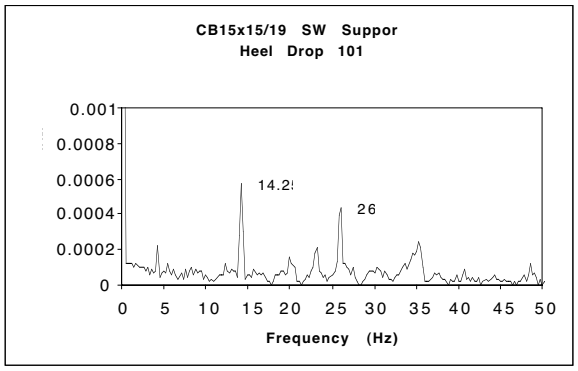

(c) SW Support

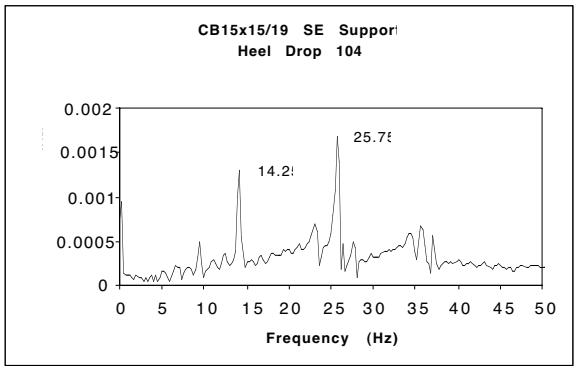

(d) SE Support

Figure B.7 CB15 x 15/19 Support Frequency Spectra

B.3 CB27 x 35/50 Summary and Description of Specimen

The CB27 x 35/50 specimen was an asymmetric section with different top and bottom root sections. It was cut from a W18 x 35 and W18 x 50 hot rolled section and spanned 58 ft between each support. Figure B.5 shows the concrete and beam dimensions as found in the manufactures' catalog. The calculated and experimental frequency results for the specimen are listed in Tables B.8 and B.9, respectively.

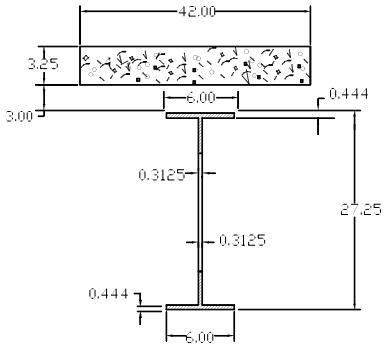

Figure B.8 Cross-section Dimensions

Table B.7 Nominal Beam Properties

CB12 X 13	
Root Top	W18 x 35
Root Bottom	W18 x 50
Weight (plf)	42.50
A_S (net)	9.35
A_S (gross)	15.48
I_x (net)	1543.74
I_x (gross)	1759.13
S_x net bottom	91.00
S_x net top	134.27

Table B.8 Vibration Analysis Parameters

LOADING	w (plf)	Δ (νι)	I_{tr} (in^4)
Loaded	302.4	0.568	4677.1
Unloaded	249.9	0.469	

Table B.9 Vibration Results

Measurement	Frequency (Hz)	
	Unloaded	Loaded
Mid-span	4.75	4.50
Avg. Support	25.00	26.25
Corrected Mid-span	4.84	4.84
Predicted	5.17	4.69
% Difference	4.57%	0.49%

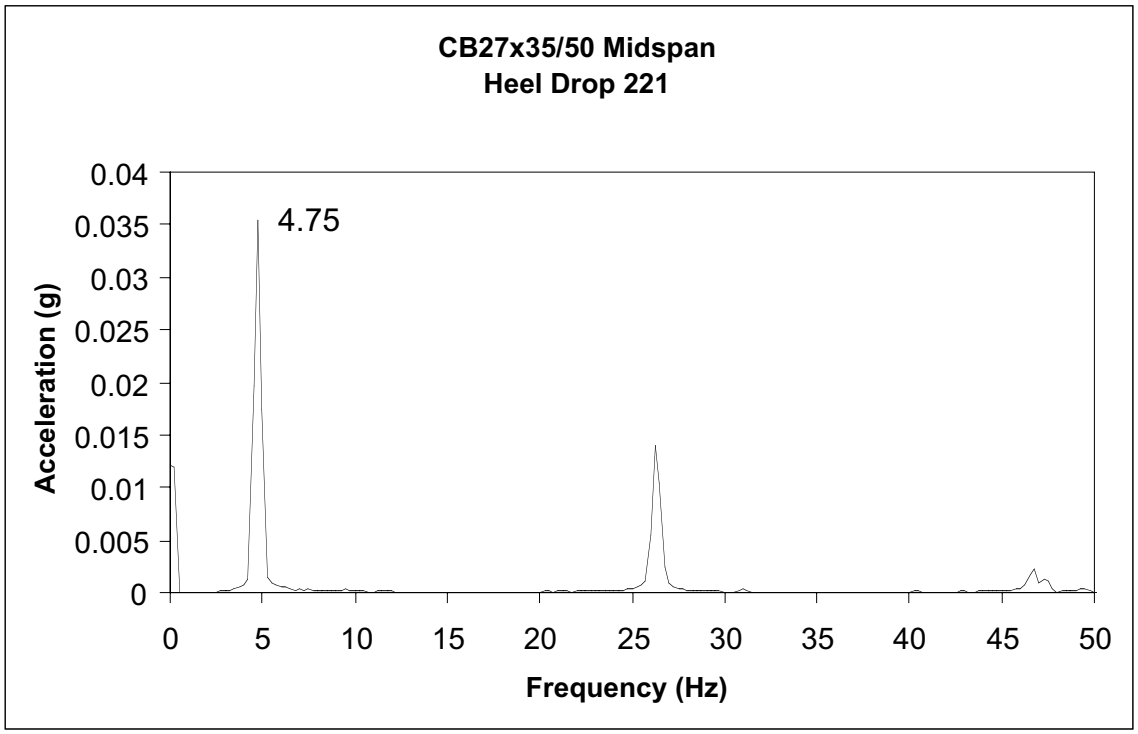

(a) Unloaded

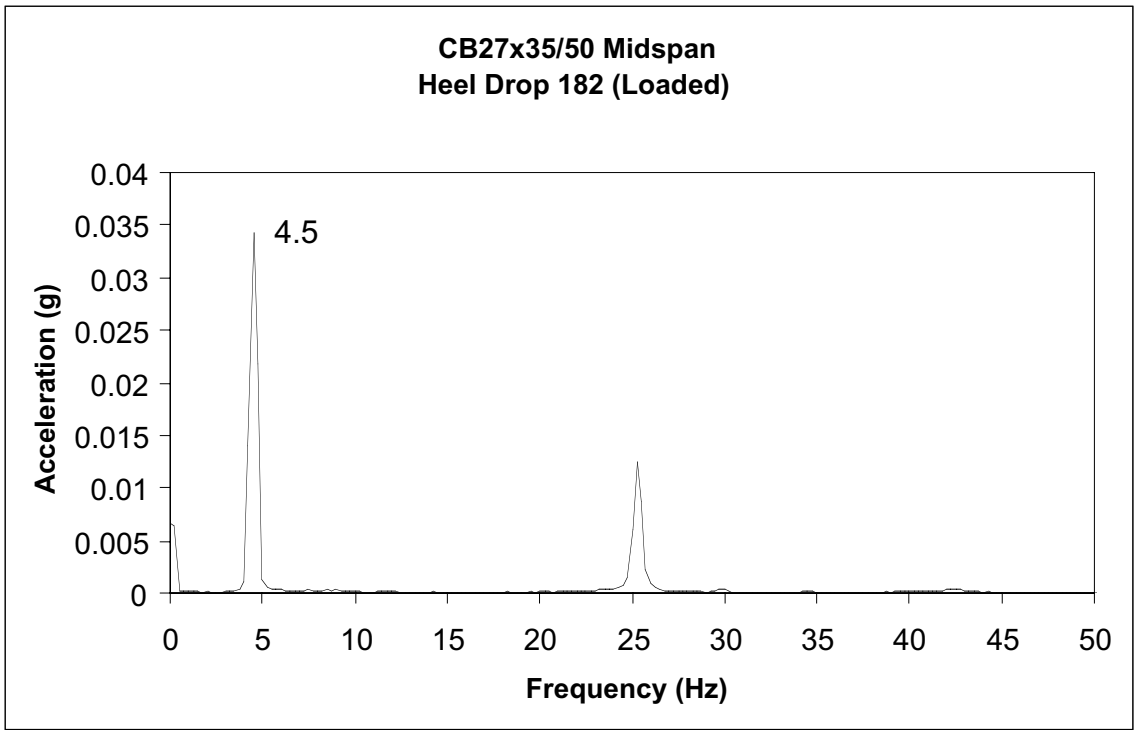

(b) Loaded

Figure B.9 CB27 x 35/50 Mid-span Frequency Spectra

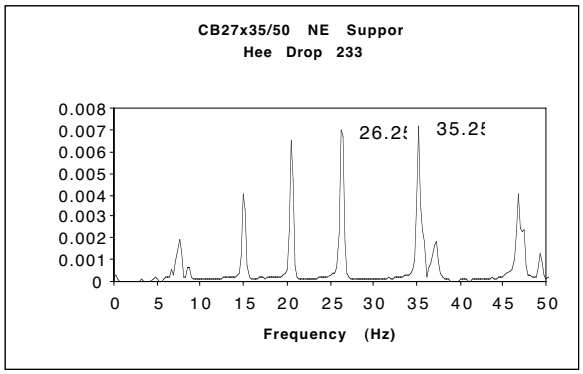

(a) NE Support

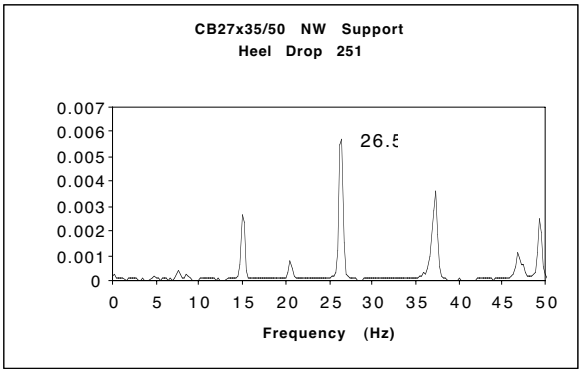

(b) NW Support

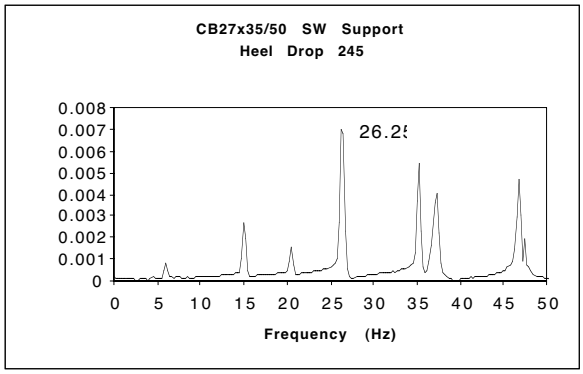

(c) SW Support

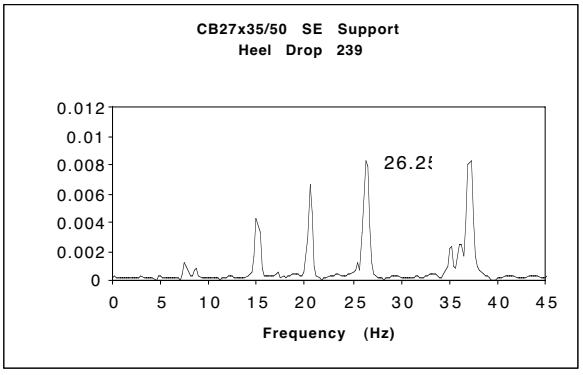

(d) SE Support

Figure B.10 CB27 x 35/50 Support Frequency Spectra

APPENDIX C

CB12 X 13 STATIC LOAD TEST RESULTS

CASTELLATED BEAM TEST SUMMARY

TEST IDENTIFICATION: CB12x13-30 Test 1
DATE: 9/19/01

TEST DESCRIPTION:

Loading	Gravity
Span	30 ft- 0 in
Beam Spacing	7 ft o.c. with 6 in deck overhang
Number of Beams	2
Web Stiffeners	2-3/16 in @ ea. Support
Decking	3 in Deep – 22 Gauge
Concrete Slab	6-1/4 in Total Depth
Shear Studs	16 - _ in Dia. x 5-1/2 in
Composite Strength	77%

FAILURE MODE:

Excessive mid-span deflection with flexural yielding at maximum moment through mid-span web opening and bottom flange.

MAXIMUM EXPERIMENTAL LOAD:

Total Applied Load	= 8 Point loads @ 3.6 kips/beam
Maximum Applied Moment	= 113.7 kip-ft
Weight of Beam	= 13.0 plf / beam
Weight of Deck/Concrete	= 207.3 plf / beam
Weight of Spreader Beams	= 33.5 plf / beam (equivalent)
Applied Line Loading	= 937.2 plf / beam (equivalent)
Total Applied Load	= 1191 plf / beam (equivalent)

THEORETICAL FAILURE LOAD: (Measured F_Y = 53 ksi)

Moment =	117.6 kip-ft
Equivalent Line Load =	1045.0 plf

R-VALUE:

R = Maximum Moment/Theoretical	1191.0/1045.0 = 1.14

DISCUSSION:

Two hydraulic actuators were used to apply load to spreader beams to create eight points loads for each beam. Wire type potentiometers were used to measure vertical deflection at supports and mid-span of each beam. The average of the two support deflections of each beam were subtracted from the measured mid-span deflection. Linear displacement transducers were used to measure horizontal slip between concrete slab and decking.

C.1 Predicted Ultimate Moment Strength Calculations

The following procedures were used to calculate the predicted ultimate moment strength of the CB12 x 13 specimen tested in this study. The ultimate moment strength is equal to the resistance provided by the castellated beam in tension and a equivalent area of concrete in compression. Figure C.1 illustrates the couple developed by these forces.

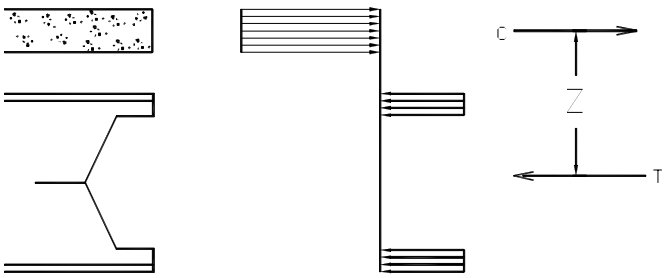

Figure C.1 Concrete Slab and Beam Couple

$$T = A_s \times F_y \tag{C.1}$$

where

T = tensile force at C.G. of both stress blocks
A_s = area of beam cross section
F_y = yield stress

The effective depth of concrete in compression is calculated by using the Whitney Stress block.

$$a = \frac{A_s F_y}{0.85 \times f_c^{'} \times b} \tag{C.2}$$

where:

a = depth of stress block
f_c' = concrete compressive strength
b = width of stress block

The following is shows the moment strength calculations of the CB12 x 13 composite beam using 53 ksi, and concrete compressive strength of 3000 psi.

Given:

Beam Properties:

Span = 30 ft

Nominal depth = 11.50

Nominal $A_{(net)}$ = 3.03 in^3

y = 5.74 in. (c.g. distance from bottom flange)

Measured $I_{tr(net)}$ = 411.6 in^4

Slab Dimensions:

Width = 42 in.

Total depth = 6.25 in.

Measured f_c' = 3000 psi

Deck Dimensions:

h_r = 3.0 in

w_r = 6.0 in

Stud Dimensions:

Dia. = 0.75 in.

H_s = 5.5 in.

F_u = 70 ksi

Total number of studs = 16

Moment Strength M_u

Shear stud strength

$$Q = SRF \times 0.5 \times A_{sc}\sqrt{f_c' \times E_c} \le A_{sc} \times F_u$$

Shear reduction factor

$$SRF = \frac{0.85}{\sqrt{N_r}}\frac{w_r}{h_r}\left[\frac{H_s}{h_r} - 1.0\right] \le 0.75 \qquad \text{where } N_r = 1.0$$

$$= \frac{0.85}{\sqrt{1.0}}\left(\frac{6.0}{3.0}\right)\left[\frac{5.5}{3} - 1.0\right] = 1.41 \ge 0.75 \qquad \text{use } 0.75$$

Shear stud strength

$$Q = 0.75 \times 0.5 \times 0.442\sqrt{3.0 \times 29000} = 15.44 kips \le 0.442 \times 70 = 30.94 kips$$

= 15.44 kips (with SRF=1.0, Q = 20.6)

Horizontal shear forces

$$C_f \le \begin{cases} 42 \times 3.0 \times 3.25 \times 0.85 = 348.0 kips \\ 3.03 \times 53 = 160.6 kips \\ 8 \times 15.44 = 123.5 kips \leftarrow controls \end{cases}$$

(with SRF = 1.0, C_f = 164.8 kips)

where 8 = half the number of studs for 77 % composite action

Concrete depth used

$$a = \frac{123.5}{0.85 \times 3.0 \times 42} = 1.15 \text{ in.}$$ (with SRF = 1.0, a = 1.54 in.)

Couple moment arm

$$Z = 17.75 - \left(\frac{1.15}{2} + 5.74 \right) = 11.43 \text{ in.}$$ (with SRF = 1.0, Z = 11.2 in.)

Predicted ultimate moment strength

$$M_u = 123.49 \times \frac{11.43}{12} = 117.64 \text{ kip-ft}$$ (with SRF = 1.0, M_u = 154.4 kip-ft)

Applied Yield Moment Strength M_y

Dead Load of concrete and metal deck

$$W_{concrete} = 145 \times \frac{4.75}{12} \times \frac{42}{12} = 200.88 \, lb/ft$$

$$W_{deck} = 1.87 \times 3.5 = 6.55 \, lb/ft$$

Concrete and Deck

$$W_D = 200.88 + 6.55 = 207.43 \, lb/ft$$

Beam weight

$$W_B = 13.0 \, lb/ft$$

Spreader Beams – W6 x 20 – 8 @ 4'-6"
W6 x 25 – 4 @ 8'-0"
W8 x 35 – 2 @ 7'-0"

Spreader Beam Weight

$$P_1 = 20 \times 4.5 \times 8 = 720 lb$$
$$P_2 = 25 \times 8 \times 4 = 800 lb$$
$$P_3 = 35 \times 7 \times 2 = 490 lb$$
$$P_{total} = 720 + 800 + 490 = 2010 lb$$

$$W_s = \frac{2010}{30} = 33.5 \, lb/ft$$

Moment caused by spreader beams

$$M_S = \frac{33.5(30\times12)^2}{8\times1000\times12} = 45.23 \text{ kip-in}$$

Moment caused by beam weight

$$M_B = \frac{13.0(30\times12)^2}{8\times1000\times12} = 17.55 \text{ kip-in}$$

Solve for M_y

Moment caused by concrete and deck

$$M_D = \frac{207.43(30\times12)^2}{8\times1000\times12} = 280.03 \text{ kip-in}$$

Applied Yield Moment

$$\sigma_y = \frac{M_B + M_D}{S_n} + \frac{M_s}{S_c} + \frac{M_{y,applied}}{S_c}$$

Non-composite section modulus

$$S_n = \frac{I_{net}}{d/2} = \frac{83.5}{5.74} = 14.6 \text{ in}^3$$

Composite Section Modulus

$$S_{c(net)} = \frac{I_{tr(net)}}{y_c}$$ y_c = 14.86 from section A.1

$$= \frac{375.60}{14.86} = 25.67 \text{ in}^3$$

Subtracting weight of concrete, beam, deck, and spreader beams

$$53 = \frac{17.55 + 280.03}{14.86} + \frac{45.23}{25.67} + \frac{M_{y,applied}}{25.67}$$

$M_{y,applied}$ = <u>66.7 kip-ft</u>

Maximum applied moment subtracting weight of concrete, beam, deck, and spreader beams is

$$M_{u,applied} = 117.64 - \left(\frac{17.55 + 280.03 + 45.23}{12}\right) = \underline{89.0 \text{ kip-ft}}$$

(with SRF = 1.0, M_u = <u>125.8 kip-ft</u>)

C.2 Photos of CB12 x 13 Test

The following photos were taken before, after, and during the CB12 x 13 test.

View of east side of test set-up before test

View from south east of testing setup before loading

View from south side of test setup during loading

First yield at mid span

Shear stud placement

APPENDIX D

CB15 X 15/19 STATIC LOAD TEST RESULTS

CASTELLATED BEAM TEST SUMMARY

TEST IDENTIFICATION: CB15x15/19-40 Test 2
DATE: 11/29/01

TEST DESCRIPTION:

Loading	Gravity
Span	40 ft- 0 in
Beam Spacing	5 ft o.c. with 6 in deck overhang
Number of Beams	2
Web Stiffeners	2-3/16 in @ ea. Support
Decking	3 in Deep – 22 Gauge
Concrete Slab	6-1/4 in Total Depth
Shear Studs	14 - _ in Dia. x 5-1/2 in
Composite Strength	54%

FAILURE MODE:

Excessive mid-span deflection with flexural yielding at maximum moment through mid-span web opening and bottom flange.

MAXIMUM EXPERIMENTAL LOAD:

Total Applied Load =	= 8 Point loads @ 4 kips
Maximum Applied Moment	= 160.0 kip-ft
Weight of Beam =	=17.0 plf / beam
Weight of Deck/Concrete =	=207.3 plf / beam
Weight of Spreader Beams =	= 75.0 plf / beam (equivalent)
Applied Line Loading =	= 800.0 plf / beam (equivalent)
Total Applied Load =	=1099.3 plf / beam (equivalent)

THEORETICAL FAILURE LOAD: (Assumed F_Y = 53 ksi)

Moment =	129.6 kip-ft (SRF = 0.75)
Equivalent Line Load =	648.0 plf

R-VALUE:

R = Maximum Load/Theoretical	1099.3/648.0 = 1.70

DISCUSSION:

Two hydraulic actuators were used to apply load to spreader beams to create 8 points loads for each beam. Wire type potentiometers were used to measure vertical deflection at supports and mid span of each beam. The average of the two support deflections of each beam were subtracted from the measured mid span deflection. Linear displacement transducers were used to measure horizontal slip between concrete slab and decking.

D.1 Predicted Ultimate Moment Strength Calculations

The following procedures were used to calculate the predicted ultimate moment strength of the CB15 x 15/19 specimen tested in this study. The ultimate moment strength is equal to the resistance provided by the castellated beam in tension and an equivalent area of concrete in compression. Figure D.1 illustrates the couple developed by these forces.

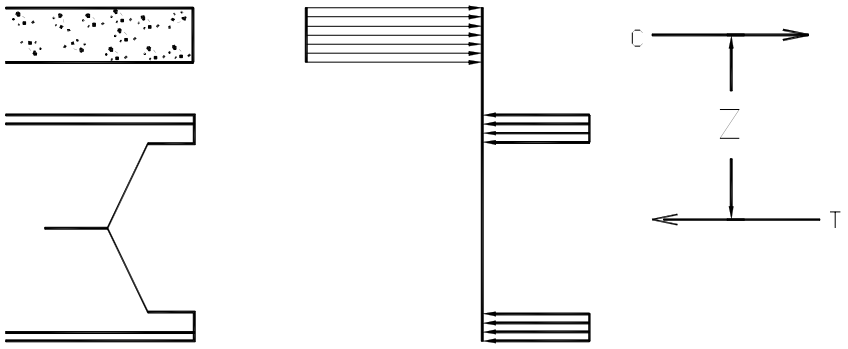

Figure C.1 Concrete Slab and Beam Couple

$$T = A_s \times F_y \tag{D.1}$$

where:

T = tensile force at C.G. of both stress blocks
A_s = area of beam cross section
F_y = yield stress

The effective depth of concrete in compression is calculated by using the Whitney Stess block.

$$a = \frac{A_s F_y}{0.85 \times f_c' \times b} \tag{D.2}$$

where:

a = depth of stress block
f_c' = concrete compressive strength
b = width of stress block

The following is shows the moment strength calculations of the CB15 x 15/19 using 53 ksi, and concrete compressive strength of 3000 psi.

Given:

Beam Properties:

Span = 40 ft

Nominal depth = 15.25

Nominal $A_{(net)}$ = 3.78 in^3

y = 6.62 in. (c.g. distance from bottom flange)

$I_{tr(net)}$ = 772.5 in^4

Slab Dimensions:

Effective width = 42 in.

Total Depth = 6.25 in.

Measured f_c' = 3740 psi

Deck Dimensions:

h_r = 3.0 in

w_r = 6.0 in

Stud Dimensions:

Dia. = 0.75 in.

H_s = 5.5 in.

F_u = 50 ksi

Total number of studs = 14

Moment Strength M_u

Shear stud strength

$$Q = SRF \times 0.5 \times A_{sc}\sqrt{f_c' \times E_c} \le A_{sc} \times F_u$$

Shear reduction factor

$$SRF = \frac{0.85}{\sqrt{N_r}}\frac{w_r}{h_r}\left[\frac{H_s}{h_r} - 1.0\right] \le 0.75 \quad \text{where } N_r = 1.0$$

$$= \frac{0.85}{\sqrt{1.0}}\left(\frac{6.0}{3.0}\right)\left[\frac{5.5}{3} - 1.0\right] = 1.41 \ge 0.75 \quad \text{use } 0.75$$

$$Q = 0.75 \times 0.5 \times 0.442\sqrt{3.0 \times 29000} = 15.44 kips \le 0.442 \times 50 = 22.1 kips$$

= 15.44 kips (with SRF=1.0, Q = 20.6)

Horizontal shear forces

$$C_f \le \begin{cases} 42 \times 3.74 \times 3.25 \times 0.85 = 434.0 kips \\ 3.78 \times 53 = 200.3 kips \\ 7 \times 15.44 = 108.1 kips \leftarrow controls \end{cases}$$

(with SRF = 1.0, C_f = 144.2 kips)

where 7 = half the number of studs for 54% composite action

Concrete depth used

$$a = \frac{108.1}{0.85 \times 3.74 \times 42} = 0.81 \text{ in.}$$ (with SRF = 1.0, a = 1.35 in.)

Couple moment arm

$$Z = 21.5 - \left(\frac{.81}{2} + 6.62 \right) = 14.38 \text{ in.}$$ (with SRF = 1.0, Z = 14.2 in.)

Predicted ultimate moment strength

$$M_u = 108.1 \times \frac{14.38}{12} = 129.6 \text{ kip-ft}$$ (with SRF = 1.0, M_u = 170.8 kip-ft)

Applied Yield Moment Strength M_y

Dead Load of concrete and metal deck

$$W_{concrete} = 145 \times \frac{4.75}{12} \times \frac{42}{12} = 200.88 \, lb/ft$$

$$W_{deck} = 1.87 \times 3.5 = 6.55 \, lb/ft$$

Concrete and Deck

$$W_D = 200.88 + 6.55 = 207.43 \, lb/ft$$

Moment caused by concrete and deck

$$M_D = \frac{207.43(40 \times 12)^2}{8 \times 1000 \times 12} = 497.83 \text{ kip-in}$$

Beam weight

$$W_B = 17.0 \, lb/ft$$

Speader Beams – W6 x 20 – 8 @ 4'-6"
W6 x 25 – 4 @ 8'-0"
W14 x 53 – 2 @ 14'-0"

Spreader Beam Weight

$$P_1 = 20 \times 4.5 \times 8 = 720lb$$
$$P_2 = 25 \times 8 \times 4 = 800lb$$
$$P_3 = 53 \times 14 \times 2 = 1484lb$$
$$P_{total} = 1484 + 800 + 490 = 3004lb$$

$$W_s = \frac{3004}{40} = 75.0 lb/ft$$

Moment caused by spreader beams

$$M_S = \frac{75(40 \times 12)^2}{8 \times 1000 \times 12 \times 2} = 90.0 \text{ kip-in}$$

Moment caused by beam weight

$$M_B = \frac{17.0(40 \times 12)^2}{8 \times 1000 \times 12} = 40.8 \text{ kip-in}$$

Solve for M_y

Applied Yield Moment

$$\sigma_y = \frac{M_B + M_D}{S_n} + \frac{M_s}{S_c} + \frac{M_{y,applied}}{S_c}$$

Non-composite Section Modulus

$$S_{net} = \frac{I_{net}}{y} = \frac{195.3}{6.62} = 29.5 \text{ in}^3$$

Composite Section Modulus

$$S_{c(net)} = \frac{I_{tr(net)}}{y_c}$$

$$= \frac{772.5}{16.70} = 46.26 \text{ in}^3$$

Subtracting weight of concrete, beam, deck, and spreader beams

$$53 = \frac{497.8 + 40.8}{29.5} + \frac{90.0}{46.26} + \frac{M_{y,applied}}{46.26}$$

$$M_{y,applied} = 126.43 \text{ kip-ft}$$

Maximum applied moment subtracting the weight of concrete, beam, deck, and spreader beams

$$M_{u,applied} = 129.6 - \left(\frac{497.83 + 40.8 + 90}{12} \right) = 77.21 \text{ kip-ft}$$

(with SRF = 1.0, M_u = 118.4 kip-ft)

D.2 Photos of CB15 x 15/19 Test

The following photos were taken before, after, and during the CB15 x 15/19 test.

View of east side of set-up before test

View from south east of testing setup before loading

View from south side of test setup during loading

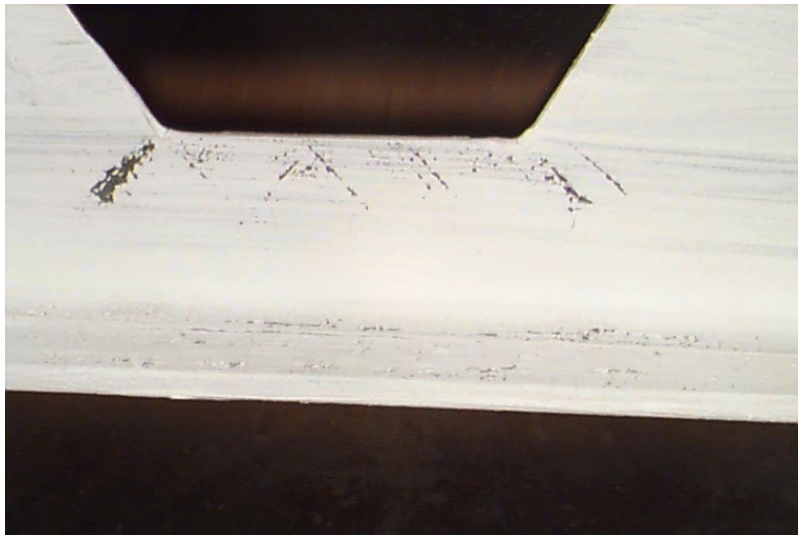

First yield at mid span

Vierendeel bending

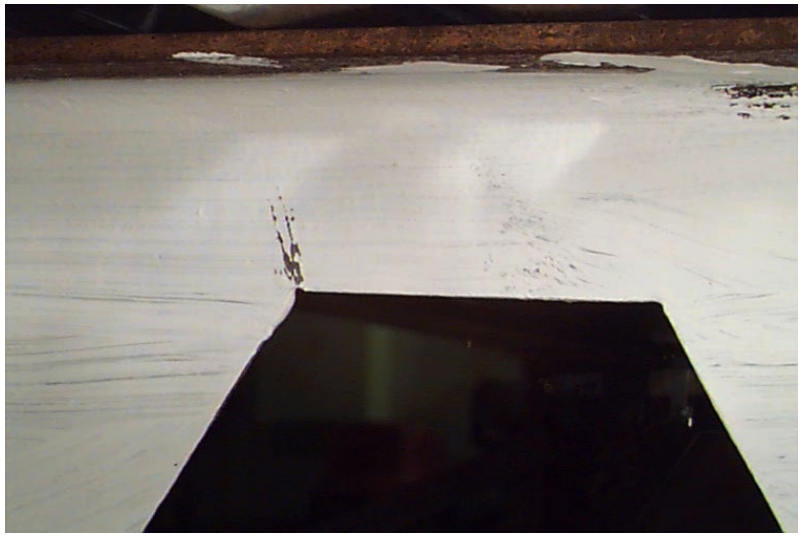

APPENDIX E

CB27 X 35/50 STATIC LOAD TEST RESULTS

CASTELLATED BEAM TEST SUMMARY

TEST IDENTIFICATION: CB27x35/50-58 Test 3
DATE: 12/19/01

TEST DESCRIPTION:

Loading	Gravity
Span	58 ft- 0 in
Beam Spacing	7 ft o.c. with 6 in deck overhang
Number of Beams	2
Web Stiffeners	2-3/16 in @ ea. Support
Decking	3 in Deep – 22 Gauge
Concrete Slab	6-1/4 in Total Depth
Shear Studs	22 - _ in Dia. x 5-1/2 in
Composite Strength	34%

FAILURE MODE:

Excessive mid-span deflection with flexural yielding at maximum moment through mid-span web opening and bottom flange.

MAXIMUM EXPERIMENTAL LOAD:

Total Applied Load	= 8 Point loads @ 11 kips/beam
Maximum Applied Moment	= 640.0 kip-ft
Weight of Beam	= 42.5 plf / beam
Weight of Deck/Concrete	= 207.3 plf / beam
Weight of Spreader Beams	= 51.8 plf / beam (equivalent)
Applied Line Loading	= 1576 plf / beam (equivalent)
Total Applied Load	= 1888 plf / beam (equivalent)

THEORETICAL FAILURE LOAD: (Measured F_Y = 53 ksi)

Moment =	844.0 kip-ft (SRF = 0.75)
Equivalent Line Load =	2007 plf

R-VALUE:

R = Maximum Moment/Theoretical 1888/2007 = 0.94

DISCUSSION:

Two hydraulic actuators were used to apply load to spreader beams to create eight points loads for each beam. Wire type potentiometers were used to measure vertical deflection at supports and mid-span of each beam. The average of the two support deflections of each beam were subtracted from the measured mid-span deflection. Linear displacement transducers were used to measure horizontal slip between concrete slab and decking.

E.1 Predicted Ultimate Moment Strength Calculations

The following procedures were used to calculate the predicted ultimate moment strength of the CB27 x 35/50 specimen tested in this study. The ultimate moment capacity is equal the resistance provided by the castellated beam in tension and an equivalent area of concrete and top flange of beam in compression. Figure E.1 illustrates the couple developed by these forces.

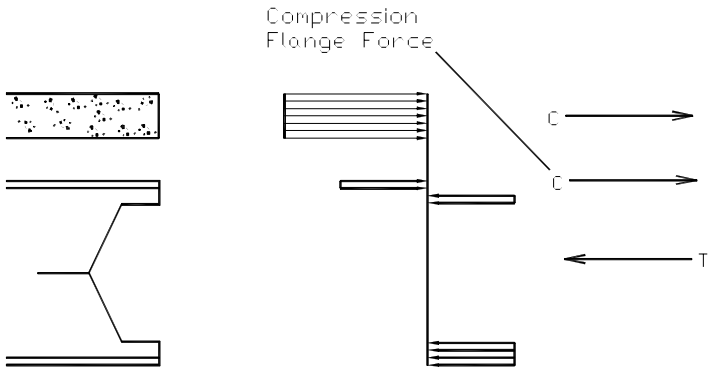

Figure E.1 Concrete Slab and Beam Couple

$$T = A_s \times F_y \tag{E.1}$$

where:

T = tensile force at C.G. of both stress blocks
A_s = area of beam cross section
F_y = yield stress

The effective depth of concrete in compression is calculated by using the Whitney Stess block.

$$a = \frac{A_s F_y}{0.85 \times f_c' \times b} \tag{E.2}$$

where:

a = depth of stress block
f_c' = concrete compressive strength
b = width of stress block

The following is shows the calculations of the moment strength CB27 x 35/50 using 55 ksi, and concrete compressive strength of 3000 psi.

Given:

Beam Properties:

Span = 58 ft

Nominal depth = 27.25

Nominal $A_{(net)}$ = 9.35 in^3

y = 10.99 in. (c.g. distance from bottom flange)

$I_{tr(net)}$ = 4677.1 in^4

Slab Dimensions:

Effective width = 42 in.

Total depth = 6.25 in.

Measured f_c' = 3300 psi

Deck Dimensions:

h_r = 3.0 in

w_r = 6.0 in

Stud Dimensions:

Dia. = 0.75 in.

H_s = 5.5 in.

F_u = 50 ksi

Total number of studs = 22

Moment Strength M_u

Shear stud strength

$$Q = SRF \times 0.5 \times A_{sc}\sqrt{f_c' \times E_c} \le A_{sc} \times F_u$$

Shear reduction factor

$$SRF = \frac{0.85}{\sqrt{N_r}}\frac{w_r}{h_r}\left[\frac{H_s}{h_r} - 1.0\right] \le 0.75 \quad \text{where } N_r = 1.0$$

$$= \frac{0.85}{\sqrt{1.0}}\left(\frac{6.0}{3.0}\right)\left[\frac{5.5}{3} - 1.0\right] = 1.41 \ge 0.75 \qquad \text{use } 0.75$$

Shear stud strength

$$Q = 0.75 \times 0.5 \times 0.442\sqrt{3.0 \times 29000} = 15.44 kips \le 0.442 \times 70 = 30.94 kips$$

= 15.44 kips (with SRF=1.0, Q = 20.6)

Horizontal shear forces

$$C_f \le \begin{cases} 42 \times 3.3 \times 3.25 \times 0.85 = 382.9 kips \\ 9.35 \times 55 = 514.3 kips \\ 11 \times 15.44 = 169.4 kips \leftarrow controls \end{cases}$$ (with SRF = 1.0, C_f = 226.6 kips)

where 11 = half the number of studs for 34 % composite action

Assumed flange Force

$$C_2 = \frac{(-169.4 + 514.3)}{2} = 172.5 \text{ kips}$$

Compression flange depth

$$a = \frac{172.5}{6 \times 55} = 0.52 \ge 0.444 = t_f$$ (stress block in stem)

Actual flange force

$C_2 = 0.44 \times 6.0 \times 55 = 145.2$ (with SRF = 1.0, C_2 = 143.8 kips)

Stem force

$C_3 = 172.5 - 145.2 = 27.3$ (with SRF = 1.0, no compression force in stem)

Stem force depth

$$a_1 = \frac{27.3}{0.3 \times 55} = 1.65 \text{ in.}$$

Concrete depth in compression

$$a_1 = \frac{169.4}{0.85 \times 3.3 \times 42} = 1.44 \text{ in}$$ (with SRF = 1.0, a = 2.11 in.)

Nominal ultimate moment strength

$$M_u = 169.4 \times \frac{(33.5 - 0.72)}{12} + 145.2 \frac{(27.25 - 0.22)}{12} \times 2 + 27.2 \times \frac{27.25 - (0.44 + 0.73)}{12} \times 2$$

$$- 514.3 \times \frac{10.99}{12} = 764.1 \text{ kip-ft}$$ (with SRF = 1.0, M_u = 791.0 kip-ft)

Applied Yield Moment Strength M_y

Dead Load of concrete and metal deck

$$W_{concrete} = 145 \times \frac{4.75}{12} \times \frac{42}{12} = 200.88 \, lb/ft$$

$$W_{deck} = 1.87 \times 3.5 = 6.55 \, lb/ft$$

Concrete and Deck

$$W_D = 200.88 + 6.55 = 207.43 \, lb/ft$$

Beam weight

$W_B = 42.5 lb/ft$

Spreader Beams – W6 x 20 – 8 @ 4'-6"
W6 x 25 – 4 @ 8'-0"
W14 x 53 – 2 @ 14'-0"

Spreader Beam Weight

$P_1 = 20 \times 4.5 \times 8 = 720 lb$

$P_2 = 25 \times 8 \times 4 = 800 lb$

$P_3 = 53 \times 14 \times 2 = 1484 lb$

$P_{total} = 1484 + 800 + 490 = 3004 lb$

$$W_s = \frac{3004}{58} = 51.8 lb/ft$$

Moment caused by concrete and deck

$$M_D = \frac{207.43(58 \times 12)^2}{8 \times 1000 \times 12} = 1046.69 \text{ kip-in}$$

Moment caused by spreader beams

$$M_S = \frac{51.8(58 \times 12)^2}{8 \times 1000 \times 12} = 261.34 \text{ kip-in}$$

Moment caused by beam weight

$$M_B = \frac{42.5(58 \times 12)^2}{8 \times 1000 \times 12} = 214.45 \text{ kip-in}$$

Solve for M_y

Applied Yield Moment

$$\sigma_y = \frac{M_B + M_D}{S_n} + \frac{M_s}{S_c} + \frac{M_{y,applied}}{S_c}$$

Non-composite section modulus

$$S_{net} = \frac{I_{net}}{y} = \frac{1682}{10.99} = 153 \text{ in}^3$$

Concrete Section Modulus

$$S_{c(net)} = \frac{I_{tr(net)}}{y_c}$$

$$= \frac{4677.1}{23.79} = 196.6 \text{ in}^3$$

Subtracting weight of concrete, beam, deck, and spreader beams

$$55 = \frac{1046.69 + 214.45}{153} + \frac{261.34}{196.6} + \frac{M_{y,applied}}{196.6}$$

$M_{y,applied}$ = <u>738.3 kip-ft</u>

Ultimate Applied Moment subtracting weight of concrete, beam, deck, and spreader beams

$$M_{u,applied} = 764.1 - \left(\frac{1046.69 + 214.45 + 261.34}{12} \right) = \underline{637.2 \text{ kip-ft}}$$

(with SRF = 1.0, M_u = <u>664.6 kip-ft</u>)

E.2 Photos of CB27 x 35/50 Test

The following photos were taken before, after, and during the CB27 x 35/50 test.

Entire Set-up before test began

Specimen loaded during test

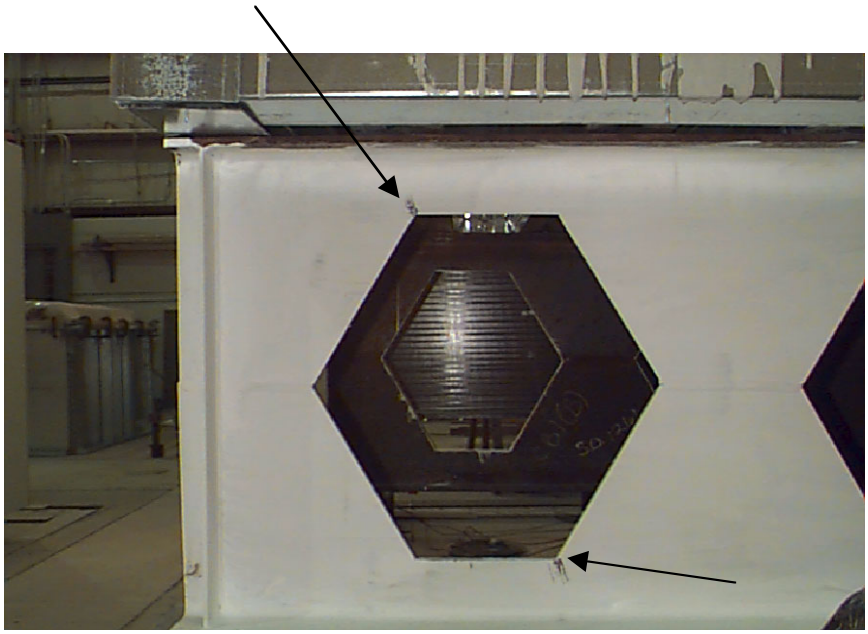

Vierendeel Bending Indicated by White Wash

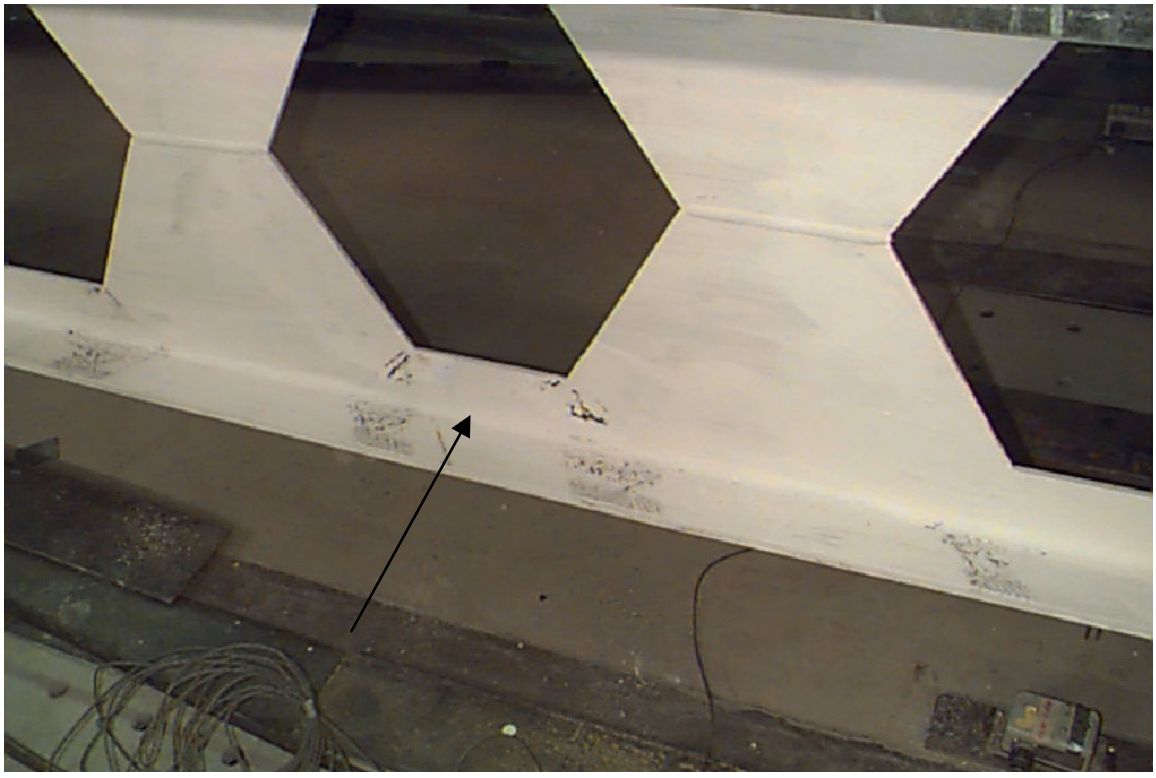

Mid-span Yielding During Test

APPENDIX F

FINITE ELEMENT INPUT FILE

S A P 2 0 0 0

Structural Analysis Programs

Version 7.00

27 Dec 2001 21:25:32

PROGRAM:SAP2000/FILE:\WINDOWS\DESKTOP\sap\12x13.EKO

S Y S T E M D A T A

STEADY STATE LOAD FREQUENCY - - - - - - - - - 0.0000E+00

LENGTH UNITS - - - - - - - - - - - - - - - - - IN
FORCE UNITS - - - - - - - - - - - - - - - - - KIP

UP DIRECTION - - - - - - - - - - - - - - - - - +Z

GLOBAL DEGREES OF FREEDOM - - - - - - - - - - UX
- - - - - - - - - - UZ
- - - - - - - - - - RY

PAGINATION BY - - - - - - - - - - - - - - - - SECTIONS
NUMBER OF LINES PER PAGE - - - - - - - - - - 59
INCLUDE WARNING MESSAGES IN OUTPUT FILE - - Y

C S I / S A P 2 0 0 0 - FINITE ELEMENT ANALYSIS OF STRUCTURES

PROGRAM:SAP2000/FILE:\WINDOWS\DESKTOP\sap\12x13.EKO

G E N E R A T E D J O I N T C O O R D I N A T E S

JOINT	X	Y	Z
1	-180.000	0.000	0.000
2	180.000	0.000	0.000
3	-180.000	0.000	10.540
4	180.000	0.000	10.540
5	-180.000	-21.000	13.395
6	180.000	-21.000	13.395
7	180.000	21.000	13.395
8	-180.000	21.000	13.395
9	-120.000	-21.000	13.395
10	-120.000	0.000	13.395
11	-180.000	0.000	13.395
12	-120.000	21.000	13.395
13	-60.000	-21.000	13.395
14	-60.000	0.000	13.395
15	-60.000	21.000	13.395
16	0.000	-21.000	13.395
17	0.000	0.000	13.395
18	0.000	21.000	13.395
19	60.000	-21.000	13.395
20	60.000	0.000	13.395
21	60.000	21.000	13.395
22	120.000	-21.000	13.395
23	120.000	0.000	13.395
24	120.000	21.000	13.395
25	180.000	0.000	13.395

26	-120.000	0.000	0.000
27	-60.000	0.000	0.000
28	0.000	0.000	0.000
29	60.000	0.000	0.000
30	120.000	0.000	0.000
31	-120.000	0.000	10.540
32	-60.000	0.000	10.540
33	0.000	0.000	10.540
34	60.000	0.000	10.540
35	120.000	0.000	10.540

C S I / S A P 2 0 0 0 - FINITE ELEMENT ANALYSIS OF STRUCTURES

PROGRAM:SAP2000/FILE:\WINDOWS\DESKTOP\sap\12x13.EKO

R E S T R A I N T D A T A

JOINT			
1	U1	U2	U3
2		U2	U3

C S I / S A P 2 0 0 0 - FINITE ELEMENT ANALYSIS OF STRUCTURES

PROGRAM:SAP2000/FILE:\WINDOWS\DESKTOP\sap\12x13.EKO

M A T E R I A L P R O P E R T Y D A T A

MAT LABEL	NUMBER TEMPS	WEIGHT PER UNIT VOL	MASS PER UNIT VOL	DESIGN CODE
STEEL	1	0.2830E-03	0.7324E-06	S
CONC	1	0.8680E-04	0.2652E-06	C
OTHER	1	0.8680E-04	0.2246E-06	N
DECK	1	0.2830E-03	0.2582E-06	C
MASSLESS	1	0.2830E-03	0.0000E+00	S

C S I / S A P 2 0 0 0 - FINITE ELEMENT ANALYSIS OF STRUCTURES

PROGRAM:SAP2000/FILE:\WINDOWS\DESKTOP\sap\12x13.EKO

T E M P E R A T U R E D E P E N D E N T D A T A

MATERIAL PROPERTIES

MAT LABEL	TEMP	MODULUS OF ELASTICITY E1	E2	E3	SHEAR MODULII G12	G13	G23

STEEL 0.00 0.290E+05 0.290E+05 0.290E+05 0.112E+05 0.112E+05
0.112E+05

CONC 0.00 0.360E+04 0.360E+04 0.360E+04 0.150E+04 0.150E+04
0.150E+04

OTHER 0.00 0.360E+04 0.360E+04 0.360E+04 0.150E+04 0.150E+04
0.150E+04

DECK 0.00 0.290E+05 0.290E+05 0.290E+05 0.112E+05 0.112E+05
0.112E+05

MASSLESS 0.00 0.290E+05 0.290E+05 0.290E+05 0.112E+05 0.112E+05
0.112E+05

C S I / S A P 2 0 0 0 - FINITE ELEMENT ANALYSIS OF STRUCTURES

PROGRAM:SAP2000/FILE:\WINDOWS\DESKTOP\sap\12x13.EKO

T E M P E R A T U R E D E P E N D E N T D A T A

THERMAL EXPANSION COEFFICIENTS

MAT TEMP COEFFICIENTS OF THERMAL EXPANSION
LABEL A1 A2 A3 A12 A13
A23

STEEL 0.00 0.650E-05 0.650E-05 0.650E-05 0.000E+00 0.000E+00
0.000E+00

CONC 0.00 0.550E-05 0.550E-05 0.550E-05 0.000E+00 0.000E+00
0.000E+00

OTHER 0.00 0.550E-05 0.550E-05 0.550E-05 0.000E+00 0.000E+00
0.000E+00

DECK 0.00 0.650E-05 0.650E-05 0.650E-05 0.000E+00 0.000E+00
0.000E+00

MASSLESS 0.00 0.650E-05 0.650E-05 0.650E-05 0.000E+00 0.000E+00
0.000E+00

C S I / S A P 2 0 0 0 - FINITE ELEMENT ANALYSIS OF STRUCTURES

PROGRAM:SAP2000/FILE:\WINDOWS\DESKTOP\sap\12x13.EKO

T E M P E R A T U R E D E P E N D E N T D A T A

MATERIAL PROPERTIES

MAT TEMP POISSONS RATIO
LABEL U12 U13 U23 U14 U24 U34 U15 U25 U35 U45 U16 U26 U36
U46 U56

STEEL 0.00 0.3 0.3 0.3 0.0 0.0 0.0 0.0 0.0 0.0 0.0 0.0 0.0 0.0 0.0 0.0

CONC 0.00 0.2 0.2 0.2 0.0 0.0 0.0 0.0 0.0 0.0 0.0 0.0 0.0 0.0 0.0 0.0

OTHER 0.00 0.2 0.2 0.2 0.0 0.0 0.0 0.0 0.0 0.0 0.0 0.0 0.0 0.0 0.0 0.0

DECK 0.00 0.3 0.3 0.3 0.0 0.0 0.0 0.0 0.0 0.0 0.0 0.0 0.0 0.0 0.0 0.0

MASSLESS 0.00 0.3 0.3 0.3 0.0 0.0 0.0 0.0 0.0 0.0 0.0 0.0 0.0 0.0 0.0 0.0

C S I / S A P 2 0 0 0 - FINITE ELEMENT ANALYSIS OF STRUCTURES

PROGRAM:SAP2000/FILE:\WINDOWS\DESKTOP\sap\12x13.EKO

MATERIAL PROPERTIES

MAT LABEL	TEMP	YIELD FY
CONC	0.00	36.00
DECK	0.00	36.00

C S I / S A P 2 0 0 0 - FINITE ELEMENT ANALYSIS OF STRUCTURES

PROGRAM:SAP2000/FILE:\WINDOWS\DESKTOP\sap\12x13.EKO

F R A M E S E C T I O N P R O P E R T Y D A T A - P R I S M A T I C

SECTION LABEL	SHAPE TYPE	DEPTH	FLANGE WIDTH TOP	FLANGE THICK TOP	WEB THICK	FLANGE WIDTH BOTTOM	FLANGE THICK BOTTOM
FSEC1	R	3.000	0.250				

FSEC2	T	2.250	4.000	0.255	0.230
FSEC3	P	3.000	3.000	0.000	0.000

C S I / S A P 2 0 0 0 - FINITE ELEMENT ANALYSIS OF STRUCTURES

PROGRAM:SAP2000/FILE:\WINDOWS\DESKTOP\sap\12x13.EKO

F R A M E S E C T I O N P R O P E R T Y D A T A - P R I S M A T I C

SECTION LABEL	AXIAL AREA	TORSIONAL CONSTANT	MOMENTS OF INERTIA I33	I22	SHEAR AREAS A2	A3
FSEC1	0.750E+00	0.148E-01	0.563E+00	0.391E-02	0.625E+00	0.625E+00
FSEC2	0.148E+01	0.296E-01	0.558E+00	0.136E+01	0.518E+00	0.850E+00
FSEC3	0.707E+01	0.795E+01	0.398E+01	0.398E+01	0.636E+01	0.636E+01

C S I / S A P 2 0 0 0 - FINITE ELEMENT ANALYSIS OF STRUCTURES

PROGRAM:SAP2000/FILE:\WINDOWS\DESKTOP\sap\12x13.EKO

F R A M E S E C T I O N P R O P E R T Y D A T A - P R I S M A T I C

SECTION LABEL	MAT LABEL	ADDITIONAL MASS PER LENGTH	ADDITIONAL WEIGHT PER LENGTH
FSEC1	MASSLESS	0.000E+00	0.000E+00
FSEC2	STEEL	0.000E+00	0.000E+00
FSEC3	STEEL	0.000E+00	0.000E+00

F R A M E E L E M E N T D A T A

ELEMENT LABEL	JOINT END-I	JOINT END-J	ELEMENT LENGTH	END-OFFSET-LENGTHS END-I	END-J	RIGID-END FACTOR	NUMBER OF SEGMENTS
3	1	3	10.540	0.000	0.000	0.0000	2
4	3	11	2.855	0.000	0.000	0.0000	2
5	2	4	10.540	0.000	0.000	0.0000	2
6	4	25	2.855	0.000	0.000	0.0000	2
7	1	26	60.000	0.000	0.000	0.0000	4
8	26	27	60.000	0.000	0.000	0.0000	4
9	27	28	60.000	0.000	0.000	0.0000	4
10	28	29	60.000	0.000	0.000	0.0000	4
11	29	30	60.000	0.000	0.000	0.0000	4
12	30	2	60.000	0.000	0.000	0.0000	4
13	3	31	60.000	0.000	0.000	0.0000	4
14	31	32	60.000	0.000	0.000	0.0000	4
15	32	33	60.000	0.000	0.000	0.0000	4
16	33	34	60.000	0.000	0.000	0.0000	4
17	34	35	60.000	0.000	0.000	0.0000	4
18	35	4	60.000	0.000	0.000	0.0000	4
19	10	31	2.855	0.000	0.000	0.0000	2
20	14	32	2.855	0.000	0.000	0.0000	2
21	33	17	2.855	0.000	0.000	0.0000	2
22	20	34	2.855	0.000	0.000	0.0000	2
23	35	23	2.855	0.000	0.000	0.0000	2
24	30	35	10.540	0.000	0.000	0.0000	2

26	26	31	10.540	0.000	0.000	0.0000
2						
27	33	28	10.540	0.000	0.000	0.0000
2						
28	34	29	10.540	0.000	0.000	0.0000
2						
29	32	27	10.540	0.000	0.000	0.0000
2						

F R A M E E L E M E N T D A T A

ELEMENT LABEL	SECTION LABEL	LOCAL PLANE	COORD SYSTEM	PLN 1ST	PLN 2ND	PLANE JOINTA	PLANE JOINTB	COORD ANGLE
3	FSEC1	12	0	+Z	+X	0	0	0.00
4	FSEC3	12	0	+Z	+X	0	0	0.00
5	FSEC1	12	0	+Z	+X	0	0	0.00
6	FSEC3	12	0	+Z	+X	0	0	0.00
7	FSEC2	12	0	+Z	+X	0	0	180.00
8	FSEC2	12	0	+Z	+X	0	0	180.00
9	FSEC2	12	0	+Z	+X	0	0	180.00
10	FSEC2	12	0	+Z	+X	0	0	180.00
11	FSEC2	12	0	+Z	+X	0	0	180.00
12	FSEC2	12	0	+Z	+X	0	0	180.00
13	FSEC2	12	0	+Z	+X	0	0	0.00
14	FSEC2	12	0	+Z	+X	0	0	0.00
15	FSEC2	12	0	+Z	+X	0	0	0.00
16	FSEC2	12	0	+Z	+X	0	0	0.00
17	FSEC2	12	0	+Z	+X	0	0	0.00
18	FSEC2	12	0	+Z	+X	0	0	0.00
19	FSEC3	12	0	+Z	+X	0	0	0.00
20	FSEC3	12	0	+Z	+X	0	0	0.00
21	FSEC3	12	0	+Z	+X	0	0	0.00
22	FSEC3	12	0	+Z	+X	0	0	0.00
23	FSEC3	12	0	+Z	+X	0	0	0.00
24	FSEC1	12	0	+Z	+X	0	0	0.00
26	FSEC1	12	0	+Z	+X	0	0	0.00
27	FSEC1	12	0	+Z	+X	0	0	0.00
28	FSEC1	12	0	+Z	+X	0	0	0.00
29	FSEC1	12	0	+Z	+X	0	0	0.00

C S I / S A P 2 0 0 0 - FINITE ELEMENT ANALYSIS OF STRUCTURES

PROGRAM:SAP2000/FILE:\WINDOWS\DESKTOP\sap\12x13.EKO

T O T A L W E I G H T S A N D M A S S E S

SECTION LABEL	WEIGHT	MASS

FSEC1	0.0157	0.0000
FSEC2	0.3013	0.0008
FSEC3	0.0400	0.0001
TOTAL	0.3570	0.0009

C S I / S A P 2 0 0 0 - FINITE ELEMENT ANALYSIS OF STRUCTURES

PROGRAM:SAP2000/FILE:\WINDOWS\DESKTOP\sap\12x13.EKO

S H E L L S E C T I O N P R O P E R T Y D A T A

SECTION LABEL	MAT LABEL	ELEMENT TYPE	ELEMENT TYPE	ELEMENT THICKNESS	BENDING THICKNESS	MATERIAL ANGLE
SSEC1	CONC	SHELL	THICK	0.1000E+01	0.4750E+01	0.000

C S I / S A P 2 0 0 0 - FINITE ELEMENT ANALYSIS OF STRUCTURES

PROGRAM:SAP2000/FILE:\WINDOWS\DESKTOP\sap\12x13.EKO

S H E L L E L E M E N T D A T A

ELEMENT LABEL	JOINT 1	JOINT 2	JOINT 3	JOINT 4
2	5	9	11	10
3	11	10	8	12
4	9	13	10	14
5	10	14	12	15
6	13	16	14	17
7	14	17	15	18
8	16	19	17	20
9	17	20	18	21
10	19	22	20	23
11	20	23	21	24
12	22	6	23	25
13	23	25	24	7

C S I / S A P 2 0 0 0 - FINITE ELEMENT ANALYSIS OF STRUCTURES

PROGRAM:SAP2000/FILE:\WINDOWS\DESKTOP\sap\12x13.EKO

S H E L L E L E M E N T D A T A

ELEMENT LABEL	SECTION LABEL	LOCAL PLANE	COORD SYSTEM	PLN 1ST	PLN 2ND	PLANE JOINTA	PLANE JOINTB	COORD ANGLE
2	SSEC1	32	0	+Z	+Y	0	0	0.00
3	SSEC1	32	0	+Z	+Y	0	0	0.00

4	SSEC1	32	0	+Z	+Y	0	0	0.00
5	SSEC1	32	0	+Z	+Y	0	0	0.00
6	SSEC1	32	0	+Z	+Y	0	0	0.00
7	SSEC1	32	0	+Z	+Y	0	0	0.00
8	SSEC1	32	0	+Z	+Y	0	0	0.00
9	SSEC1	32	0	+Z	+Y	0	0	0.00
10	SSEC1	32	0	+Z	+Y	0	0	0.00
11	SSEC1	32	0	+Z	+Y	0	0	0.00
12	SSEC1	32	0	+Z	+Y	0	0	0.00
13	SSEC1	32	0	+Z	+Y	0	0	0.00

C S I / S A P 2 0 0 0 - FINITE ELEMENT ANALYSIS OF STRUCTURES

PROGRAM:SAP2000/FILE:\WINDOWS\DESKTOP\sap\12x13.EKO

T O T A L W E I G H T S A N D M A S S E S

MATERIAL LABEL	WEIGHT	MASS
SSEC1	1.3124	0.0040
TOTAL	1.3124	0.0040

C S I / S A P 2 0 0 0 - FINITE ELEMENT ANALYSIS OF STRUCTURES

PROGRAM:SAP2000/FILE:\WINDOWS\DESKTOP\sap\12x13.EKO

L O A D C O N D I T I O N LOAD1

SELF-WEIGHT MULTIPLIER FOR ENTIRE STRUCTURE = 0.1000E+01

JOINT FORCES IN LOCAL COORDINATES

JOINT LABEL	FORCE 1	FORCE 2	FORCE 3	MOMENT 1	MOMENT 2	MOMENT 3
17	0.000E+00	0.000E+00	-0.500E+01	0.000E+00	0.000E+00	0.000E+00

L O A D C O N D I T I O N 15KIP

SELF-WEIGHT MULTIPLIER FOR ENTIRE STRUCTURE = 0.1000E+01

C S I / S A P 2 0 0 0 - FINITE ELEMENT ANALYSIS OF STRUCTURES

PROGRAM:SAP2000/FILE:\WINDOWS\DESKTOP\sap\12x13.EKO

M O D E S D A T A

NUMBER OF EIGENVALUES	1
EIGEN CONVERGENCE TOLERANCE	0.1000E-04
EIGEN CUTOFF FREQUENCY	0.0000E+00
EIGEN FREQUENCY SHIFT	0.0000E+00
INCLUDE RESIDUAL-MASS MODES	NO

C S I / S A P 2 0 0 0 - FINITE ELEMENT ANALYSIS OF STRUCTURES

PROGRAM:SAP2000/FILE:\WINDOWS\DESKTOP\sap\12x13.EKO

L O A D C O M B I N A T I O N M U L T I P L I E R S

COMBO LABEL		DSTL1					
COMBO TYPE		ADD					
	LOAD LABEL	MODE NUM	SPEC LABEL	HIST LABEL	MOVE LABEL	COMBO LABEL	SCALE FACTOR
	LOAD1						1.000
COMBO LABEL		DSTL2					
COMBO TYPE		ADD					
	LOAD LABEL	MODE NUM	SPEC LABEL	HIST LABEL	MOVE LABEL	COMBO LABEL	SCALE FACTOR
	LOAD1						1.000
	15KIP						1.000

C S I / S A P 2 0 0 0 - FINITE ELEMENT ANALYSIS OF STRUCTURES

PROGRAM:SAP2000/FILE:\WINDOWS\DESKTOP\sap\12x13.EKO

I N P U T C O M P L E T E

VITA

Rahsean L. Jackson was born on November 14, 1975 in St. Paul, Minnesota. He graduated from Rolling Meadows high school in Rolling Meadows, Illinois. He received his Bachelor of Science in Civil Engineering from Southern University in Baton Rouge, Louisiana in May of 2000. He enrolled in the graduate program at Virginia Tech in the fall of 2000 and plans to work for a design firm in Washington DC after completion.

_____

Rahsean L. Jackson